A SYSTEMATIC FRAMEWORK FOR ANALYZING THE SECURITY AND PRIVACY OF CELLULAR NETWORKS

A Dissertation

Submitted to the Faculty

of

Purdue University

by

Syed Rafiul Hussain

In Partial Fulfillment of the

Requirements for the Degree

of

Doctor of Philosophy

December 2018

Purdue University

West Lafayette, Indiana

THE PURDUE UNIVERSITY GRADUATE SCHOOL
STATEMENT OF DISSERTATION APPROVAL

Dr. Elisa Bertino, Chair

Department of Computer Science

Dr. Sonia Fahmy

Department of Computer Science

Dr. Ninghui Li

Department of Computer Science

Dr. Mike Atallah

Department of Computer Science

Dr. Omar Chowdhury

Department of Computer Science, University of Iowa

Approved by:

Dr. Voicu S. Popescu

Head of the Graduate Program

In dedication to my parents and my wife who love me unconditionally.

ACKNOWLEDGMENTS

I owe to many people who directly or indirectly helped me to touch this milestone. At first, I sincerely thank my adviser, committee members, mentors, professors, collaborators, and colleagues for their never-ending and invaluable support, advice and guidance that helped me to reach the end of this long but rewarding journey. I am also grateful to all the staffs of the computer science department and graduate school who made this journey less stressful and pleasant. I am forever in debt to every individual from whom I have learned no matter to what extent.

Words can only do so much to thank my sister, brother-in-law, and my two wonderful nieces for their continuous encouragement for my graduate study, but my words would be incomplete without directly acknowledging them for taking care of my parents during my absence at home. I want to express my deepest gratitude to my parents for their unconditional love and support. None of my achievements would have been possible without their countless sacrifices and infinite patience to give me the best possible education.

Last but not least, no words is enough to thank my lovely wife, Shagufta Mehnaz, for her never-ending support, sacrifice, understanding, encouragement, and patience throughout my Ph.D. years. I am grateful to her for spending numerous hours to discuss my research problems, for having belief in me, and for being the greatest supporter of my crazy ideas. I feel blessed for having her by my side during my peaks and valleys. Her very presence is calming at even the most stressful moments. I am so fortunate I get to share my life with her and I enjoy every bit of growing together.

TABLE OF CONTENTS

Page

Page

Page

Page

LIST OF TABLES

LIST OF FIGURES

Figure Page

ABSTRACT

Hussain, Syed Rafiul PhD, Purdue University, December 2018. A Systematic Framework For Analyzing the Security and Privacy of Cellular Networks. Major Professor: Elisa Bertino.

Cellular networks are an indispensable part of a nation's critical infrastructure. They not only support functionality that are critical for our society as a whole (e.g., business, public-safety message dissemination) but also positively impact us at a more personal level by enabling applications that often improve our quality of life (e.g., navigation). Due to deployment constraints and backward compatibility issues, the various cellular protocol versions were not designed and deployed with a strong security and privacy focus. Because of their ubiquitous presence for connecting billions of users and use for critical applications, cellular networks are, however, lucrative attack targets of motivated and resourceful adversaries.

In this dissertation, we investigate the security and privacy of 4G LTE and 5G protocol designs and deployments. More precisely, we systematically identify design weaknesses and implementation oversights affecting the critical operations of the networks, and also design countermeasures to mitigate the identified vulnerabilities and attacks. Towards this goal, we developed a systematic model-based testing framework called LTEInspector. LTEInspector can be used to not only identify protocol design weaknesses but also deployment oversights. LTEInspector leverages the combined reasoning capabilities of a symbolic model checker and a cryptographic protocol verifier by combining them in a lazy fashion. We instantiated LTEInspector with three critical procedures (i.e., *attach*, *detach*, and *paging*) of 4G LTE. Our analysis uncovered 10 new exploitable vulnerabilities along with 9 prior attacks of 4G LTE all of which have been verified in a real testbed. Since identifying all classes of attacks with a unique

framework like LTEInspector is nearly impossible, we show that it is possible to identify sophisticated security and privacy attacks by devising techniques specifically tailored for a particular protocol and by leveraging the findings of LTEInspector. As a case study, we analyzed the paging protocol of 4G LTE and the current version of 5G, and observed that by leveraging the findings from LTEInspector and other side-channel information and by using a probabilistic reasoning technique it is possible to mount sophisticated privacy attacks that can expose a victim device's coarse-grained location information and sensitive identifiers when the adversary is equipped only with the victim's phone number or other soft-identity (e.g., social networking profile). An analysis of LTEInspector's findings shows that the absence of broadcast authentication enables an adversary to mount a wide plethora of security and privacy attacks. We thus develop an attack-agnostic generic countermeasure that provides broadcast authentication without violating any common-sense deployment constraints. Finally, we design a practical countermeasure for mitigating the side-channel attacks in the paging procedure without breaking the backward compatibility.

1. INTRODUCTION

Cellular networks have not only enabled instantaneous and inexpensive communication among people living in any part of the world, but have also been a major enabling factor for the modernization of infrastructures and application sectors, such as transportation infrastructure, agriculture, education, health, government and business. Cellular networks are, therefore, considered as a nation's critical infrastructure. The proliferation of low-cost cellular devices, the explosive growth of high-bandwidth mobile applications (such as audio and video), and the overall mobile connectivity by the end users have resulted in increased complexity and challenging requirements against such networks, and thus fueling the demand for continuous network evolution. As a result, even after decades of their emergence with the first generation protocol (1G), cellular communication protocols have been evolving in terms of speed, technology, frequency, data capacity, and latency to enhance quality of services and thus have become the driving force behind many advancements. For instance, the first generation (1G) enabled the basic analog voice communication, while the second generation (2G) enabled digital voice communication and dealt with capacity and coverage. The third generation (3G) ushered in mobile data, and provided multimedia support whereas the fourth generation (4G) paved the way for widespread mobile Internet usage and access to a wide range of telecommunication services. The fifth generation (5G) is going to revolutionize mobile and Internet-of-Things (IoT) markets by assuring better connectivity, reduced latency, and enhanced security to smart cellular devices.

1.1 Insecurity of Cellular Communication

Though cellular networks have been evolving every 10 years with newer generation of access technologies, the security and privacy safeguards for such critical infrastruc-

ture have not kept pace with its growing importance. Because of their ubiquitous presence and use for critical applications (e.g., emergency alert systems), cellular networks have been attractive attack targets for malicious parties. For instance, resourceful adversaries (e.g., nation states, foreign intelligence agencies, terrorists) can rely on an ingenious range of attack strategies and wreak havoc by exploiting vulnerabilities of the cellular network ecosystem (e.g., surveillance [1], cyberwarfare [2]). The potential of such attacks is exacerbated by the increasingly wide adoption of cellular communication enabled smart devices [3] and systems (e.g., autonomous vehicles) which often reside in individuals' personal space. If cellular networks are not adequately protected, the damage may result in huge losses of dollars, strategic advantage, and even of human lives.

1.2 A Vision for Secure Cellular Network and the Key Research Direction

We envision a future in which the security and resiliency of cellular networks will be unquestionable and will not crumble even against the strongest possible adversaries. Achieving this goal will require advances in many research directions. Among them the foremost research direction is the secure system design and rigorous verification of the desirable security and privacy properties of the system. Since many vulnerabilities in the implementations arise from specification misinterpretation and evaluation in isolation, it is, therefore, also critical to investigate the existing design and deployments of cellular networks for detecting potential vulnerabilities.

The 3rd Generation Partnership Project (3GPP) [4] develops the standard/specification of cellular communication protocols and provides guidelines for conformance testing [5] which only evaluates if the implementation is compliant with the specifications. While such testing approaches have been shown to be useful for checking functional requirements, gaps in the protocol design and insufficient checking for the adversary entry points have resulted in the discovery of new vulnerabilities. There-

fore, it is imperative to analyze the security and privacy of cellular network standards and thus ensure their resiliency against powerful attackers.

1.3 Challenges in the Analysis of Cellular Networks

Developing suitable methodologies and tools for the analysis of the security and privacy of cellular networks requires addressing several non-trivial challenges: (a) *Protocol complexity*: Cellular protocols—comprising of multiple (cryptographic) sub-protocols—are *stateful* in nature [6]. Also, analyses will likely experience scalability challenges due to the presence of multiple types of protocol participants, and messages containing data with large domains. (b) *Lack of formal specification*: Cellular protocols lack formal specifications, and the standards [4, 7] often suffers from ambiguity and under-specification. (c) *Closed systems*: A majority of the deployed cellular systems (both network operators and cellular devices) are proprietary and closed systems which require any testing approach to be black-box and system-agnostic. (d) *Legal barriers*: Regulatory requirements [8] prohibit transmission in the licensed spectrum making dynamic network testing and attack validation challenging.

1.4 Existing Efforts

There exists a substantial amount of research work that has analyzed the security and privacy of different protocols of telecommunication systems in isolation, and also identified design weaknesses of the standard [4, 7] and unsafe practices by the responsible stakeholders [6, 9–20]. Such work, however, suffers from one or more of the following limitations: (A) Analyses use clever intuitions but do not use systematic methodologies for attack discovery [9–17, 19]; (B) Analyses focus on prior generations of the protocols only [9–16, 20], and hence some of the findings do not directly apply to recent protocols, such as LTE 4G and 5G; (C) Analyses do not explicitly reason about adversarial actions [6].

1.5 Dissertation Focus

It is evident that the state-of-the-art of systematic analysis frameworks and vulnerability mitigation techniques for ensuring the resilience of cellular standards against attacks are far away from the security level that we want to achieve. In this dissertation, we, therefore, first address the following research question: *is it possible to develop a systematic framework for scrutinizing different protocols in the cellular network standard to uncover vulnerabilities that can be shown to be realizable in practice by an adversary*?

Designing a uniform framework for verifying all classes of (security and privacy) properties and exploring all kinds of attacks for such complex cellular systems is an undecidable problem. Though fine-grained protocol-behavior abstraction (including low-level details) of the massive cellular systems may be capable of identifying a wide range of attacks, it is likely to trigger the state explosion problem which would make the analysis intractable. The coarse-grained behavior abstraction, on the other hand, facilitates efficient reasoning but is unable to identity the side-channel attack vectors. In this dissertation, we, therefore, address the second research question: *is it possible to identify side-channel attacks in a particular sub-protocol of the cellular system by leveraging insights drawn from a systematic approach and by exploiting sophisticated probabilistic reasoning techniques?*

While systematic analysis helps identifying the root causes of the vulnerabilities, mitigation techniques are required to augment the inventory of defense mechanisms. Attack-specific countermeasures, or in other words, hot-patches to a particular vulnerability have been shown to be fruitful for an already deployed cellular system whereas attack-agnostic countermeasures seal-off the root cause of a class of vulnerabilities and require major overhaul to the protocol standard and thus are difficult to integrate with the already deployed system. Hence, in this dissertation, we address the third research question: *is it possible to design attack-agnostic countermeasures*

that can be incorporated into both the current and the newer generations of cellular networks without breaking the backward compatibility?

Note that we address these research questions from the perspective of 4G and 5G networks and our proposed techniques are general enough to adapt for both older and newer generations of cellular networks.

1.6 Thesis Statement

In this doctoral thesis, we demonstrate that: (i) carefully designed systematic framework can soundly and scalably discover the vulnerabilities in closed systems and is useful in evaluating cellular networks to understand how well they ensure security and privacy; (ii) the use of sophisticated techniques tailored for specific sub-protocols makes it possible to identify side-channel attacks in cellular networks; and (iii) attack-specific countermeasures often do not hold under detailed security analysis, whereas attack-agnostic and clean-slate defense techniques are more effective in mitigating the root cause of many active attacks; however, they require careful optimization and engineering to keep the protocol overhead low while at the same time assuring backward compatibility.

1.7 Contributions

In this dissertation, we make the following contributions

1.7.1 A Systematic Framework for Analyzing Security and Privacy of Cellular Networks

We investigate the security and privacy of the three critical procedures of the 4G LTE protocol (i.e., attach, detach, and paging), and in the process, uncover potential design flaws of the protocol and unsafe practices employed by the stakeholders. For exposing vulnerabilities, we propose a model-based testing approach LTEInspector

which lazily combines a symbolic model checker and a cryptographic protocol verifier in the symbolic attacker model. Using LTEInspector, we have uncovered 10 new attacks along with 9 prior attacks, categorized into three abstract classes (i.e., security, user privacy, and disruption of service), in the three procedures of 4G LTE. Notable among our findings is the *authentication relay attack* that enables an adversary to spoof the location of a legitimate user to the core network without possessing appropriate credentials. To ensure that the exposed attacks pose real threats and are indeed realizable in practice, we have validated 8 of the 10 new attacks and their accompanying adversarial assumptions through experimentation in a real testbed. Note that LTEInspector is generalized enough that it works like a plug-and-play analysis tools for both older and newer generations of cellular networks which drew attention [21–26] from all over the world and paved the way to make a real impact through collaborating with the leading cellular stakeholders (e.g., Qualcomm and Intel).

1.7.2 Identification of Privacy Attacks on the 4G and 5G Cellular Paging Protocols Using Side Channel Information

The cellular paging (broadcast) protocol strives to balance between a cellular device's energy consumption and quality-of-service by allowing the device to *only* periodically poll for pending services in its idle, low-power state. For a given cellular device and serving network, the exact time periods when the device polls for services (called the *paging occasion*) are fixed by design in the 4G/5G cellular protocol. In this work, we show that the fixed nature of paging occasions can be exploited by an adversary to associate a victim's soft-identity (e.g., phone number, Twitter handle) with its paging occasion, with only a modest cost, through an attack dubbed `ToRPEDO`. Consequently, `ToRPEDO` can enable an adversary to infer a victim's coarse-grained location information, inject fabricated paging messages, and mount denial-of-service attacks. We also demonstrate that, in 4G and 5G, it is plausible for an adversary to retrieve a victim device's persistent identity (i.e., IMSI) with a brute-force `IMSI-Cracking` attack

while using ToRPEDO as an attack sub-step. Our further investigation on 4G paging protocol deployments also identified an *implementation oversight* of several network providers which enables an adversary to launch an attack, named PIERCER, for associating a victim's phone number with its IMSI; subsequently allowing targeted user location tracking. All of our attacks have been validated and evaluated in the wild using commodity hardware and software.

1.7.3 Securing the Insecure Connection Bootstrapping in Cellular Networks: The Root of all Evil

Current cellular ecosystem lacks authentication in its bootstrapping signaling and it allows a malicious, fake base station to lure unsuspecting cellular device to connect to it which can then enable the adversary to launch many known active attacks. Though several efforts have been undertaken to detect fake base stations and also to protect the privacy of subscribers' permanent identifier (IMSI/IMEI), very little has been done to empower cellular devices to authenticate legitimate base stations. The 3GPP is aware of the danger of unauthenticated broadcast signals and has outlined two possible approaches—based on symmetric and asymmetric key cryptography—to mitigate this insecurity. These authentication approach-sketches, however, are not incorporated in the recent generation of the protocol (5G). The rationale for not incorporating broadcast authentication in 5G is, however, not clear. In addition, it is not clear what would be the challenges and trade-offs required for the deployment of such authentication approaches within the 5G protocols. In this work, we, thereby, first develop clean-slate designs of these two approaches and evaluate their efficacy from a purely technical point of view. Based on our initial evaluation, we observed that the approach based on symmetric key cryptography does not provide the desired level of assurances whereas the approach based on Public-key Infrastructure (PKI) is feasible without breaking the backward compatibility. Further evaluation on a real test-bed shows that it is feasible to deploy a *light-weight* PKI-based authentication mechanism

leveraging precomputation of digital signatures without incurring substantial latency and bandwidth overhead.

1.7.4 Hardening against Privacy Attacks Exploiting Side-Channel Information

The fixed nature of paging occasions in 4G and 5G networks is a fundamental weakness which the adversary may exploit to associate a victim's soft identity, e.g., phone number or Twitter Handle with its paging occasion. This further enables the adversary to perform ToRPEDO attack through which the adversary can infer a victim's coarse-grained location information, inject fabricated paging messages, and mount denial-of-service attacks. In this work, we first explore the solution space against the ToRPEDO attack and then outline a clean-slate countermeasure making the paging occasions and the identities anonymous to any devices. Our initial evaluation, however, reveals the impractical overhead incurred by this solution which leads us to develop a viable noise-based countermeasure in which a legitimate base station carefully injects fake paging messages containing legitimate devices' TMSIs. We evaluated its efficacy with real network traces for different operators. In our evaluation, we observed that with $\sim$ 600 fake paging messages injected within $\sim$ 40 seconds interval can prevent the adversary to perform the ToRPEDO attack with as many as $\sim$ 500 phone calls.

1.8 Dissertation Outline

The remainder of this dissertation is organized as follows:

Chapter 2 provides a background on 4G LTE and 5G networks. Chapter 3 presents LTEInspector, a model-based testing approach, for analyzing the security and the privacy of 4G LTE networks. Chapter 5 demonstrates how the adversary exploits the fixed paging occasion of a device to perform a number of privacy attacks. Chapter 5 describes the PKI-based lightweight broadcast authentication scheme for preventing fake base stations. Chapter 6 addresses the side channel attacks uncovered in the

paging procedure. Chapter 7 presents the state-of-the-art summary of the related work. Finally, Chapter 8 provides a discussion of concluding remarks and future research directions.

2. BACKGROUND

In this chapter, we provide a brief primer of 4G LTE and 5G networks. We begin by introducing the 4G network architecture. For the ease of exposition, we simplify the network architecture substantially (see Figure 2.1) and only focus on the aspects relevant to most critical network operations including *bootstrapping*, *attach*, *paging*, and *detach* procedures. While presenting these for 4G LTE, we also discuss the counterparts of attach and detach procedures in 5G networks, i.e., the *registration* and *paging* procedures. Since a complete treatment of 4G LTE and 5G networks in this thesis is simply not possible as the standard documents have several thousand pages, we intend this chapter to focus on the architectural elements and critical procedures of the 4G LTE and 5G that are required for understanding the discussions in the following chapters. We refer the readers interested in further exploring additional specific details of both 4G [7, 27, 28] and 5G [29–33] networks to the documentation available through the Third Generation Partnership Project (3GPP) [4].

2.1 LTE Network Architecture

The LTE network is broadly comprised of the following three components: the cellular device (also known as user equipment or UE), the radio access network (or, (E-UTRAN), and the core network or Evolved Packet Core (EPC).

UE: UE is the cellular device equipped with a universal subscriber identity module known as SIM card. The SIM card securely stores the unique international mobile subscriber identity (IMSI) number and its associated cryptographic keys used for the UE identification and authentication during the UE's connection initiation with the EPC. The UE also has its own device-specific unique identity, called the international mobile equipment identity (IMEI), also used for identification. The IMSI and IMEI

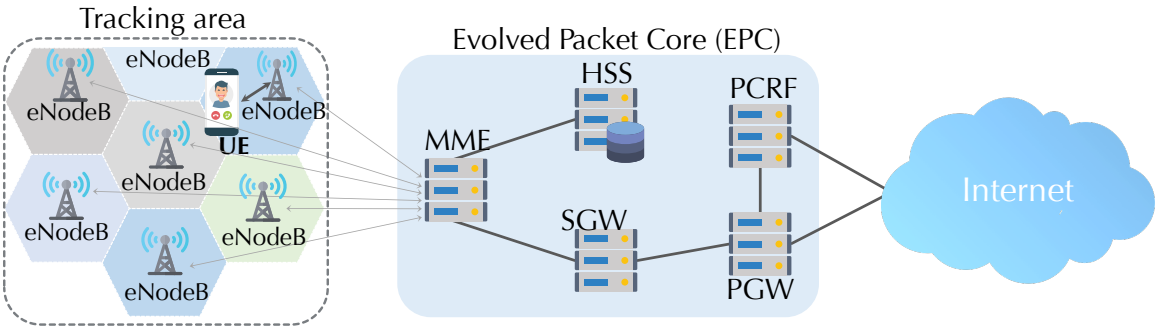

Figure 2.1.: The LTE Network Architecture

are sensitive in the sense that exposing them can make the UE prone to illegitimate tracking/impersonation. Table 2.1 shows a list of UE identities that are used in 4G and 5G networks.

E-UTRAN: A geographical area, in the context of LTE, is partitioned into hexagonal cells (see Figure 2.1) where each cell is serviced by a single base station (i.e., eNodeB), providing its nearby cellular devices the connectivity to the Internet through the carrier's core network. The eNodeB can be roughly viewed as an intermediary facilitating the connection between the UE and the EPC. In essence, the E-UTRAN is the network between a UE and the eNodeB, and between pairs of eNodeBs.

Table 2.1.: UE Identities used in 4G and 5G networks.

Identifiers	**Network**	**Full Form**
IMSI	4G	International Mobile Subscriber Identity
IMEI	4G & 5G	International Mobile Equipment Identity
TMSI	4G & 5G	Temporary Mobile Subscriber Identity
GUTI	4G	Globally Unique Temporary Identifier
SUPI	5G	Subscription Permanent Identity
SUCI	5G	Subscription Concealed Identity

EPC: We now describe those EPC components of 4G LTE that are relevant to our discussion, i.e., the MME (Mobility Management Entity) and the HSS (Home Subscriber Server).

(1) Mobility Management Entity (MME): The MME manages attach (including authentication and key agreement), paging, and detach procedures of the UEs in a particular tracking area (formed by a set of hexagonal cells). It is also responsible for keeping track of the locations of the UEs residing in its designated tracking area.

(2) Home Subscriber Server (HSS): The HSS stores UEs' identities (e.g., IMSI and IMEI) and subscription data (e.g., QoS profile) along with the cryptographic master keys from which it generates the authentication challenges and the symmetric session keys for each subscriber.

Other EPC components include the Serving-Gateway (SGW), the PCRF (Policy and Charging Rules Function) server, and the Packet Data Network Gateway (P-GW) which are responsible for enabling incoming and outgoing services (phone calls and SMS). 4G LTE provides packet switch (PS) services for Internet access and VoLTE (Voice over LTE) phone calls. It also supports circuit switch (CS) voice services using the Circuit-Switched Fallback (CSFB) technique which moves UEs from 4G to 3G network to access 3G voice services, and then returns them to the 4G network.

2.1.1 Corresponding EPC Components in 5G

5G has introduced a service-driven network architecture and included a number of new core elements to efficiently meet diversified service requirements. A major portion of the 5G architecture is, however, similar to 4G which induces a deep similarity between some EPC components of the 4G and 5G core networks. A majority of control-plane interactions between the UE and the core network are thus equivalent for 4G and 5G. We, therefore, briefly discuss the 5G network components that are equivalent to MME and HSS in 4G:

(1) Access and Mobility Management Function (AMF): The AMF supports registration (resp, attach in 4G) management, connection management, mobility management, access authentication and authorization, and security context management.

(2) Unified Data Management (UDM): The UDM supports generation of Authentication and Key Agreement (AKA) credentials, user identification handling, access authorization, and subscription management.

2.2 Bootstrapping Signals

Synchronization Signals. Primary Synchronization Signal (PSS) and Secondary Synchronization Signal (SSS) are two specific physical layer signals that are used for radio frame synchronization and physical cell identification.

Master Information Block (MIB). A base station periodically (every 40 ms) broadcasts master_info_block messages to advertise the existence of the network irrespective of any user's presence in a cell area. Therefore, the very first step for a UE to gain initial access to the network is to read the master_info_block (MIB) message that includes the downlink channel bandwidth, configuration parameters for decoding subsequent messages, and the current system frame number (**SFN**) for UE's time/frame synchronization with the network. We further elaborate the discussion on SFN and time/frame synchronization in Section 2.3.

System Information Block (SIB). A base station also periodically (every 80 ms) broadcasts system_info_block_type_1 message that includes information regarding whether a UE is allowed to access the cell. It also defines the scheduling of the other system_info_block messages (e.g., system_info_block_type_2), and carries cell ID, mobile country code (MCC), mobile network code (MNC), tracking area code (a tracking area consists of multiple cells), mapping information for other system_info_block messages.

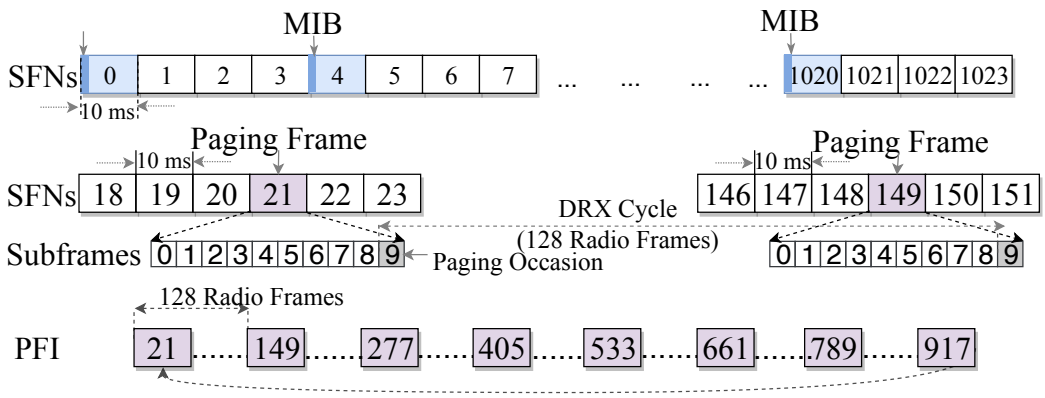

Figure 2.2.: Network time/frame synchronization, and paging frame and paging occasion calculation.

2.3 Network Time/Frame Synchronization in LTE

LTE supports full duplex radio communication between a UE and a base station through frequency division duplex (FDD) mode in which the transmitter and receiver operate on different carrier frequencies. In LTE-FDD, communications are carried out through *radio frames* (also called *system frames* or type-1 LTE frames) each of which spans 10 milliseconds. In this thesis, we simply call them *frames*. They are indexed with a 10-bit circular counter (resetting to 0 after counting up to 1023), and thus have System Frame Numbers (SFN) in the range of $[0, 1023]$. Thus for every 10.24 seconds, SFN will repeat. Each frame is further partitioned into 10 *sub-frames* each of which spans 1 millisecond (Figure 2.2). As already discussed in Section 2.2, connection bootstrapping starts with a UE capturing the master_info_block (MIB) message, which is periodically (more precisely, every 40 milliseconds) broadcast by base stations. The MIB includes the current SFN and other connection-related parameters used by the UE uses to synchronize itself and connect to the base station.

2.4 UE's Cell Section and Initial Connection Establishment

The cellular device scans the frame synchronization signals broadcast by nearby base stations in the frequency bands that the device is allowed to operate on and for each frequency it identifies the strongest among all the suitable/acceptable cells. A suitable/acceptable cell is the one for which the measured cell attributes satisfy the cell selection criteria. When an acceptable cell is found, the UE camps on that cell and initiates the cell reselection procedure, if required. The UE reads the MIB message sent by the selected cell, and synchronizes the time. The UE learns the connection-related parameters' values from the SIB messages after which it initiates connection (as shown in Figure 2.3) to the base station (at the radio resource control or RRC layer) and to the core network (at Network Access Stratum or NAS layer).

2.5 Attach Procedure

When a UE wants to connect to the EPC (e.g., at the time of device reboot), the UE starts off by establishing a (RRC-layer) connection (see Figure 2.3) with the eNodeB whose signal power it perceives to be the highest. As we illustrate later, this step (i.e., connecting to the highest powered eNodeB) can be exploited to set up a malicious eNodeB, prevalently in the context of IMSI catchers [18, 20]. Once the UE has established a connection with the eNodeB, the attach procedure can proceed according to the following four stages.

Identification: The UE starts the attach procedure by sending the attach_request message to the MME through the eNodeB (see Figure 2.3). The UE includes its identity, i.e., the IMSI/IMEI and its security capabilities (e.g., supported cipher suites) in this attach_request message in plaintext.

Authentication: For verifying the authenticity of the UE, the MME, upon reception of an authentication challenge generated by the HSS, sends an authentication_request message including this challenge to the UE. The UE using its master key solves the challenge and sends an authentication_response message to the UE. If the authentica-

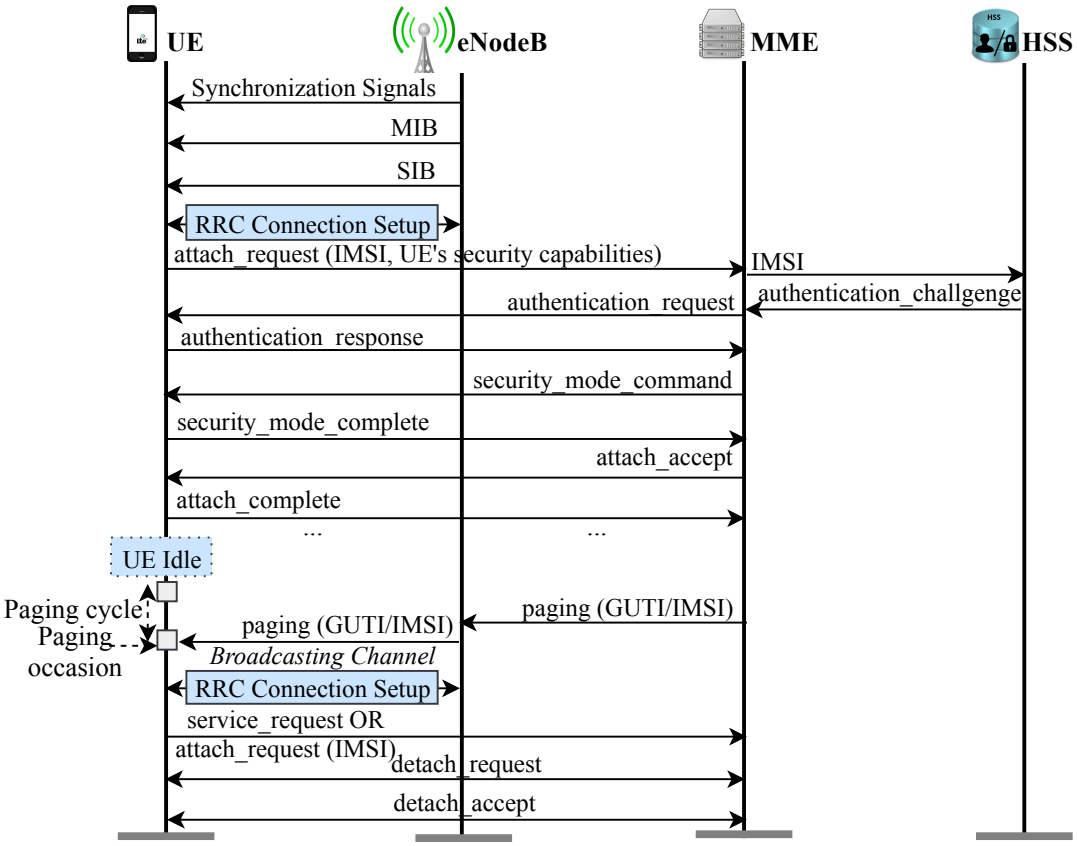

Figure 2.3.: Attach, paging, and detach procedures of 4G LTE.

tion is successful, the UE and the MME enter next stage, that is, security algorithm negotiation.

Security algorithm negotiation: The MME chooses one of the algorithm pairs (i.e., encryption and integrity) that the UE supports, obtained from the security capabilities sent with the attach_request. The MME then sends the integrity protected security_mode_command message to the UE in which the MME replays with the UE's security capabilities so that the UE verifies whether the security capabilities in the security_mode_command message are same as the ones sent by the UE in the attach_request message. After a successful verification of the message authentication code (MAC) included in the security_mode_command, the MME then sends an encrypted and integrity protected security_mode_complete message. The UE and the

MME then create a shared security context, i.e., the shared keys for protecting confidentiality and integrity of the future message exchanges.

Secure temporary identifier exchange: The MME then sends an encrypted and integrity-protected attach_accept message which includes a temporary identity called GUTI (Globally Unique Temporary Identity)[1] for the UE. TMSI is randomly assigned by the MME to an UE and is local to a tracking area, and so it has to be updated each time the UE moves to a new geographical area. The MME can also update a UE's TMSI if it desires to do so. To limit the exposures of sensitive IMSI/IMEI, the TMSI is used in all subsequent communications between the UE and the eNodeB/MME. The UE concludes the *attach* procedure by sending an attach_complete message. The UE and the eNodeB then also create a security context by generating a pair of shared keys for their secure communication.

2.5.1 Registration Procedure in 5G

Except for the *identification* phase, the registration procedure in 5G is similar to the attach procedure in 4G. Instead of sending the IMSI in the registration_request (resp., attach_request for 4G) message, in 5G the UE sends a randomized encryption of the SUPI (Subscription Private Identifier). The SUPI is a SIM card-specific persistent identity for a UE in 5G. The UE uses the core network's public key to encrypt its SUPI (the encrypted SUPI is referred to as SUCI or Subscription Concealed Identifier) whereas the UDM in 5G core network uses the private key for decrypting the SUCI.

2.6 Paging Procedure

When a UE is not actively communicating with a base station, it enters an idle, low-energy mode for conserving battery power. When the UE is in the idle mode, the base station uses the paging protocol to notify the UE about emergencies (e.g.,

[1]GUTI = MME identifier + TMSI (Temporary Mobile Subscriber Identity). The MME/eNodeB uses few bytes of GUTI as TMSI to represent the temporary identifier. Therefore, for simplifying the discussion, we use the terms TMSI and GUTI interchangeably in the rest of the thesis.

Tsunami warning) or pending network services (e.g., incoming calls, SMS, or other services). This is called Discontinuous Reception (DRX).

Service paging. For notifying an idle UE about a pending service, if *smart paging* is used, the MME first asks the UE's last connected base station to broadcast a paging message for the UE. If there is no response from the UE, then the MME asks all base stations in its tracking area to broadcast the paging message through a Paging Control Channel (PCCH). For non-smart paging, the first step is skipped. If the UE still does not respond, it is assumed that the UE either left the tracking area or is not communicating to the network.

Paging messages. A paging message contains between 1 and 16 *paging records*. Each paging record notifies one UE that there are incoming services for it. Such a record contains the MME identifier, the domain (PS or CS), and the target UE's paging identity, which can be either the IMSI or the TMSI, determined by the MME.

Paging occasion. A UE in idle state wakes up periodically to check whether there is a paging message. If there is a paging message, the UE iterates over the paging records in the message while searching for its paging identity (IMSI or TMSI). It re-establishes the connection with the base station if it finds its identity. The paging protocol ensures that when a base station sends a UE's paging record in at a given time, the UE also wakes up at that time to check. That is, a base station and a UE must agree on when to send/receive paging records for the UE.

2.6.1 Paging Synchronization

The paging occasion for a UE (i.e., when it wakes up to check for paging messages) is given by three numbers: the paging cycle T $\in \{32, 64, 128, 256\}$; the Paging Frame Index PFI, which is an integer between 0 and $T - 1$; and a sub-frame index s, $0 \leq s \leq 9$. The UE wakes up at sub-frame s in any frame whose SFN is congruent to PFI modulo T. For example, when $s = 9$, $T = 128$ and PFI $= 21$, the UE will wake up at sub-frame 9 in frames with SFN $21 + i * 128$ for $0 \leq i \leq 7$. For every cycle of

T frames (of total length $10T$ ms), the UE needs to wake up for only 1 ms. We now explain how these numbers are computed.

Paging Cycle (T). The base station broadcast a proposed value for T. The UE can choose to use that value or propose another value, in which case the minimum of these two values are chosen.

Paging Frame Index (PFI). Computing the PFI requires the UE's UE_ID, defined as:

$$\text{UE\_ID} = \text{IMSI mod } 1024.$$

In addition, it requires another public parameter (**nB**) set by the base station, and chosen from the set $\{4\text{T}, 2\text{T}, \text{T}, \frac{\text{T}}{2}, \frac{\text{T}}{4}, \frac{\text{T}}{8}, \frac{\text{T}}{16}, \frac{\text{T}}{32}\}$. PFI is defined using the following formula:

$$\text{PFI} = \frac{\text{T}}{N} \times (\text{UE\_ID mod } N) \text{ where } N = \min(\text{T}, \text{nB}).$$

Equivalently,

$$\text{PFI} = \begin{cases} \text{UE\_ID mod T} & \text{when T} \leq nB \\ \frac{\text{T}}{\text{nB}} \times (\text{UE\_ID mod nB}) & \text{when T} > \text{nB} \end{cases}$$

Sub-frame Index. The sub-frame index s can be calculated using the lookup Table 2.2 where

$$N_s = \max\left(1, \frac{\text{nB}}{\text{T}}\right); \;\; i_s = \left\lfloor \frac{\text{UE\_ID}}{N} \right\rfloor \text{ mod } N_s.$$

Note that when nB $\leq$ T and $N_s = 1$, all UEs will use sub-frame 9. When nB = 2T, a UE uses either sub-frame 4 or sub-frame 9, depending on whether its UE_ID is even or odd. When nB = 4T, the UEs are partitioned into 4 groups, each using one sub-frame.

Example. An example is shown in Figure 2.2 illustrating the calculation of the PFI, the System Frame Numbers during which the UE should wake up, and the sub-frame index, where nB=T=128 and UE_ID=21.

Table 2.2.: Sub-frame index s

	$i_s = 0$	$i_s = 1$	$i_s = 2$	$i_s = 3$
$N_s = 1$	9	**N/A**	**N/A**	**N/A**
$N_s = 2$	4	9	**N/A**	**N/A**
$N_s = 4$	0	4	5	9

2.6.2 Calculating Paging Occasion in 5G

In 5G, the calculation of the paging occasion is very similar to that for LTE. The paging occasion for a UE is given by the same three numbers: the paging cycle T; the Paging Frame Index PFI; and the sub-frame index s, which are computed exactly as in LTE. The only difference is that 5G introduced another public-parameter broadcast called PF_offset (clause 7 of RRC Idle mode specification [33]). The UE wakes up at the sub-frame s in any system frame whose SFN+PF_offset is congruent to PFI modulo T.

2.6.3 Abstraction of Paging

Abstractly, UEs are partitioned into a number of paging groups that time-share the channel through which paging messages are sent. Paging messages for UEs from two different groups will be sent at different times, and can be identified as such. For ease of exposition, we consider the case where T = nB when describing our attacks. Under this case, each UE wakes up once every T frames. Three of the four wireless carriers we have observed use T = nB = 128, while the other uses $\mathrm{T} = 128, \mathrm{nB} = 8$. Our attacks can be generalized to the case where T $\neq$ nB, since the same time-sharing principle applies.

2.7 Detach Procedure

The UE/MME can choose to terminate the established connection by generating a detach_request including the cause of detach. In response to the detach_request, the UE/MME is *expected* to send a detach_accept message.

3. LTEInspector: A SYSTEMATIC APPROACH FOR ADVERSARIAL TESTING OF 4G LTE

The adoption of Fourth generation Long Term Evaluation (4G LTE)—the de facto standard for cellular telecommunication—has seen a stable growth in recent years, replacing prior generations due to its promise of improved assurances (e.g., higher bandwidth, reliable connectivity, enhanced security). 4G LTE has not only influenced our society as a whole but also made impact at a more personal level by enabling applications that often improve our quality of life. 4G LTE are also often used for quickly broadcasting public safety/warning messages in the case of natural (e.g., hurricane) or man-made (e.g., toxic gas emission) disasters. Although different aspects of 4G LTE have been investigated [17, 34] using ad hoc analysis techniques, there is no concerted effort/framework to systematically inspect the 4G LTE standard/specification for identifying security and user privacy vulnerabilities. The grand vision of this work is to develop a framework which can enable automated analysis of the 4G LTE standard for finding weaknesses and operational oversight that can be exploited by adversaries for violating the inherent security, user privacy, and service guarantees desired from 4G LTE networks.

Problem and scope. The 4G LTE protocol can be viewed as an amalgamation of multiple critical procedures, such as attach, paging, detach, handover, and calls — to name a few. Each of these procedures is complex and requires an in-depth security and privacy analysis of its own. Among the different procedures, attach, paging, and detach are critical for the correct and reliable functionality of the other procedures. For instance, without a correct and secure attach procedure (i.e., the initial secure connection setup), the security bootstrapping process is likely to be vulnerable; this may have serious consequences, such as man-in-the-middle attacks, spurious mobile billing, or even life threatening risks. This work described in this

chapter thus addresses the following central research question: *is it possible to develop a systematic approach for scrutinizing the attach, detach, and paging procedures to uncover vulnerabilities that can be shown to be realizable in practice by an adversary*?

Approach. For analyzing the critical procedures of 4G LTE, in this work, we propose LTEInspector which employs a property-driven adversarial model-based testing philosophy. LTEInspector considers the standard symbolic adversary model (alternatively known as the Dolev-Yao model [35]) for its analysis. LTEInspector takes the relevant 4G LTE abstract model $\mathcal{M}$ and a desired property φ, and tries to find a violation of φ in $\mathcal{M}$. The set of properties that LTEInspector aims to check include *authenticity* (e.g., disallowing impersonation), *availability* (e.g., preventing service denial), *integrity* (e.g., restricting unauthorized billing), and *secrecy* of user's sensitive information (e.g., preventing activity profiling).

As a prerequisite of LTEInspector's analysis, we first construct the 4G LTE ecosystem model by consulting the standard [4, 7]. Our model $\mathcal{M}$ (publicly available in `https://github.com/relentless-warrior/LTEInspector`) captures the *abstract* functionality (ignoring low-level implementation details) of the 4G LTE ecosystem—only relevant to the analysis of the three procedures—as synchronous communicating finite state machines (FSM). Each FSM captures the stateful functionality of a protocol participant's (i.e, user's cellular device and the core network) at the Non-Access Stratum (NAS) protocol layer [4, 7]. The two FSMs communicate with each other through public (adversary-controlled) communication channels by sending each other NAS layer messages.

Our analysis is an instance of the parameterized system verification problem (i.e., parameterized by the number of protocol participants) which is generally undecidable [36]; achieving both soundness and completeness is thus impossible. Consequently, we follow the conventional method of aiming for soundness instead of completeness, that is, if our approach reports a violation, it is indeed a violation; we cannot, however, detect all violations. Also, checking compliance of the protocol model against desired security and privacy properties often requires simultaneously reason-

ing about: (❶) temporal ordering of different events/actions (i.e., trace properties such as response properties [37]), (❷) cryptographically-protected messages and constructs (e.g., encryption, hashing), and (❸) other rich constraints (e.g., linear integer arithmetic constraints). General purpose model checkers [38, 39] have shown promise in successfully reasoning about properties concerning ❶ and ❸. Cryptographic protocol verifiers [40–45], although proficient in verifying cryptography related properties, for tractability reasons only provide primitive support at best for properties concerning ❶ and ❸. This naturally leads us to the question: *is it possible to get the best of both these techniques*?

To this end, LTEInspector lazily (or, on an on-demand basis) combines the reasoning powers of a symbolic model checker and a cryptographic protocol verifier. To the best of our knowledge, in the context of 4G LTE, the use of symbolic model checking and a cryptographic protocol verifier to reason about rich temporal trace properties is novel. In this approach, we first abstract away all cryptography-related constructs from the model $\mathcal{M}$ and the desired property φ and only reason about aspects ❶ and ❸ of the φ (denoted by φ_{abs}). For any violation of φ_{abs} in $\mathcal{M}$, the symbolic model checker would yield a counterexample π demonstrating the violation. Now, π may include adversary actions which may not be realizable due to cryptographic assumption violations (e.g., constructing a valid ciphertext of a message without possessing the encryption key). To rule out such cases, for each adversary action in π, we query a cryptographic protocol verifier to check the action's feasibility with accordance to the cryptographic assumptions. In case all adversary actions in π turn out to be feasible, we can report π to be a feasible vulnerability. If, however, there exists one adversary action in π which is not feasible, we refine the property φ_{abs} to rule out traces in which the adversary takes that action. The analysis is then run again with the refined property. For further confidence, we validate π by concretely executing it in a testbed.

Finally, we show the application of a technique we call *attack chaining* in which seemingly low-impact attacks are stitched together to yield a damaging high-impact

attack. We show its successful application by chaining together attacks, exposed using LTEInspector, to allow an adversary to carry out an authentication relay attack in the 4G LTE network.

Findings. Notable among our findings is the *authentication relay attack* which enables an adversary to connect to the core networks—without possessing any legitimate credentials—while impersonating a victim cellular device. Through this attack the adversary can poison the location of the victim device in the core networks, thus allowing setting up a false alibi or planting fake evidence during a criminal investigation.

Other notable attacks reported in this work enable an adversary to obtain user's coarse-grained location information and also mount denial of service (DoS) attacks. In particular, using LTEInspector, we obtained the intuition of an attack which enables an adversary to possibly hijack a cellular device's paging channel with which it can not only stop notifications (e.g., call, SMS) to reach the device but also can inject fabricated messages resulting in multiple implications including energy depletion and activity profiling.

Contributions. In summary, this work makes the following technical contributions:

(1) We propose LTEInspector—a systematic model-based adversarial testing approach—that leverages the combined power of a symbolic model checker and a protocol verifier for analyzing three critical procedures (i.e., attach, detach, and paging) of the 4G LTE network. The general principle employed by LTEInspector is to be tool-agnostic, that is, it can be instantiated through any generic symbolic model checker and cryptographic protocol verifier.

(2) We show the effectiveness of our approach in finding new vulnerabilities as well as 9 prior attacks. Our approach has contributed to exposing 10 new attacks.

(3) We show that the majority of our new attacks (i.e., 8 out of 10) are realizable in practice through experimentation in a low cost (i.e., $\$3,900$), real test-bed while adhering to ethical, legal, and moral practices.

3.1 Design Overview of LTEInspector

In this section, we first present our threat model, and then describe the major components of LTEInspector's architecture (see Figure 3.1). Finally, we explain LTEInspector's adversarial-testing approach with a concrete example.

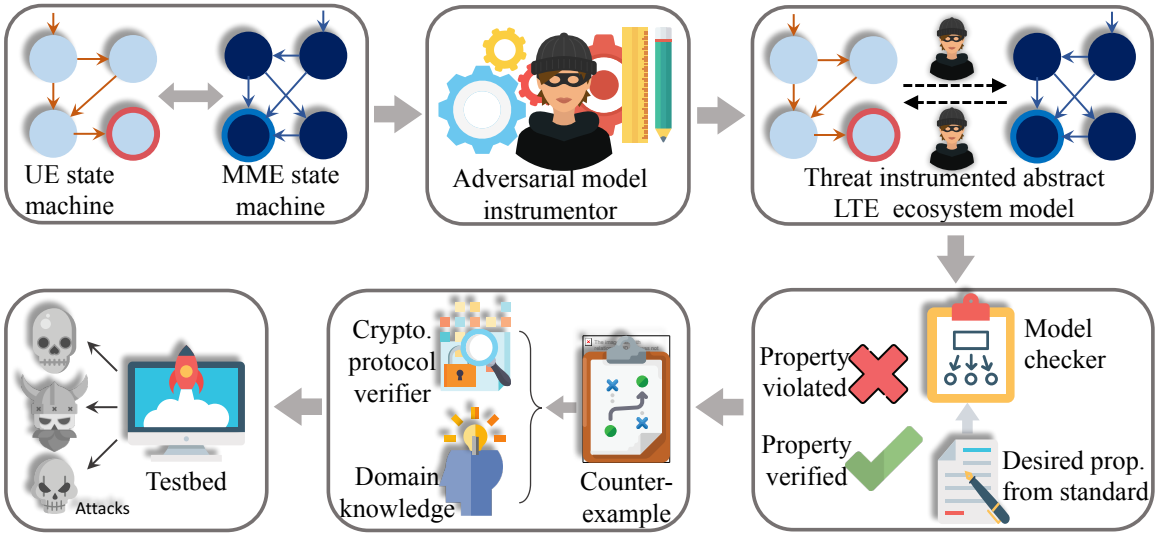

Figure 3.1.: Architecture of LTEInspector

Adversary model. For our analysis, we consider a Dolev-Yao-style network adversary Adv^{+c} [35] with the following capabilities: **(A-1)** It can *drop* or *modify* any messages in the public communication channel. **(A-2)** It can impersonate a legitimate protocol participant and can *inject* messages in the public communication channel on the victim's behalf. **(A-3)** It adheres to all cryptographic assumptions. For instance, Adv^{+c} can decrypt an encrypted message *only if* it possesses the decryption key. Cryptographic constructs are considered to be perfectly secure in this model.

Our choice of Adv^{+c} is motivated by the following three aspects: (1) Adv^{+c} is very powerful and any protocol that is secure against it, is *likely* to be secure in weaker threat models; (2) Automatic tools can analyze protocols in this model (e.g., ProVerif [40], Tamarin [41]); (3) It is often possible to realize (a majority of the)

$\mathsf{Adv}^{+\mathsf{c}}$ capabilities in our context. We do not adopt the computational model [46, 47] as proving properties in this model often requires manual intervention.

3.1.1 High-Level Approach

LTEInspector in an on-demand basis combines the reasoning power of a general purpose model checker (**MC**) and a cryptographic protocol verifier (**CPV**). We first construct a protocol model in the propositional logic level and use a **MC** [38, 39] to check for violations of the abstracted input property. Along with the propositional level abstraction, we also abstract away cryptographic constructs from the model and the input property. During checking compliance of the model with respect to the property with a **MC**, as part of abstracting the cryptographic constructs, we carry out our analysis with respect to an adversary $\mathsf{Adv}^{-\mathsf{c}}$ which is the cryptography-agnostic version of the $\mathsf{Adv}^{+\mathsf{c}}$. Any counterexample generated by the **MC** hence may not be feasible due to such an abstraction. To rule out such infeasible counterexamples, we check the feasibility of the counterexample with a cryptographic protocol verifier (**CPV**) [40, 41] which although operates on the first-order logic level can only verify certain types of queries. In the case **CPV** cannot find an attack, we refine the input property to rule out such spurious counterexamples.

One natural question readers may have is that why do not we use a **CPV** [40, 41] to begin with. This is because the level of abstraction and the scope with which we model the protocol enables us to efficiently reason about rich *temporal trace properties* (e.g., safety and liveness [37]). **CPV**s, even though can support unbounded parallel sessions, cryptographically sophisticated adversaries, and rich constructs, for the sake of tractability often limit their analyses to specific syntactic forms of safety properties (e.g., *correspondence* [48], *secrecy* [49]) which may not be sufficient for capturing all the desired properties we have observed. In the same vein, for tractability reasons, **CPV**s do not allow us to model the rich constructs (e.g., constraints on linear integer arithmetic) on which a **MC** can reason very efficiently, for instance, authen-

tication desynchronization vulnerability described in our running example. Finally, even infeasible counterexamples may give us insights about other possible attacks.

3.1.2 LTEInspector Components

We now describe the major components of LTEInspector.

Abstract LTE model. We model the LTE protocol from the point of view of two participants: a UE and an MME. Although there are other protocol participants (e.g., eNodeBs, HSS), for ease of modeling, we combine their functionality inside the MME as their identity distinction does not impact the analysis of the attach, detach, and paging procedures. Also, we only consider the NAS layer messages between the two entities[1].

We abstractly model only the portion of the 4G LTE protocol that is relevant to the analysis of attach, detach, and paging procedures—without fine-grained implementation details—as two synchronous communicating finite state machines (FSM) (denoted by $\mathcal{M}_{\text{vanilla}}$). The two FSMs in $\mathcal{M}_{\text{vanilla}}$ (one for the UE and another for the MME) communicate with each other by sending messages through public communication channel. We model the communication channel between the two FSMs $\mathcal{M}_{\text{UE}}$ and $\mathcal{M}_{\text{MME}}$ with two uni-directional channels; one from $\mathcal{M}_{\text{UE}}$ to $\mathcal{M}_{\text{MME}}$ and another from $\mathcal{M}_{\text{MME}}$ to $\mathcal{M}_{\text{UE}}$. The choice of two unidirectional channels instead of a single bidirectional channel is not only for modeling convenience but also for effortlessly modeling weaker adversaries than $\mathsf{Adv}^{+\mathsf{c}}$ during adversary model instrumentation (e.g., only one direction of the public channel to be adversary controlled).

To keep the analysis tractable, in $\mathcal{M}_{\text{vanilla}}$, we do not model message data with arbitrarily large domains. For instance, the attach_request message can possibly contain IMSI as a data; in our model, we do not capture the IMSI and just model attach_request as a possible message type. We, however, model message data-dependent

[1]Although paging messages are Radio Resource Control (RRC) protocol layer messages [4, 7], as we model the core network and the base-station as a single entity, without loss of generality, we simplify the modeling by considering paging messages as NAS layer messages in our abstract model.

conditions as environment-controlled (or, in short, *environmental*) Boolean variables. For instance, for each message that can have integrity protection, we capture its integrity verification with a *unique* Boolean variable mac_failure whose value is nondeterministically set by the environment during model checking. $\mathcal{M}_{\text{vanilla}}$ can capture an unbounded number of sequential sessions. It, however, can neither capture an unbounded number of parallel sessions nor an unbounded number of protocol participants; the latter is shown to be undecidable [50].

Adversarial model instrumentor. The adversarial model instrumentor takes $\mathcal{M}_{\text{vanilla}}$ and instruments it to incorporate the presence of an adversary to obtain a new model $\mathcal{M}_{\text{adv}}$. We model a cryptography-agnostic adversary $\mathsf{Adv}^{-\mathsf{c}}$ which possesses the same capabilities of $\mathsf{Adv}^{+\mathsf{c}}$ except for its cryptographic proficiency (i.e., **A-3**). We model the $\mathsf{Adv}^{-\mathsf{c}}$ capabilities for each unidirectional public channel **ch** in the following manner. Capability **A-1** is modeled as **ch**'s property, that is, **ch** *nondeterministically* drops any message **msg** passing through it (represented as a no_operation) or replaces it with another plausible message including the current message **msg**.

Modeling capability **A-2** for **ch** requires considering an adversarial FSM which nondeterministically injects one of the possible messages including no_operation. We call such adversary FSMs the *injection adversaries*. In the case both the legitimate protocol participant and the adversary simultaneously push messages $\mathbf{msg}_{\mathsf{v}}$ and $\mathbf{msg}_{\mathsf{adv}}$, respectively, into **ch**, the message received on the other side is decided by the value of an environmental Boolean variable adv_turn; the value of adv_turn is nondeterministically chosen by the environment. Precisely, the other side of **ch** will receive $\mathbf{msg}_{\mathsf{adv}}$ only if the value of adv_turn is set to be true by the environment. *The nondeterministic behavior of the channels and the injection adversaries are crucial for reasoning about all possible adversary strategies.* Our instrumentation makes it effortless to customize the capabilities of the adversary, for instance, independently making each **ch** to have adversarial interference.

General-purpose Model Checker (MC). **MC** takes as input $\mathcal{M}_{\text{adv}}$ and a desired abstract property φ, and checks to see whether all possible executions of $\mathcal{M}_{\text{adv}}$ (considering all possible values of the environmental variables) satisfy φ. In the case **MC** finds an execution π of $\mathcal{M}_{\text{adv}}$ which violates φ, **MC** outputs π as an evidence of the violation (also, known as the *counterexample*). π includes the adversary actions which were used to violate φ, and alternatively, can be viewed as the attack strategy. The $\mathsf{Adv}^{-\mathsf{c}}$ used when model checking $\mathcal{M}_{\text{adv}}$ does not have the necessary cryptographic proficiency of $\mathsf{Adv}^{+\mathsf{c}}$ (i.e., **A-3**), and hence π can violate cryptographic assumptions, making it unrealizable in practice. We rule out such spurious πs through the following process.

Validating counterexamples with CPV. For a given counterexample π, we check each sub-step of π that requires manipulating some crytographically-protected message type. We model each small sub-step in a **CPV**, denoted as $\mathsf{M}_{\mathsf{crypto}}$. We then pose a query to **CPV** that will be violated in $\mathsf{M}_{\mathsf{crypto}}$ only if the $\mathsf{Adv}^{+\mathsf{c}}$ has the specific capability that π requires. For few message types, such as, paging, we know from the 3GPP standard that there are no confidentiality and integrity protections; for those message types we do not invoke the **CPV**.

Testbed experimentation. Once both **MC** and **CPV** adjudicate a given π to be feasible, we try to realize this attack in a testbed. This is essential because π may not be realizable in practice due to possible technical safeguards. Any π validated in the testbed experiment can thus be considered a vulnerability. We built a testbed using low-cost software defined radios and open-source LTE software stack having a price tag of around $\$3,900$ which we would argue is within the reach of a motivated adversary.

3.1.3 Example Demonstrating LTEInspector's Effectiveness

We now show the effectiveness of LTEInspector's vulnerability detection through a concrete example. For ease of exposition, we rely on a simplified and partial model of the LTE ecosystem shown in Figure 3.2 for this example.

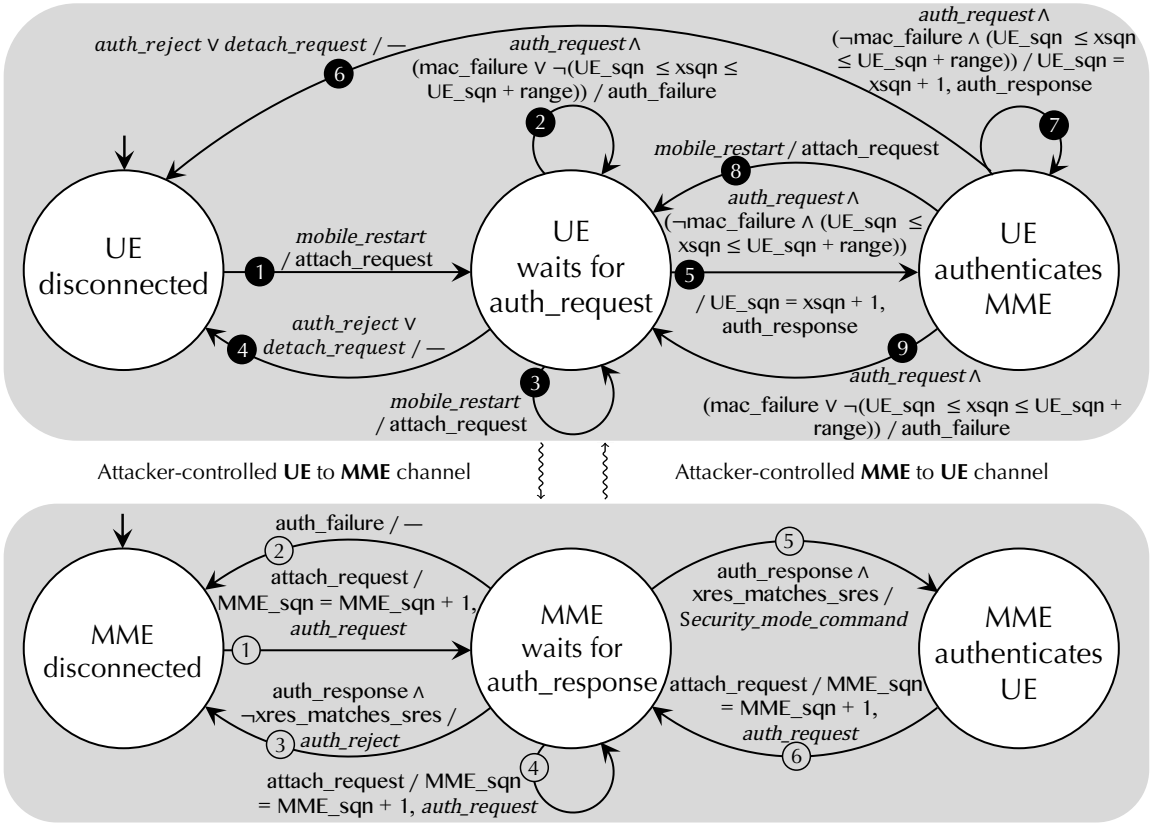

Figure 3.2.: A simplified LTE ecosystem model.

In the example, the UE FSM (the top FSM) has 3 states and 9 transitions whereas the MME FSM (the bottom FSM) has 3 states and 6 transitions. Transition labels are of the form "condition/actions" in which condition is a propositional logic formula specifying the condition under which the transition will be triggered whereas the actions component refers to a sequence of actions that will be performed (in their appearance order) by the FSM after the transition is taken. Although the actions component can be empty (denoted with –), the condition component cannot be empty. We represent

Table 3.1.: CPV Properties used in the motivating example.

ID	MC property details
φ_1	It is always the case that whenever the UE FSM is in the wait for auth_request state, it will eventually move to the state where the UE authenticates the MME.
φ_2	Refinement over φ_1: Once UE FSM moves to the wait for &auth_request state, the environment will never set the value of mobile_restart to be true.
φ_3	Refinement over φ_2: mac_failure is never set to true by the environment.
φ_4	Refinement over φ_3: UE FSM never receives the detach_req message.
φ_5	Refinement over φ_4: UE FSM never receives the auth_reject message.

Table 3.2.: **MC** properties used in the motivating example.

ID	CPV property details
Ψ_1	Every attach_request message received by the MME should be preceded by a unique attach_request message sent by the UE.

the states with barebone arrows (i.e., arrows with no condition and action) as the initial states of the FSMs. We use ❶, ❷,. . . to denote the UE transitions whereas we use ①, ②,. . . , to denote the MME transitions. The FSMs have the following environmental variables: mobile_restart (signifying UE rebooting); mac_failure (improper MAC for auth_request message); xres_matches_sres (correct authentication_response message for a given authentication_request message). Both the FSMs start with their respective sequence numbers to be 0.

The response property we want to verify is the following: "*It is always the case that whenever the UE FSM is in the* wait for auth_request *state, it will eventually move*

to the state where the UE authenticates the MME" (denoted by φ_1). The property is desirable as its violation signifies a denial-of-service attack in which the UE cannot proceed to the next stage of the attach procedure after initiating it.

When φ_1 is checked against the given $\mathcal{M}_{\text{adv}}$, it gives the trivial counterexample π in which after the UE FSM moves to the wait for auth_request state, it continuously observes the value of the environmental variable mobile_restart to be true (triggering transition ❸)—signifying the repeated restart of the UE—which even though plausible, is not interesting as the $\mathsf{Adv}^{+\mathsf{c}}$ has no control over UE reboot. One possible way of removing this π is to refine φ_1 to add the restriction that once UE FSM moves to the wait for auth_request state, the environment will never set the value of mobile_restart to be true. When this refined property (denoted by φ_2—see Table 3.2) is checked, the **MC** yields a π in which all the auth_request messages received by the UE fails the MAC verification (triggering transition ❷) because the **MC** assigns the value of the mac_failure to be continuously true. We then refine φ_2 further to ensure that mac_failure is never set to true by the **MC** and obtain the property φ_3.

Attack 1: Checking $\mathcal{M}_{\text{adv}}$ against φ_3 using **MC** yields another π in which after UE FSM moves to the wait for auth_request state, it receives a network initiated detach request (detach_req)–injected by the adversary—triggering transition ❹ which moves it to the disconnected state and due to avoiding reboot after transitioning to wait for auth_request state (in φ_2), stops the UE FSM to get out of the disconnected state. This is a legitimate attack and we would like to know whether it is possible for the attacker to forge a network initiated detach_request. A close inspection of the standard reveals that once the security context has been established between the UE and the MME, the network initiated detach_request should be integrity protected only. Our experiment with the UE, however, revealed that the UE does not actually check the validity of the MAC for detach_req even in the case the security context has been established. This means such an attack is plausible and we have verified it in our testbed. We then refine φ_3 further to exclude this π and ensure that the UE FSM

never receives the network initiated detach request; as a result, we obtain the refined property φ_4.

Attack 2: We then check $\mathcal{M}_{\text{adv}}$ against φ_4, and it yields another similar π in which the UE FSM receives an auth_reject message (triggering transition ❹); this moves the FSM to the disconnected state. Again, one needs to determine whether the adversary can fabricate an auth_reject message. A close inspection of the standard revealed that the auth_reject message is never integrity protected and our experimentation validated it. In a similar way, we refine φ_4 to exclude any auth_reject message and obtain our final property φ_5.

Attack 3: Finally, checking $\mathcal{M}_{\text{adv}}$ against φ_5 with **MC** results in a very interesting π in which the adversary sends the **range** (a UE-specific constant non-negative integer) number of fake attach_request messages to the MME, before the UE reboots and sends the attach request. After receiving each attach_request message, the MME increases its own sequence number (according to transitions ① and ④) and uses the value of the sequence number to provide replay protection to the auth_request message which it sends to the UE. As the UE is still in the disconnected state (with its sequence number 0, i.e., $UE\_sqn = 0$) and there is no transition that is triggered by the auth_request when the UE is in the disconnected state (see Figure 3.2), these auth_request messages are ignored. Then the UE observes a mobile_restart (triggering transition ❶) and sends an attach request to the MME which the adversary allows to reach the MME. After the MME receives it (transitions ①, ④, and ⑥), the MME as usual responds with an auth_request with the sequence number $\mathbf{range} + 1$. The adversary also allows the auth_request from the MME to reach the UE. Upon receiving the message, the UE checks for mac_failure (which cannot be true as we excluded it while refining φ_2 to obtain φ_3) and checks whether the received sequence number from MME (denoted with $xsqn$) satisfies the following: $UE\_sqn \leq xsqn \leq UE\_sqn + \mathbf{range}$; this condition will fail as $xsqn = \mathbf{range} + 1$ resulting in the UE not being able to attach with the MME. To ensure that validity of the π, one has to verify whether the $\mathsf{Adv}^{-\mathsf{c}}$ can inject a fake attach_request message; we use the **CPV** to validate it. We pose

an injective-correspondence [48] query, Ψ_1 (shown in Table 3.2) which asserts that every attach_request message received by the MME should be preceded by a unique attach_request message sent by the UE. The **CPV** produced an attack in which the adversary injected an attach_request; validating the desired sub-step of π. We have also observed the feasibility of this attack in our testbed. We call this attack **the authentication synchronization failure attack**; this attack is also applicable against a recent proposal for defeating IMSI catchers [20]. One of the challenges of detecting such an attack through **CPV**s is to precisely capture the sanity check corresponding to the sequence number. It is not immediately clear to us how one would directly capture such a requirement in the **CPV** in a fine-grained fashion. The **MC**, however, can efficiently reason about such requirement precisely. *This shows the effectiveness of combining a* **MC** *with a* **CPV** *for attack discovery.*

This example demonstrates the analysis power of LTEInspector's approach, that is, based on the violation of a single desired property (and, its refinements) LTEInspector was able to find three different attacks which have been shown to be realizable in practice. As we will demonstrate later, Attacks 1 or 2 can be stitched with a relay attack to yield the authentication relay attack.

3.1.4 Implementation

We now discuss some additional details of LTEInspector.

MC and CPV: We instantiate LTEInspector's **MC** component with NuSMV [38] and use ProVerif [40] for **CPV**.

Model. We manually construct the abstract LTE model by consulting the 3GPP standard [4, 7]. Our model has a total of 13 states and 107 transitions. Our current model and the respective properties are publicly available at `https://github.com/relentless-warrior/LTEInspector`.

Properties. Our properties were extracted from the 3GPP standard [4, 7]. We have tested $\mathcal{M}_{\text{adv}}$ against 14 properties in total in which 7 properties were analyzed with

NuSMV whereas 7 properties were analyzed with ProVerif. Note that, we do not claim our list of properties to be exhaustive.

3.2 LTEInspector Findings

In this section, we highlight the findings of LTEInspector. For readers' convenience, we have provided a summary of the attacks and their implications in Table 3.3.

3.2.1 Attacks Against Attach Procedure

We now present our findings on the attach procedure.

A-1 Authentication Synchronization Failure Attack

This attack exploits the UE's sequence number sanity check to disrupt its attach procedure. Precisely, the adversary interacts with the HSS through the MME to ensure that the sequence numbers of the UE and the HSS are out-of-sync. As a result, the authentication challenge received through the legitimate auth_request message fails the UE's sanity check and consequently is discarded by the UE.

Adversary assumptions. For successfully carrying out this attack, the adversary is required to set up a malicious UE and also is required to the know the victim UE's IMSI. Such a threat is very practical and has been validated through experimentation in our testbed (see Section 3.3.1).

Detection. We exposed this attack by first model checking $\mathcal{M}_{\text{adv}}$ with respect to a refinement φ_5 of the following property: "*It is always the case that whenever the UE FSM is in the wait for* auth_request *state, it will eventually move to the state where the UE authenticates the MME*" (see Table 3.2 for details). We observed a violation of φ_5 in $\mathcal{M}_{\text{adv}}$ where the $\mathsf{Adv}^{-\mathsf{c}}$ fabricates attach_request messages and sends them to the MME. To validate the $\mathsf{Adv}^{-\mathsf{c}}$'s capability of forging an attach_request message,

we leverage ProVerif which showed that forging attach_request messages are possible; validating the feasibility of the attack.

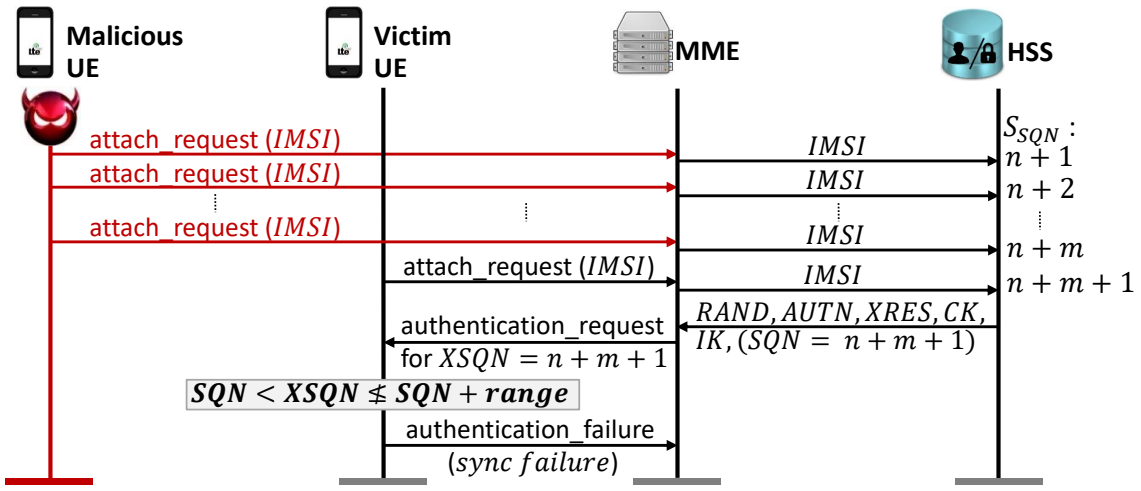

Figure 3.3.: Authentication synchronization failure attack.

Attack description: The steps of this attack are shown in Figure 3.3. It is very similar to the description of Attack 3 in Section 3.1.3 with one caveat. It is just not sufficient to send the same attach_request message m times (where $m >$ **range**). The malicious UE needs to send different security capabilities (by selecting different encryption and integrity protection algorithms) in successive attach_request messages. This is crucial as the HSS only processes an attach_request message only if one or more of the information elements in the current attach_request message differs from the already received one. In which case, in accordance to subclause 5.5.1.2 of 3GPP standard [27], the previously initiated attach procedure is aborted and the new attach_request message is processed (including, the increment of the sequence number).

Re-synchronization: When the sequence number sanity check fails on the UE side, it sends an auth_failure message (cause: sync. failure) to the EPC with $AUTS$ parameter containing the UE's current sequence number resulting in the EPC to re-synchronize its sequence number. Even after re-synchronization, the adversary can

continue repeating step 1 to make the UE and the HSS sequence numbers to go out-of-sync again; preventing the UE from connecting to the EPC.

Implication: The major implication of this attack is the service disruption suffered by the victim UE.

A-2 Traceability Attack

This attack exploits the responses of security_mode_command messages to track a particular victim UE. Typically during the attach procedure, the MME uses the security_mode_command message to choose one of the UE-supported cipher suites to use for communication. When the UE receives this message, it is expected to respond with a security_mode_complete message when the received message satisfies the MAC validation. In case of MAC failure, the UE responds with a security_mode_reject message. The MME can also send a security_mode_command message to an already attached UE for changing the current cipher suite. This message is recommended to be integrity- and replay-protected [27].

Adversary assumptions. We assume that the adversary has already obtained an authentic security_mode_command message sent to the victim UE in the previous attach procedure. We also assume that the adversary can set up a malicious eNodeB.

Detection. We model check the $\mathcal{M}_{\text{adv}}$ against the following property: *the UE responds with a* security_mode_complete *message only if the MME sent a* security_mode_command *message which passes the sanity checks.* This is trivially violated by a counterexample in which the adversary injects a security_mode_command message. As the security_mode_command message is cryptographically protected this seems to be a spurious counterexample. Coincidentally, we observed that none of the four major US carriers make the security_mode_command message replay-protected (they do not include the recommended fresh nonce). Then, we used ProVerif's capability of reasoning about observational equivalence to pose the query: *is it possible for the adversary*

to distinguish two UEs based on their responses to a security_mode_command *message? ProVerif provided an attack strategy for distinguishing two UEs.*

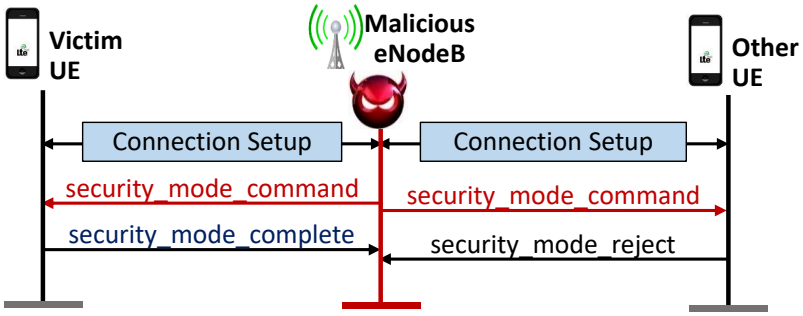

Figure 3.4.: Traceability attack using security_mode_command.

Attack description: The UEs in a particular eNodeB cell get connected with the malicious eNodeB. The malicious eNodeB then replays the captured security_mode_command message to all the UEs as shown in Figure 3.4. The victim UE verifies the integrity and the UE's security capabilities of the received message, and responds with the security_mode_complete message to the malicious eNodeB whereas the rest of the UEs in that cell respond with security_mode_reject messages due to integrity check failure. The malicious eNodeB thus identifies the presence of a particular UE in an area.
Implications: This attack can enable an adversary to track a particular victim UE.

A-3 Numb Attack

In this attack, the adversary injects an out-of-sequence control-plane protocol message to severely disrupt the service of a victim UE.
Adversary assumption. For successfully carrying out this attack, the adversary is required to set up a malicious eNodeB.
Detection. We observed this attack after model checking $\mathcal{M}_{\text{adv}}$ with respect to a refinement φ_3 of the property φ_1 in Table 3.2. The counterexample produced by the model checker shows that whenever the UE receives an auth_reject message injected by the Adv^{-c}, the UE FSM moves to the disconnected state. To realize this attack

the Adv^{-c} has to be able to inject auth_reject message which is feasible as the message is not cryptographically protected according to the standard.

Attack description: As soon as the victim UE connects with the malicious eNodeB, the malicious eNodeB sends an auth_reject message to the victim UE irrespective of the context of the victim UE.

Implications: Along with the most straightforward implication of severe service disruption, this finding may be chained with another attack (possibly, some form of impersonation attack) which requires the UE to be inactive or re-initiate the attach procedure. We have observed that upon reception of the auth_reject message in one of the popular cellular device, the UE first detaches itself from the network, completely shuts down all cellular activities, and does not even attempt to downgrade/connect to 3G/2G networks. In this situation, even re-insertion of SIM card does not allow the victim UE to connect to the EPC again. The victim UE remains in such a numb state until the user restarts her UE.

3.2.2 Attacks Against Paging Procedure

In this section, we present attacks that we have exposed against the paging procedure.

Adversary assumptions. For the following attacks on the paging procedure, the adversary needs to setup a malicious eNodeB and also needs to know the victim UE's IMSI. For the linkability attack, we assume the adversary knows the previous **pseudo-IMSIs** (or, in short, PMSIs[2]) [20].

Detection. We obtain the intuition for the *paging channel hijacking* attack (**P-1**) after observing our model $\mathcal{M}_{\text{adv}}$'s violation of the following property: *the UE sends a service request only if the MME has sent a* paging *message that is pending.*

[2]To protect against IMSI catching attacks, Broek et al. [20] proposed an enhancement over the 3GPP standard where the IMSI is replaced with a changing pseudonym, called Pseudo-IMSI or PMSI, that only the SIMs HSS can link to the SIMs identity. Therefore, instead of sending the IMSI, the UE uses different PMSIs in different attach_request messages. To the best of our knowledge, support for PMSIs have not been implemented in 4G LTE.

The model checker produces a counterexample in which the Adv^{-c} injects a paging message. After consulting the standard [27], we observed that paging messages do not have any cryptographic protection. This signifies that an adversary can inject paging messages. *The rest of the attacks in this section are direct consequences of the paging channel hijacking attack.*

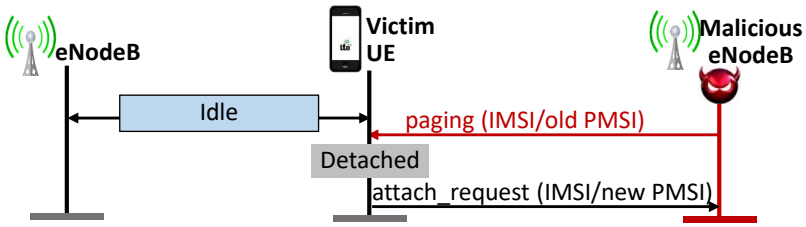

Figure 3.5.: Detach attack using paging.

P-1 Paging Channel Hijacking

For hijacking the paging channel, the malicious eNodeB operates in the same frequency band as the legitimate eNodeBs so that the victim UE does not perceive any network changes. The malicious eNodeB then broadcasts fake **empty** paging messages in the shared paging channel. However, a UE does not listen to the paging channel continuously for incoming paging messages. It usually remains in the *sleep* state and wakes up in its paging cycle for pending paging message. Therefore, it is crucial for the adversary to make its eNodeB's paging cycle same as the victim UE's. Detailed synchronization procedure is presented in Section 3.3.

Although both malicious and legitimate eNodeBs broadcast the paging messages at the same time intervals, the UE only responds to the first received message. To address this challenge, the malicious eNodeB broadcasts paging messages with higher signal power. Thereby, the adversary hijacks the victim UE's paging channel and makes the victim UE unable to receive legitimate paging messages from the MME. This means that the victim does not receive any service (e.g., incoming phone call-

s/SMS) notifications which would result in customer dissatisfaction, revenue loss and reputation damage of the network operators. *One of the interesting consequences of this attack is that the victim UE is completely unaware of paging channel hijacking which lets the adversary silently drop incoming services.*

P-2 Stealthy kicking-off Attack

The steps of this attack are shown in Figure 3.5 and described as follows:

After hijacking the victim UE's paging channel, the malicious eNodeB creates a paging message with one paging record consisting of the victim UE's IMSI. The adversary sets other fields of the paging record similar to an original paging message. Upon reception of the paging message with IMSI, the victim UE finds its IMSI in the first paging record. As a result, it first disconnects from the EPC and then sends an attach_request message. *This attack can also be used as a prerequisite of the authentication relay attack.* The major implication of this attack is service disruption.

P-3 Panic Attack

In this attack, the adversary wants to inject fake emergency paging messages to a large number of UEs. The adversary thus sends a paging message with empty records but with fake emergency warnings. To ensure that such a fake paging message reaches a large number of UEs, the adversary keeps broadcasting this message for all possible paging occasions of the legitimate eNodeB. *This can create artificial emergency which can be exploited by malicious parties for hiding their agenda.*

P-4 Energy Depletion Attack

The idea of this attack is to make the victim UE perform expensive cryptographic operations. One way to achieve this is to force the UE to keep carrying out the expensive attach procedure over and over again, by sending a paging message with

Table 3.3.: Summary of our findings (●=validated, ◓=partially validated, ○=not validated) of the reported attacks.

ID	Attack name	Affected procedure	Adversary assumptions	Assumption validation	Standard/ Stakeholder slip-up	New attack?	Detection process	Notable implications	Validated	Setup cost
A-1	Auth. sync. failure	Attach	Known IMSI, malicious UE	IMSI [17], Section 3.3.1	3GPP	Yes	LTEInspector	Denial-of-attach or Denial-of-services.	●	$2600 (2 USRPs)
A-2	Traceability	Attach	Valid security_mode command, malicious eNodeB	Section 3.3.1	Operational networks, mobile devices	Inspired by [14]	LTEInspector	Coarse-grained location information leakage.	●	$2600 (2 USRPs)
A-3	Numb using auth_reject	Attach	Malicious eNodeB	Section 3.3.1	3GPP	Yes	LTEInspector	Denial of all cellular services.	●	$1300 (1 USRP)
A-4	Auth. relay	Attach	Known IMSI, malicious eNodeB	IMSI [17]; Section 3.3.1	3GPP, operational networks	Yes	LTEInspector, attack chaining	Reading incoming/outgoing messages of victim, stealthy denial of all/selective services, location history poisoning.	●	$3900 (3 USRPs)
P-1	Paging channel hijacking	Paging	Known IMSI, malicious eNodeB	IMSI [17], Section 3.3.1	3GPP	Yes	Intuition from LTEInspector, domain Knowledge	Stealthy denial of incoming services.	●	$1300 (1 USRP)
P-2	Stealthy kicking-off	Paging	Known IMSI, malicious eNodeB	IMSI [17], Section 3.3.1	3GPP	Yes	Consequence of **P-1**, domain knowledge	Detaching a victim from the network surreptitiously.	●	$1300 (1 USRP)
P-3	Panic	Paging	Malicious eNodeB	Section 3.3.1	3GPP	Yes	Consequence of **P-1**, domain knowledge	Life threatening impact against mass people, e.g., artificial chaos for terrorist activity.	○	$1300 (1 USRP)
P-4	Energy depletion	Paging	Known IMSI, GUTI, malicious eNodeB	IMSI [17]; GUTI [12], Section 3.3.1	3GPP	Inspired by [51, 52]	Consequence of **P-1**, domain knowledge	Battery depletion.	◓	$1300 (1 USRP)
P-5	Linkability	Paging	Known IMSI or old pseudo-IMSI	Section 3.3.1	3GPP, enhanced AKA [20]	Yes	ProVerif only	Coarse-grained location information leakage	○	$1300 (1 USRP)
D-1	Detach/ Downgrade	Detach	Malicious eNodeB, known IMSI (for targeted version)	IMSI [17]; Section 3.3.1	3GPP	Inspired by [17]	LTEInspector, attack chaining (for targeted version)	Denial of services/- Downgrade to 2G/3G.	●	$1300 (1 USRP)

IMSI between two successive attach procedures. In case the adversary knows the GUTI of the victim [12], it can send a paging message with GUTI which the UE responds with a cryptographically-involved service_request message.

P-5 Linkability Attack

This attack (see Figure 3.5) focuses on breaking the unlinkability guarantees (i.e., attacker cannot link any two successive pseudo-IMSIs/PMSIs) provided by Broek et al. [20]. From the assumption that the adversary knows the old PMSI which it uses to issue a paging message which the victim responds with an attach_request with the new PMSI enabling us to link the two PMSIs. *Note that, the above attack is not applicable to 4G LTE because the mechanism of Broek et al. [20] is not adopted for 4G LTE.* In case of 4G LTE, however, the adversary may use the same philosophy for tracing a victim UE in a cell area. After broadcasting a paging with the victim UE's IMSI, if the adversary observes an attach_request with the same IMSI, the adversary can confirm the victim UE's presence.

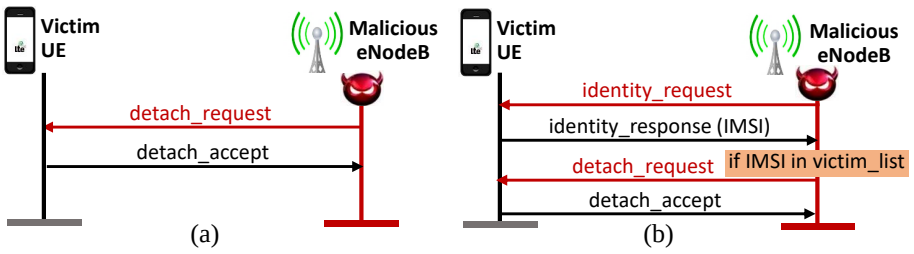

Figure 3.6.: (a) Indiscriminately- (b) targeted- detach/downgrade a UE using the network initiated detach_request message.

3.2.3 Attacks Against Detach Procedure

We now describe an attack on the detach procedure that LTEInspector has exposed.

D-1 Detach/Downgrade Attack

In this attack, the adversary injects the network initiated detach_request to disrupt the service of a victim UE irrespective of the UE context.

Adversary assumptions. The adversary needs to setup a malicious eNodeB and also needs to know the IMSI of the victim.

Detection. Attack detection is similar to the numb attack.

Attack description. The steps of this attack are shown in Figure 3.6(a). Whenever the victim UE connects to the malicious eNodeB, it sends a network initiated detach_request message which force the UE to move to the disconnected state and to send detach_accept message.

Targeted variant of detach/downgrade attack. This attack (see Figure 3.6(b)) can be adopted to a more targeted setting in which the adversary targets specific UEs. For the targeted variation, before the detach_request is sent, the eNodeB will send an identity_request message which the UE will respond with an identity_response message containing the UE's IMSI. If the IMSI is in the attacker's victim list, it will send the detach_request, otherwise, it will ignore that UE.

Implications: Along with its direct consequence of severe service disruption, this finding can be stitched with another attack (possibly, some form of impersonation attack) which requires the UE to be inactive and re-initiate the attach process.

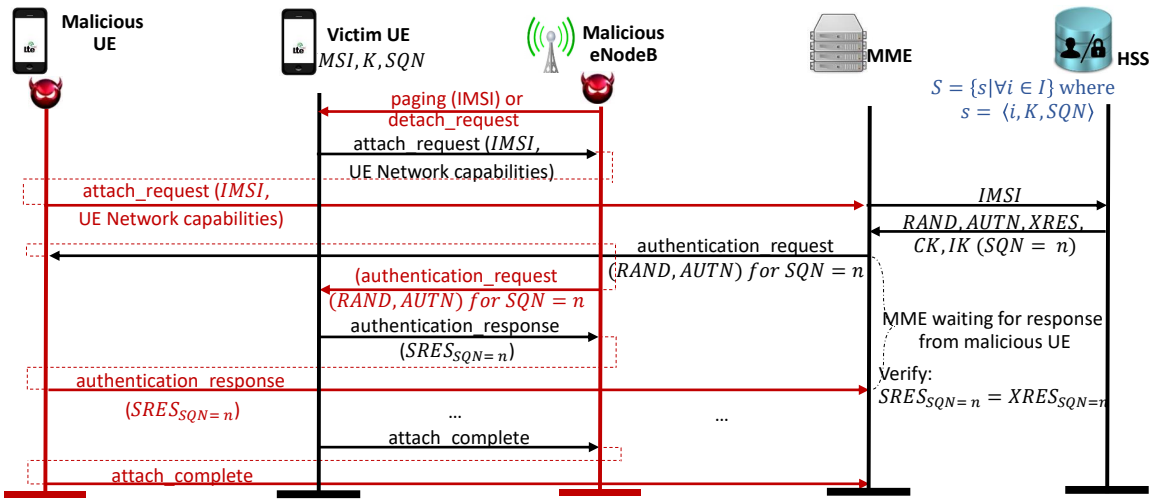

Figure 3.7.: Authentication relay attack

3.2.4 Attack Chaining

We now demonstrate the application of the attack chaining technique through the authentication relay attack.

A-4 Authentication Relay Attack

In this attack, one of our exposed attacks (e.g., paging with IMSI) is stitched with a relay attack with which an adversary impersonates the victim UE to connect to the EPC without possessing proper credentials, and in the process, spoof the victim UE's location in the core networks.

Adversary assumptions. For this attack, the adversary is required to setup a malicious eNodeB ($\mathsf{eNodeB}_{\mathsf{adv}}$) and a malicious UE ($\mathsf{UE}_{\mathsf{adv}}$), and also needs to know the IMSI of the victim UE. We assume there is a private channel between the $\mathsf{eNodeB}_{\mathsf{adv}}$ and the $\mathsf{UE}_{\mathsf{adv}}$.

Attack description. In this attack, the adversary impersonates an already attached victim UE ($\mathsf{UE}_{\mathsf{vic}}$) to connect to the EPC by collaborating with the $\mathsf{eNodeB}_{\mathsf{adv}}$ and the $\mathsf{UE}_{\mathsf{adv}}$. Suppose the $\mathsf{UE}_{\mathsf{vic}}$ is already attached with the legitimate eNodeB denoted by $\mathsf{eNodeB}_{\mathsf{benign}}$. The attack can be broken down into two main goals: (i) Force $\mathsf{UE}_{\mathsf{vic}}$ to disconnect from the EPC; (ii) $\mathsf{UE}_{\mathsf{adv}}$ pretends to be $\mathsf{UE}_{\mathsf{vic}}$ to connect to the EPC.

Disconnecting $\mathsf{UE}_{\mathsf{vic}}$ *from the EPC*: For disconnecting the $\mathsf{UE}_{\mathsf{vic}}$ from the EPC, we use our paging with IMSI attack. This can also be achieved with our network initiated detach_request or auth_reject attacks.

$\mathsf{UE}_{\mathsf{adv}}$ *connecting to the EPC by impersonating as* $\mathsf{UE}_{\mathsf{vic}}$: As the $\mathsf{UE}_{\mathsf{vic}}$ detached itself from the EPC due to a paging with IMSI message, it will try attach to the eNodeB with the highest signal strength; which is the $\mathsf{eNodeB}_{\mathsf{adv}}$. The $\mathsf{UE}_{\mathsf{vic}}$ will send an attach_request message m_{req} to the $\mathsf{eNodeB}_{\mathsf{adv}}$ which the $\mathsf{eNodeB}_{\mathsf{adv}}$ forwards to the $\mathsf{UE}_{\mathsf{adv}}$. The $\mathsf{UE}_{\mathsf{adv}}$ then sends the same attach request m_{req} to the $\mathsf{eNodeB}_{\mathsf{benign}}$. The legitimate MME will send an authentication challenge c to the $\mathsf{UE}_{\mathsf{adv}}$ through the $\mathsf{eNodeB}_{\mathsf{benign}}$ upon receipt of m_{req}. The $\mathsf{UE}_{\mathsf{adv}}$ will forward the c to the $\mathsf{eNodeB}_{\mathsf{adv}}$

which the $\mathsf{eNodeB}_{\mathsf{adv}}$ will send to the $\mathsf{UE}_{\mathsf{vic}}$. After the $\mathsf{UE}_{\mathsf{vic}}$ receives c, unaware that the $\mathsf{eNodeB}_{\mathsf{adv}}$ sent it, it will solve the challenge c to generate the correct response r. The $\mathsf{UE}_{\mathsf{vic}}$ will then send r to the $\mathsf{eNodeB}_{\mathsf{adv}}$ which it will forward to the $\mathsf{UE}_{\mathsf{adv}}$. The $\mathsf{UE}_{\mathsf{adv}}$ then will use r to respond to the MME challenge. Using the same principle, the $\mathsf{UE}_{\mathsf{adv}}$ will finish the rest of the steps of the attach procedure.

Discussion. Unlike a typical man-in-the-middle attack, the adversary in this attack can neither decrypt the encrypted traffic between the victim UE and the core networks, nor can inject valid encrypted traffic unless the service provider blatantly disregards the standard's security recommendations and choose a weak-/no- security context during connection establishment.

Implications: The implications of this attack include:

(1) Deception: The adversary deceives the victim into believing that the $\mathsf{UE}_{\mathsf{vic}}$ is connected to the core network.

(2) Location History Poisoning: Since the $\mathsf{UE}_{\mathsf{adv}}$ does not need to be in the same tracking area as the $\mathsf{UE}_{\mathsf{vic}}$, it can authenticate itself to the EPC from a different tracking area and thus provide misleading location information about the $\mathsf{UE}_{\mathsf{vic}}$. Thus, the $\mathsf{UE}_{\mathsf{adv}}$ can poison the location history of the $\mathsf{UE}_{\mathsf{vic}}$ by performing this attack successively from different tracking areas. As a result, a fugitive or criminal hiding in one location can deceive the core network into believing that the criminal has attached to the core network from a different location.

(3) Loss of confidentiality: The security_mode_command message sent by the MME during the attach procedure includes the selected cipher (EEA0-EEA7) and integrity protection (EIA0-EIA7) algorithms of the MME. By observing the security_mode_command messages of all four major network providers in the US, **we have observed that at least one carrier (OP-I) never used encryption (i.e., uses EEA0—no cipher)**. Note that, to keep the four major US network operators anonymous, we use pseudonyms (i.e., OP-I, OP-II, OP-III, OP-IV) to identify them. We have observed this insecure practice multiple times in two different geographical locations.

The adversary hence can learn the $\mathsf{UE}_{\mathsf{vic}}$'s conversation, SMSs, and data through the $\mathsf{UE}_{\mathsf{adv}}$ and the $\mathsf{eNodeB}_{\mathsf{adv}}$. We reported this to the affected carrier which has now been addressed.

(4) Complete or Selective DoS: Using this attack, the $\mathsf{UE}_{\mathsf{adv}}$ and the $\mathsf{eNodeB}_{\mathsf{adv}}$ can relay the incoming/outgoing traffic of the $\mathsf{UE}_{\mathsf{vic}}$ and the EPC. Therefore, the $\mathsf{UE}_{\mathsf{adv}}$ and the $\mathsf{eNodeB}_{\mathsf{adv}}$ can deny the $\mathsf{UE}_{\mathsf{vic}}$'s phone-calls/SMS/data-transfers completely/selectively. Consequently, the operational network is deprived of the charges for the incoming/outgoing calls and SMSs.

(5) Profiling victim's service usage: Since all the incoming/outgoing communications of the $\mathsf{UE}_{\mathsf{vic}}$ take place through the $\mathsf{UE}_{\mathsf{adv}}$ and the $\mathsf{eNodeB}_{\mathsf{adv}}$, the adversary can profile the service usage pattern (i.e., patterns of phone calls, SMSs, data) of the victim.

3.2.5 Prior Attacks Detected by LTEInspector

In addition to the new attacks, LTEInspector is capable of detecting 9 [13–15, 17, 20,53] out of 13 prior attacks (see Table 3.4) that are relevant in the context of attach, detach, and paging procedures. The previous attacks [12, 16, 17] that LTEInspector cannot detect exploit one of the following which LTEInspector currently does not support: (1) message data, (2) multiple instances of UEs or MMEs, (3) other layers' (e.g., RRC layer) messages, (4) 2G/3G procedures that are different from 4G LTE, (5) properties about sets of traces, and (6) performance related parameters (e.g., data transmission and reception rate).

3.3 Validation of Attacks with Testbed

In this section, we describe the verification of the new attacks (along with their adversarial assumptions) detected by LTEInspector. We have tried to exercise restraint—conforming to best practices—in validating the effectiveness of the different vulnera-

Table 3.4.: Prior attacks (related to attach, detach, and paging procedures) that are detected/not detected by LTEInspector.

#	Prior attack	Detected	How/Why?
1	Downgrade using tau_reject [17]	Yes	LTEInspector.
2	Denial of all services [17]	Yes	LTEInspector.
3	Denial of selected services [17]	No	Do not model data for attach_request.
4	Location tracking through mapping user's phone number/social network ID to GUTI [12, 17].	No	Do not model multiple instance of UEs.
5	IMSI catching [20]	Yes	LTEInspector.
6	Fine-grained location exposure [17]	No	Do not model RRC layer messages.
7	DoS exploiting race condition with paging_response [53] in 2G	Yes	LTEInspector.
8	Service hijacking exploiting race condition with paging_response [53] in 2G	Yes	LTEInspector.
9	Linkability using TMSI_reallocation_command [15] in 3G	Yes	LTEInspector.
10	Linkability of IMSI to GUTI using paging_request [14] in 3G	Yes	LTEInspector.
11	Linkability using auth_sync_failure [14] in 3G	Yes	LTEInspector.
12	Man-in-the-Middle in 2G [13]	Yes	LTEInspector.
13	Man-in-the-Middle in 3G [16]	No	Do not model data.

bilities while maintaining the validation process meaningful. To limit the impact of our attacks, we use both a custom-built LTE network and commercial networks with a logical Faraday cage [17].

3.3.1 Testbed Setup and Assumption Validation

We now describe our testbed setup for attack validation.

Malicious eNodeB Setup

We have used a Universal Software-defined Radio Peripheral device (i.e., USRP B210 [54]) connected to an Intel Core i7 machine running Ubuntu 14.04 as the hardware component and OpenLTE [55], an open source LTE protocol stack implementation, to set up a malicious eNodeB which costs around $1300 for the dedicated hardware (i.e., excluding the core i7 machine). We used OpenLTE's `LTE_Fdd_enodeb` application which simultaneously acts as a bare-minimal eNodeB, a mobility management entity (MME), and a home subscriber server (HSS). We have implemented support for the *detach* procedure in OpenLTE as it originally had support for the *attach* procedure only. We have also instrumented OpenLTE to inject different fabricated messages (e.g., network initiated detach_request message) when necessary. For validating attacks against the paging procedure, we use srsLTE [56] which we enhanced to support eNodeB-initiated paging messages; its original support only included MME-initiated paging messages.

eNodeB configuration. Our malicious eNodeB can impersonate the legitimate eNodeB of a network operator (i.e., OP-I to OP-IV) by broadcasting system_info_block_type_1 messages with higher signal power. For successful impersonation, these messages must include parameter values that are equal to that of an operator's legitimate eNodeB. The adversary uses a UE with the operator's SIM to learn the parameters in the system_info_block_type_1 messages sent by the operator's eNodeB. In our setup, we use both our custom-built sniffer and QXDM [57] to sniff the incoming and outgoing LTE messages on a consumer UE to learn the operator's parameters. Table 3.5 shows the parameters that we capture from the operator eNodeB's system_info_block_type_1 messages. We use them to configure the malicious eNodeB with OpenLTE.

Learning IMSI/IMEI. As soon as the victim UE is forced to connect with the malicious eNodeB, the malicious eNodeB sends an identity_request (IMSI/IMEI) message to the victim UE which responds with the identity_response message including its IMSI/IMEI.

Table 3.5.: Configuration parameters captured from Operator's system_info_block_type_1 messages.

Parameters	Description
band	The frequency band number of the network operator.
dl_earfcn	E-UTRA absolute radio frequency channel number.
mcc	Mobile country code specific to a country.
mnc	Mobile network code specific to a network operator.
p0_nominal_pucch	Power control parameter.
p0_nominal_pusch	Power control parameter.
q_rx_lev_min	Used for cell re-selection.
q_hyst	Used for cell re-selection
DRX cycle	Paging cycle

Learning GUTI. We use the well-known set intersection technique to find the GUTI as described in [12].

Malicious UE Setup

We use a USRP B210 [54] running srsUE [58] (open source protocol stack implementation for UE) as the malicious UE which costs around $1300.

Victim UEs and EPC Networks

We have used 3 different models of LTE-capable mobile phones and the 4 major network operators in the US. For the authentication relay and authentication synchronization failure attacks, the adversary requires a malicious UE to send messages to a commercial EPC. Since this is a violation of the Federal Communications Commission's (FCC) regulations [8], we use our custom-built network (as the EPC) and a USIM (Universal Software Identity Module) instead of commercial EPCs and

their SIMs, respectively. Our custom-built network similar to [59], operates on an experimental licensed spectrum.

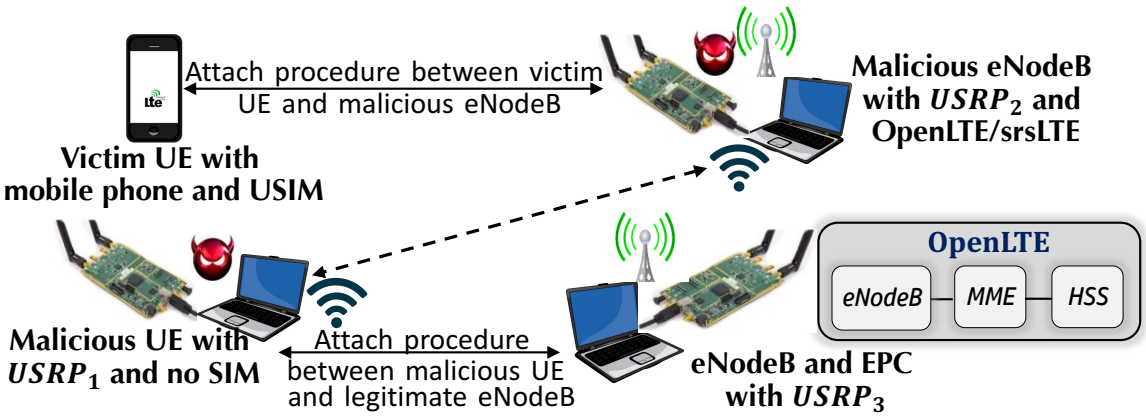

Figure 3.8.: Experiment setup for custom-built network.

Sniffer setup

We have built a low-cost, real-time LTE channel decoder (costs around $1300) using USRP [54] as the hardware whereas we used Owl [60] and srsLTE [56] as the software components. Our sniffer identifies the new c-RNTI (a lower-layer UE identifier) of a UE that joins the cell, and then decodes the unencrypted downlink messages from the MME/eNodeB.

Attack setup cost. Since different attacks (e.g., **A-4** and **P-1**) require different attack setups, we list only the dedicated hardware cost for individual attack in Table 3.3. which shows $3900 as the maximum cost required to validate the attacks.

3.3.2 Validation using Custom-built Network

We now discuss how we successfully verified the authentication synchronization failure and authentication relay attacks in our custom-built network (See Figure 3.8).

A-1 Authentication Synchronization Failure Attack

In our verification setup, the malicious UE (using the victim UE's IMSI) sent 100 attach_request messages (with different security configurations) to the legitimate MME. After the attack step, we reboot the victim UE which initiated the attach procedure by sending an attach_request message for which it received an authentication_request message from the MME. In response to that message, using our sniffer we observed that the victim UE responded with an auth_failure message (with cause sync. failure); confirming our attack.

A-4 Authentication Relay Attack

For this attack, we built a relay channel (See Figure 3.8) between the malicious UE (USRP_1) and the malicious eNodeB (USRP_2) using the Wi-Fi interfaces of the machines co-located with those USRPs. We also configured both the malicious eNodeB and the legitimate eNodeB to broadcast different tracking areas in their system_info_block_type_1 messages. After performing the attack steps, we observed that both the victim and malicious UE received the same attach_accept message and also completed the attach procedure. From the logs of the legitimate EPC and using the tracking area numbers, we confirmed that only the malicious UE was connected with the legitimate MME. On the other hand, although the victim UE was actually connected with the malicious EPC, it was deceived to realize that it was connected with the legitimate EPC. Thus, the legitimate EPC was duped about the actual location of the legitimate UE; confirming the attack.

We have also successfully verified the authentication synchronization failure and relay attacks with OpenEPC [61], which is a licensed prototype implementation of the 3GPP Evolved Packet Core (EPC).

3.3.3 Validation using Commercial Mobile Phones

For all the other attacks (except **A-1** and **A-4**), we use commercial network operators' (e.g., OP-I) SIMs for the victim UE and a malicious eNodeB as discussed in Section 3.3.1).

A-2 **Traceability Attack**

For this attack verification, we use multiple UEs among which one of them is designated as the victim UE; the one being tracked. First, using the sniffer, we capture a legitimate security_mode_command message sent by the MME to the victim UE during a benign interaction. We decoded the captured security_mode_command message and extracted all its field values including the MAC. For tracing, the malicious eNodeB then injected fabricated security_mode_command messages to all the UEs using the extracted field values. We observed that in response to the injected messages only the victim UE responded with the security_mode_complete message whereas the rest of UEs responded with a security_mode_reject message; confirming our attack. Note that, the malicious eNodeB may not always have success with this attack when it does not receive security_mode_complete messages from any of the UEs. This can be attributed to either the victim UE's absence in that cell area or the victim UE's use of a different a cipher suite.

This attack can also be performed for a specific user with only the knowledge of victim's phone number. The adversary first determines the victim UEs GUTI and her paging occasion using [12], and then hijacks her paging channel using **P-1**. Now the adversary initiates phone calls to victim's phone number which trigger the MME to send paging messages to the victim's UE. However, the victim UE's unresponsiveness due to **P-1** causes the MME to send paging with IMSI (subclause 5.5.3.2.7 [7]) which the adversary may intercept. In case the attacker receives multiple such paging with IMSI, he would use the set intersection technique [12] to uniquely identify the victim UE's IMSI. The adversary then performs the traceability attack as follows—(i) forces

the victim UE to complete an attach procedure with the legitimate EPC; (ii) captures a valid security_mode_command message; (iii) and finally replays that message to all nearby UEs.

A-3 Numb Attack and D-1 Detach/Downgrade Attack

For verifying both these attacks, we made the malicious eNodeB inject auth_reject and network initiated detach_request (with different causes) messages in different stages of the protocol, and observed the UE responses to these messages. For auth_reject messages, we observed a complete unresponsiveness of the victim UE until the SIM is re-inserted and the mobile phone is rebooted. Our observation of victim UE's responses in reaction to the detach_request messages (with different causes) are summarized in Table 3.6.

Table 3.6.: Victim UE's responses to different types of detach.

Detach Type	**Our observation of victim UE's response**
Re-attach required	No cellular signals (shows "No Service"). Requires mobile restart or SIM re-insert to get the 4G LTE back again.
Re-attach not required	Detaches from 4G LTE. Immediately downgrades to 3G/2G and sends attach_request to the 3G/2G network.
IMSI detach	Does not detach from the 4G LTE network.

P-1 Paging Channel Hijacking Attack

Successfully carrying out this attack first requires determining the victim UE's paging cycle/occasions. To this end, we captured and decoded the system_info_block_type_1 and attach_request messages—sent in plaintext by the carrier's eNodeB and the victim UE, respectively, and learned the parameters relevant for computing the victim UE's paging occasion (e.g., DRX_cycle, IMSI). The malicious eNodeB then injected

fake paging messages (with no paging records) at the paging occasions of the victim UE. We observed that the victim UE only received the fake paging messages instead of the legitimate messages.

After hijacking the victim UE's paging channel, we allowed two senders to place phone calls and send SMSs to victim's phone number triggering the (benign) MME to send multiple paging messages to the victim UE. We observed that the victim did not receive any of the legitimate paging messages, i.e., the service notifications. The victim's unresponsiveness was also noticed on the sender-side.

P-2 Stealthy Kicking-off Attack

For this attack, instead of injecting empty paging messages, the malicious eNodeB fabricated the paging messages with a paging record containing the victim UE's IMSI. As soon as the victim UE received this message, we observed that it locally detached itself from the network and sent an attach_request, confirming the attack.

P-3 Panic Attack

To inject fake paging messages to arbitrary neighboring UEs, the malicious eNodeB broadcasted paging messages at all possible paging occasions. Each of these paging messages had the ETWS (earthquake and tsunami warning system) bits set to provide the UEs an alert notification. Upon receiving such alert notification, a UE looks for the actual warning message which the eNodeB broadcasts through the system_information_block type 10 or 11 or 12 messages. Since such warning messages may be received by other mobile phones which are not subject to our experiment, we refrained the malicious eNodeB from sending the actual warning messages.

P-4 Energy Depletion Attack

We quantitatively measure the UE's energy depletion due to this attack. In particular, we leverage the strong correlation between energy consumption with message transmission rate [62]. We essentially measured the message transmission rate in the benign and attack case, and drew conclusions about energy consumption. To realize this attack, we configured the malicious eNodeB to broadcast paging message with the victim's GUTI at every third paging occasion (i.e., $\sim$ 3 seconds) of the victim UE. Upon reception of this paging message, we observed that the victim UE sent an encrypted and integrity protected service_request message to the malicious eNodeB. We also carried out this attack where the paging message included the victim's IMSI in which case, however, the victim initiated the attach procedure. For the paging with GUTI, we carried out the attack for an hour and observed that the victim sent 1200 service_request messages. In the benign case (measured from 4G LTE traces [63]), however, on average the UE responds to 156 (std. dev. 14.27) paging messages . Roughly, the energy depletion due to this attack $\sim$ 8 times to that of the benign condition. The attacker can make it worse, in case it chooses to inject the paging with GUTI in every paging occasion.

3.4 Discussion

Properties amenable to our analysis. LTEInspector can reason about temporal trace properties (with cryptographic constructs) of both safety and liveness variations. Our current model cannot handle properties that require reasoning about sets of traces (e.g., noninterference) instead of a single trace. For such properties, we mainly rely on the protocol verifier.

Defenses. We deliberately do not discuss defenses for the observed attacks as retrospectively adding security into an existing protocol without breaking backward compatibility often yields band-aid-like-solutions which do not hold up under extreme scrutiny. It is also not clear, especially, for the authentication relay attack whether

a defense exists that does not require major infrastructural or protocol overhaul. A possibility is to employ a distance-bounding protocol; realization of such protocol is, however, rare in practice [64]. This motivates us to further investigate the feasibility of symmetric-key based or public-key cryptography-based solutions (see Chapter 5) to prevent this attack.

Limitations. Although LTEInspector suggests a systematic approach, it currently requires human intervention, for instance, deciding which sub-steps of the counterexample is required to be modeled in ProVerif and how. Also, our FSM extraction is currently manual and the extracted FSMs are not complete. In the same vein, the list of properties we have checked is not exhaustive. Our current model also does not capture all the data embedded in the messages.

Threat to Validity. Our manually extracted FSMs from the 3GPP standard may not reflect the behavior of real operational networks. Inaccuracies in the FSMs may induce false positives, although, we have not observed any. Due to ethical considerations, we limit our experiments to a custom-built network for some attack validations which may not faithfully capture the operational network behavior.

3.5 Summary

In this chapter, we propose LTEInspector which employs an adversarial model-based testing philosophy for exposing attacks against three critical procedures of 4G LTE. LTEInspector harnesses the strengths of both a symbolic model checkers and a protocol verifier and is demonstrated to be effective in finding 10 novel and 9 prior attacks. We have also validated most of our attacks (i.e., 8 out of 10) in a testbed. Our proposed framework is general enough that it can be easily extended for analyzing the security and privacy of 5G networks as well.

Based on the findings by LTEInspector, we further focus into analyzing the quantitative and side-channel properties of a specific a procedure, i.e., paging for both 4G

and 5G networks (see Chapter 4) and devise a probabilistic reasoning technique to identify side-channel attacks.

4. PRIVACY ATTACKS TO THE 4G AND 5G CELLULAR PAGING PROTOCOLS USING SIDE CHANNEL INFORMATION

In cellular networks, when a device is not actively communicating with a base station, it enters an idle, low-energy mode to conserve battery power. When there is a phone call or an SMS message for the device, it needs to be notified. This is achieved by the paging protocol, which strives to achieve the right balance between the device's energy consumption and quality-of-service (e.g., timely delivery of services such as phone calls). When there is pending service(s) for a device, the network's Mobile Management Entity (MME) asks base station(s) to broadcast a paging message, which includes the Temporary Mobile Subscriber Identity (TMSI) of the device. TMSI is randomly assigned by the MME for the device, and it is recommended that the TMSI for a device should be changed frequently.

Kune et al. [12] showed that a user's presence in a geographical area can be identified by a sniffing attack that exploits the fact that in practice the TMSI is changed infrequently. An attacker can place multiple phone calls to the victim device in a short period of time and sniffs the paging messages. If the most frequent **TMSI** among the paging messages appears frequently enough, then the attacker concludes that the victim device is present. Shaik et al. [17] found that paging messages can be triggered with SMS as well as notifications from instant messengers; consequently, the same attack in [12] can be mounted by these means. These attacks exploit the deployment weakness that the TMSI is infrequently changed. Kim et al. [34] showed that some deployments choose the new TMSI predictably even when it is changed. Furthermore, such attacks can be made stealthy in the sense that the attacker can make phone calls and send SMS messages that trigger paging messages without alerting the user of the victim device.

The natural defense to these attacks is to change TMSI frequently and use random, unpredictable values for new TMSI. This renders existing attacks ineffective. However, in this work, we show that *even if TMSI is changed each time a device connects to the network* (so that the next paging message will use a different and unrelated TMSI), it is possible to carry out a similar attack to verify whether a victim user is present in a geographical cell.

We propose the ToRPEDO attack, which is able to verify whether a victim device is present in a geographical cell with less than 10 calls, even under the assumption that TMSI changes after each call. Furthermore, in the process, the attacker learns exactly when a device wakes up to check for paging messages and 7 bits of information of the device's International Mobile Subscriber Identity (IMSI). This knowledge enables two other new attacks that lead to full recovery of the device's IMSI.

When TMSI is changed each time, it appears that one can no longer link a call made by the attacker and the resulting paging message. The key insight under our novel attack is that the paging protocol requires synchronization between the base station and the device. The LTE paging protocol uses a paging cycle of T frames, each of which is 10ms long. The default value of T is 128. Each device has a Paging Frame Index (PFI), which is determined by its IMSI, and the device wakes up only once during a paging cycle, at the frame indexed by its PFI. The base station broadcast the paging message for the device at these frames. When multiple calls for a device are made, their corresponding paging messages will occur in frames indexed by the same Paging Frame Index (PFI). When the base rate of paging messages is low, that is, paging messages only appear in a small fraction of all frames, the attacker can identify which PFI is "too busy", and is thus the victim device's PFI.

PIERCER **attack for 4G.** Our investigation of paging protocol deployments revealed that in some exceptional cases, contrary to conventional wisdom and 3GPP recommendations, some service providers use IMSIs instead of TMSIs in paging messages to identify devices with pending services. A simple manual testing revealed that it is possible to give the service provider the impression that the exceptional case is

occurring which forces it to reveal the victim's IMSI. We exploited this weakness to design the PIERCER (Persistent Information ExposuRe by the CorE netwoRk) attack which enables an attacker with knowledge of the victim's phone number, a sniffer, and a fake base station in the victim's cell to associate the victim device's IMSI with its phone number while using ToRPEDO as an attack sub-step. The dangers of PIERCER are well known. Precisely, PIERCER can enhance prior attacks, which require knowledge of victim's IMSI, to a level where just knowing the victim's phone number is sufficient [13, 16–18, 65].

IMSI-Cracking **attack for 4G/5G.** We also observed that ToRPEDO enables an attacker with the knowledge of the victim's phone number to retrieve the victim's IMSI by launching a brute-force attack. For US subscribers, IMSIs can be represented as 49-bit binary numbers. IMSI's leading 18-bits (i.e., the mobile country code and the mobile network code) can be obtained from phone number using paid, Internet-based home location register lookup services [66]. Identifying victim's paging occasion with ToRPEDO additionally leaks the trailing 7 IMSI bits for US subscribers leaving 24 bits for the attacker to guess. Using a brute-force attack and two oracles (one for 4G and another for 5G) we designed, the attacker can guess the victim's IMSI in less than 13 hours.

Attack validation. We have verified ToRPEDO against 3 Canadian service providers and all the US service providers. PIERCER, on the other hand, has been verified against one major US service provider and 3 major service providers of a South Asian country. We have also noticed the presence of IMSIs in paging messages delivered by two Chinese, and one Russian service providers and speculate that PIERCER may be feasible for those service providers.

Contributions. This work makes the following contributions:

- We present the ToRPEDO attack that exploits a 4G/5G paging protocol weakness to enable an attacker that knows a victim's phone number to identify the victim's presence in a particular cellular area and in the process identify the

victim's paging occasion. It not only elevates prior attacks but also facilitate other newer attacks.

- We also present the `PIERCER` attack that exploits a 4G paging protocol deployment vulnerability to allow an attacker to associate a victim's phone number with its IMSI. Apart from its immediate implication on victim's location tracking, `PIERCER` can also lift prior attacks that require knowledge of the victim's IMSI to only require knowledge of the victim's phone number.
- We also show that `ToRPEDO` can enable an attacker to mount a brute-force `IMSI-Cracking` attack leaking a victim's IMSI for both 4G and 5G.
- All of our attacks for 4G have been validated against real networks.

4.1 ToRPEDO Attack

4.1.1 Problem setting

For our purpose, UEs are partitioned into T groups, as given by their Paging Frame Indexes (PFI). A UE's PFI depends on its IMSI. For ease of exposition, time is divided into cycles of length $10T$ ms. Such a cycle consists of T frames, each of length 10ms. We number the frames within one cycle from 0 to $T - 1$. The default value for T is 128, which is used in most networks.

When a MME receives a service for a UE, it asks base station(s) to broadcast a paging record at the next frame that has the same number as the UE's PFI. We assume that the paging record uses the TMSI (and not the IMSI) to identify the UE. Furthermore, the phone's TMSI is updated to a new one (randomly chosen by the MME) each time the phone has responded to a call. That is, the carriers have already deployed defenses suggested by earlier work. We show that attacks are nonetheless possible.

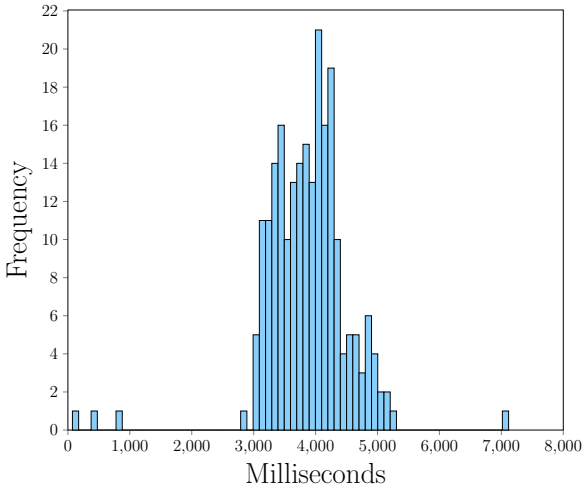

(a) Histogram of paging delay for SMS.

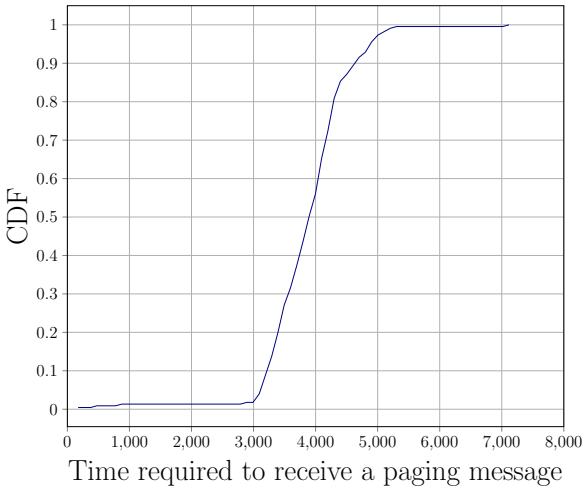

(b) Cumulative Distribution Function of paging delay for SMS.

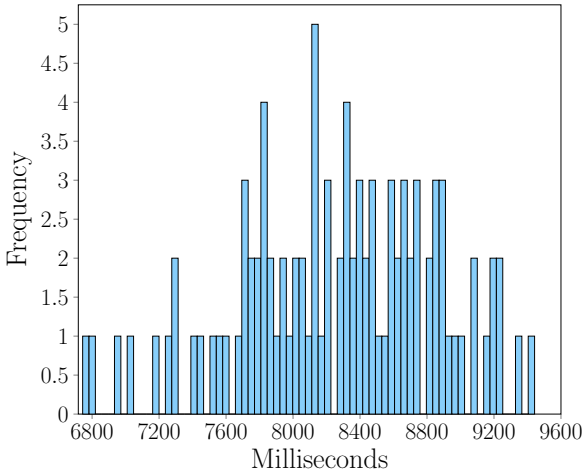

(c) Histogram of paging delay for VoLTE phone calls.

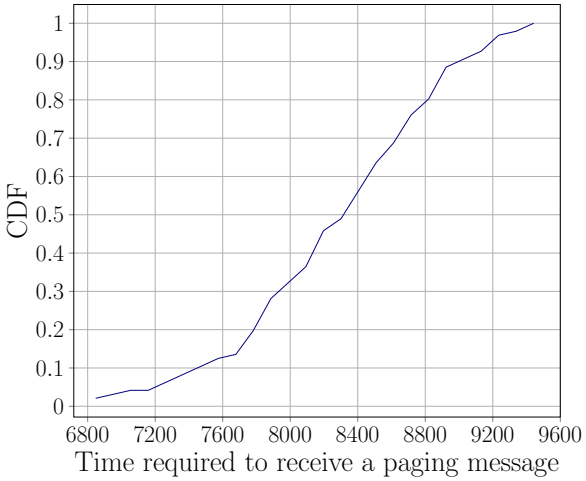

(d) Cumulative Distribution Function of paging delay for VoLTE phone calls.

Figure 4.1.: Distribution of paging delay i.e., the time between the event of initiating a phone call or SMS and the event of reaching a paging message to the receiver for that phone call/SMS.

4.1.2 Adversary Model

We assume that the adversary knows the soft identity of the target UE u_t, such as the phone number, e-mail address, or social network handler of u_t. The adversary

also knows the geographical area that u_t is likely to be in (called the target area), and sets up a sniffer (built with a Universal Software-defined Radio Peripheral (USRP)) in that area to listen on the paging broadcast channel. That is, the adversary can make a good guess about the geographical location of u_t, although the guess does not need to be correct. Through the attack, the adversary is able to find out whether the guess is correct or not. Also note that the adversary can carry out this attack simultaneously in multiple geographical areas at once against a target u_t, provided that the adversary is willing to spend the resources for doing so.

The goal of the adversary is to (i) *confirm whether or not u_t is indeed in the target area*, and (ii) *when u_t is in the area, identify the UE's* PFI *(which we use PFI_t to denote), which also yields information about the phone's IMSI.*

The adversary can make a call to u_t to trigger a paging message for u_t, and listens to the paging broadcast channel. While we use the term "*make a call*" to describe the adversary's action, the action could take the form of VoLTE or CSFB calls, SMS's, tweets, and so on.

The adversary can repeat this process of making a call and listening for paging messages multiple times. We note that these calls do not need to be made continuously. The adversary can wait between calls. The only restriction is that if the total duration of the attack is too long, then the UE may have moved out of the target area during that time.

To assess the effectiveness of such location tracking attacks, we consider the following criteria: (1) identification accuracy: when u_t is present in the area, the rate with which the attack outputs the correct PFI, (2) presence accuracy: when u_t is not present in the area, the rate with which the attack correctly concludes that u_t is not present, and (3) the number of calls required for the attacking algorithm to reach a decision.

4.1.3 High-level Intuition of the Attack

The intuition behind the attack is as follows. Let us assume, for the moment, that there is no other paging message in the system. When the adversary makes a call to u_t, there are two cases. Case one: If u_t is in the area, a paging message will be sent, and the adversary will also see the paging message at a particular PFI. Case two: u_t is not in the area, then there will be no paging message, and the adversary will not see any paging message. By making a single call to u_t and checking whether there is a corresponding paging message, the adversary can infer whether u_t is in the target area or not, and, if u_t is, what is its PFI.

The challenge of the attack is that the assumption that there is no other paging message in the system is unrealistic. When there are other paging messages, it is difficult for an adversary to associate a call she made with a particular paging record. Recall that we assume that the TMSI (instead of the IMSI) is used in a paging record, and the TMSI changes each time a UE connects to the base station. The only information to associate a call with its corresponding paging record is timing. The paging record should be sent soon after the adversary makes a call. We call the interval between the time the adversary makes a call and the time the paging record is sent the *paging delay*. Unfortunately for the adversary, the paging delay is affected by many factors, and is randomized from the adversary's perspective. Furthermore, there are paging records for other UEs in the area, as well as other services for u_t that are not from the adversary. What the adversary needs to do is to test whether paging records due to adversary-initiated calls are present for each PFI in the noise of paging records generated by the background processes.

One way to establish an association between calls and the resulting paging records is obtain a probability distribution of paging delays, and then establish a *delivery window*. Let us call the time that the adversary makes a call 0, then the delivery window is given by two times t_b, t_e. Any paging record received after t_b and before t_e is considered to be in the delivery window. The choice of t_b, t_e needs to be carefully

made. A window that is too narrow will miss associated paging records. On the other hand, if a window that is too wide, one increases the probability that paging records resulted from the background sources as associated with the call.

The distributions of paging delays differ based on the type of services, e.g., phone calls, SMS, or tweets. They are also dependent on the cell area and the load. The adversary can get a distribution of paging delays for each type of service, either by using historical knowledge, or by estimating the distributions for a particular incoming service before actually carrying out attacks. In Section 4.1.6, we discuss how to obtain empirical distributions.

Figures 4.1 shows the empirical distributions of paging delays we observed in our experiments. Fig.4.1(a) and (b) show the histogram and cumulative distribution for paging delay of SMS. Fig.4.1(c) and (d) show the same for VoLTE calls. We made 500 calls for each. From the figure, one can observe that paging delays for SMS messages are between approximately 2.8 and 5.3 seconds, whereas the paging delays for VoLTE phone calls are between approximately 6.8 and 9.4 seconds.

4.1.4 Two Simple Attacks

Because of the background traffic of paging messages, the adversary is unable to use a single call to carry out the attack, and needs to make multiple calls. When the adversary makes multiple calls over time, she expects to see a paging message after each call, and all the paging messages are delivered in frames with the same number. Here the adversary relies on the observation that the base rate of paging messages in each frame is typically low. We first present two simple attacks.

Filtering

The Filtering attack assumes *perfect delivery of paging messages*, that is, it is assumed that each time the adversary makes a call, a paging message will be reliably received during the delivery window. Starting with the set of all possible PFI values,

the adversary repeats the following steps: (1) Make a call. (2) Listen for paging messages during the delivery window. (3) Remove from the set all PFI values that do not have a paging message during the window. (4) If only one PFI value remains in the set, then it concludes that this is u_t's PFI. If the set is empty, concludes that u_t is not in the target area.

For the Filtering attack to work reliably, paging messages need to be delivered/-captured almost perfectly, which is not always possible due to different forms of noises in the sniffer-captured data. One reason is that the sniffer is not totally reliable and may miss paging messages because of signal interference. Another reason is that the call may be dropped or delayed due to network congestion, causing the paging message to either be missing, or fall outside the delivery window. Yet another reason is that the device u_t may be in the connected mode, and a paging message is not needed.

Counting

When paging messages are delivered imperfectly, we rely on the fact that a call will result in a paging message in the delivery window with high probability. The algorithm uses a parameter ϕ, which models the probability that a paging message is received by the adversary within the paging window. We set $\phi = 0.85$ for our experiments. The adversary maintains a counter (initialized to 0) for each PFI value, and iterates through the following steps: (1) Make a call. (2) Listen for paging messages during the delivering window. (3) For each PFI value, if there is a paging message for that value during the delivering window, increment the corresponding counter by 1. (4) For each PFI value that is still in the set, let v be the counter value, and n be the number of rounds, remove the PFI value if

$$\mathsf{Pr}(v : n, \phi) = \binom{n}{v} \phi^v (1-\phi)^{n-v} < \theta = 0.1$$

(5) If only one PFI value remains in the set, then it concludes that this is u_t's PFI. If the set is empty, concludes that u_t is not in the target area.

4.1.5 The ToRPEDO Attack with Likelihood Analysis

The Counting attack does not use the information of how many paging records arrive in each frame (only whether there is at least one paging record), nor does it use the information about the timing of the message's arrival. From Figure 4.1, we can see that even though the delivery window for SMS goes roughly from 2.8 to 5.4 seconds, a paging message is much more likely to arrive at, e.g., 4 seconds, than at 5.3 seconds. We now present the ToRPEDO attack, which utilizes all information to conduct a likelihood analysis and decide the PFI of u_t.

Let the time at which the adversary makes a call be $t = 0$. ToRPEDO takes as input $F(\cdot)$, the cumulative distribution of paging delay. That is, if the paging message corresponding to the call is received at all, then with probability $F(t)$, it will be received by time t. Let t_m be the smallest t such that $F(t) = 1$. Then the adversary listens for c cycles after making a call, where c is computed as follows:

$$c = \left\lceil \frac{t_m}{10T \text{ ms}} \right\rceil,$$

For each $i \in [0..\mathrm{T}-1]$, during the whole observation period, there are c frames with SFN congruent to i modulo T. Let $v_{i,j}$ (where $0 \le i < T$ and $1 \le j \le c$) denote the number of paging records received at the j-th frame that has SFN congruent to i modulo T. The time for $v_{i,j}$ can be computed as:

$$\mathsf{time}(i,j) = \begin{cases} 0 & \text{when } j == 0 \\ ((j-1)T + i - b) \cdot 10\text{ms} & \text{when } j \ge 1, b \le i \\ (j \cdot T + i - b) \cdot 10\text{ms} & \text{when } j \ge 1, b > i \end{cases} \tag{4.1}$$

where

$$b = S_0 \bmod T, \text{ where } S_0 \text{ is the SFN when the call occurs}$$

denotes the frame index within the length-T cycle at the time the call is made.

For each i, we compute the likelihood of observing the sequence $V = v_{i,1}, v_{i,2}, \cdots, v_{i,c}$ when $\mathsf{PFI}_t \neq i$ and when $\mathsf{PFI}_t = i$. When $\mathsf{PFI}_t \neq i$, the sequence V is due to the background paging records. We use the Poisson Distribution to model the probability

that we observe a certain number of paging records in a given frame. The Poisson distribution expresses the probability of a given number of events occurring in a fixed interval of time if these events occur with a known constant rate and independently of the time since the last event. The Poisson distribution is parameterized by a base rate λ_b, which the adversary can estimate empirically.

We use ℓ'_i to denote the likelihood of observing $v_{i,1}, v_{i,2}, \cdots, v_{i,c}$ when $\mathsf{PFI}_t \neq i$. It can be computed as:

$$\ell'_i = \prod_{j=1}^{c} \mathsf{Pr}\big[P(\lambda_b) = v_{i,j}\big] \tag{4.2}$$

Here $P(\lambda_b)$ is a Random Variable following the Poisson distribution with parameter λ_b.

We use ℓ_i to denote the likelihood of observing the sequence V when $\mathsf{PFI}_t = i$. To compute ℓ_i, we need to consider two cases.

- First it may be that even though $\mathsf{PFI}_t = i$, the paging message is not observed. This happens with probability $1 - \phi$, where ϕ is the same parameter as used in the Counting attack. It is an estimation of the probability that a paging message is received within the delivery window.

- Second, the paging record may be delivered during any of the c cycles, and we have to sum up the likelihood of each case. The likelihood of the paging record being delivered during the j-th cycle is a product of 3 probabilities: (1) the probability that the delay for the paging message is such that the message arrives at the j-th cycle; (2) the probability that we observe $v_{i,j}$ records given that the paging record arrives in this cycle (i.e., the background contributes $v_{i,j} - 1$ paging records; (3) observations of $v_{i,k}$ where $k \neq j$ are from the background. Thus ℓ_i can be computed as follows:

$$\begin{aligned}\ell_i = (1-\phi)\prod_{j=1}^{c}\mathsf{Pr}\big[P(\lambda_b)=v_{i,j}\big] \\ +\phi\sum_{j=1}^{c}\ (F(\mathsf{time}(i,j))-F(\mathsf{time}(i,j-1))) \\ \times\mathsf{Pr}\big[P(\lambda_b)=v_{i,j}-1\big]\prod_{k=1,k\neq j}^{c}\mathsf{Pr}\big[P(\lambda_b)=v_{i,k}\big]\end{aligned} \tag{4.3}$$

where:

ϕ	is the same parameter as used in the counting attack
$P(\lambda_b)$	is a Random Variable following the Poisson distribution with parameter λ_b
F	is the CDF of paging delay given in Fig. 4.1
time	is defined in Eq.(4.1)

Computing the global likelihood of a PFI **to be the victim's PFI.** After making each call, the adversary computes the global likelihood, $\mathcal{L}_i$ for each $i =$ PFI, $0 \leq i < T$ to belong to the u_t. The adversary also computes the global likelihood, $\mathcal{L}_{-1}$ for the case that u_t is not present. The global likelihood $\mathcal{L}_i$ and $\mathcal{L}_{-1}$ after making n calls is computed as follows:

$$\begin{aligned}\mathcal{L}_i &= \prod_{n\text{ trials}}\ell_i\prod_{m=0,m\neq i}^{T-1}\ell'_m \\ \mathcal{L}_{-1} &= \prod_{n\text{ trials}}\prod_{m=0}^{T-1}l'_m\end{aligned} \tag{4.4}$$

After each new trial, if the maximum global likelihood ($\mathcal{L}_i$) for any i becomes significantly larger (i.e., by an order of a set threshold value τ) than the second largest global likelihood value, the adversary identifies i as the PFI of the u_t. If -1 is identified this way, it concludes that u_t is not in the area.

$$\frac{\mathcal{L}_i}{\max\mathcal{L}_j, \text{where j} \neq \text{i}} \geq 10^{\tau} \tag{4.5}$$

4.1.6 Discussions

Estimating empirical distributions of paging delays. We assume that the adversary $\mathcal{A}$ owns a UE, $u_1^{\mathcal{A}}$ that is a subscriber of the target network located at cell area c. Furthermore, the adversary knows $u_1^{\mathcal{A}}$'s IMSI and TMSI, which is feasible in many cases through cellular debugging tools such as MobileInsight [63]. $\mathcal{A}$ thus can compute the PFI value for $u_1^{\mathcal{A}}$. Using another adversary-controlled UE, $u_2^{\mathcal{A}}$, the adversary sends $\mathcal{N}$ phone calls, $\mathcal{N}$ SMS, or $\mathcal{N}$ tweets to $u_1^{\mathcal{A}}$ and observes the time (in milliseconds) required to receive paging messages at $u_1^{\mathcal{A}}$ for the corresponding phone calls, SMS and tweets. Using these observations, $\mathcal{A}$ can establish an empirical paging delay distribution for each service. Note that it is necessary to wait for the device to move to the idle mode before making the next call, otherwise paging messages will not be triggered. For our experiment, we choose the conservative value of ~ 40 seconds between two consecutive calls (or, SMS/tweets) to ensure this is the case.

Clandestine Location Tracking The adversary can carry out ToRPEDO, clandestinely, i.e., without alerting the human user using u_t. For example, a phone call can be made silent [17, 34] in 4G LTE by making a call and then terminating it in a few seconds. In this case, the base station will broadcast a paging message, but the phone will not ring because the call is hanged up before the call establishment procedure succeeds. Similarly, SMS and other messages can be made silent.

Dealing with smart and non-smart paging. Wireless providers generally use non-smart paging (all base stations in a tracking area broadcast paging messages) for VoLTE phone calls, and smart paging (only one base station broadcasts paging messages) for SMS services. The adversary can thus choose which one to use based on whether adversary is certain of the exact location of u_t.

Table 4.1.: Number of paging_imsi messages observed by a single UE for different network operators.

Carrier	**Total hours of observation**	**Total number of paging with IMSI**	**Percentage of paging with IMSI**
US-1	44 hours	171	0.274 %
CH-1	10 hours	8	3.404 %
CH-2	7 hours	1	0.028 %
US-MVNO-1	15 hours	78	0.324 %
US-MVNO-2	18 hours	146	0.336 %
RU-1	4 hours	2	3.175 %

4.2 The PIERCER Attack for 4G

This section describes the PIERCER attack that enables an attacker to associate a victim's phone number with its IMSI by exploiting a deployment oversight of service providers we have discovered.

4.2.1 Attack Surface

Our investigation towards PIERCER began due to an observation we made while inspecting the network traces of different service providers' paging protocol deployment. The traces we analyzed were contributed by devices across the world in the MobileInsight [63] platform. In those traces [63], we observed that a non-negligible amount of paging messages originating from 1 major US network operator, 2 Chinese network operators, 1 Russian network operator, and 2 US mobile virtual network operators [67] contain IMSI as the identifier (in short, paging_imsi). A summary of the results are presented in Table 4.1.

Some of these observed paging_imsi messages, however, were not intended for the UEs that actually contributed the traces. They rather were intended for other UEs sharing the same paging occasion as the trace-contributing UEs. Due to the lack of contextual information about UEs for which the observed paging_imsi messages were

intended, we were unable to conclude, only from the traces, the condition(s) under which the operators sent paging_imsi. To increase the confidence of our observations, we collected network traces containing paging messages originating from all major US network operators and validated that one operator (the same one from the MobileInsight traces) sent paging_imsi. Additionally, we observed the same behavior from 3 major network providers from a South Asian country.

4.2.2 Curious Case of Paging Containing IMSIs

To establish the condition(s) under which paging_imsi was sent, we consulted the 3GPP standard and searched the Internet for relevant documentation. A manual testing of the deployments, however, revealed that the actual condition is somewhat nuanced compared to the ones found in the standard and in the Internet documentation.

3GPP Standard. According to the 3GPP standard, it is permissible for a network provider to send out a paging_imsi message in the following two cases:

A. When a lower-layer failure occurs for a UE during an interleaved TMSI reallocation and paging procedures, and the core network does not receive any response to an implementation-dependent number of paging messages containing either the old TMSI or new TMSI.

B. When the device's TMSI is unavailable due to network failure.

A recent work by Kim et al. [34], however, observed that the network operators tend to disallow the overlap of the TMSI reallocation procedure and paging protocol by ignoring the TMSI reallocation. The authors used this insight to block the network from changing a device's TMSI which can then be used to track the user. As a result, case **A** cannot be the condition under which the offending network operators in our case send paging_imsi. For case **B**, the standard does not clearly describe what constitutes a network failure preventing us to draw any conclusions.

Practitioner's observation. A quick web search led us to an article [68] discussing the following three cases in which an operator may send paging_imsi in 2G networks.

The considered cases, however, focus on the GSM network instead of the newer 4G LTE network.

1. When the VLR (Visitor Location Registry)—similar functionality as in MME—uses a volatile storage to store the different IMSI-TMSI mappings, a VLR restart would induce an inaccessible IMSI-TMSI mappings. When VLR restarts, any paging will be with IMSI.
2. If the VLR has a limited amount of RAM, a user's IMSI-TMSI mapping may be evicted when a new mapping needs to be inserted. Any paging for users whose mapping are not in the RAM will be with IMSI.
3. The IMSI-TMSI mapping is expired for users who have not shown activity for a long time. Any paging for users whose IMSI-TMSI mappings have expired will result in paging_imsi.

The infrastructure that supports the newer protocol versions arguably does not have the same limitation of using an unreliable, small volatile storage to store the IMSI-TMSI mapping for devices. This argument is further strengthened by our observation that network operators always try with 1-2 paging_tmsi messages before trying with a paging_imsi. This means that network operators usually do not lose the IMSI-TMSI mappings neither because of limited volatile storage nor due to network nodes' abrupt restart. Nonetheless, the findings by Shaik et al. [17] who observed that operators did not change TMSIs for some devices for up to 7 days also invalidates the practitioner's observation of paging with IMSI for 2G networks.

Manual testing. Since neither the standard nor the web article [68] provided a convincing condition to why the network may send paging_imsi, we resort to a manual testing approach. We first collected traces in a cellular device UE_{test} equipped with the offending networks SIM card while placing phone calls from another cellular device periodically at a regular interval. We, however, did not see any paging_imsi intended for UE_{test}. This led us to conclusion that paging_imsi is sent only under exceptional/error cases.

One of the exceptional cases we considered is to block UE_{test} from receiving the paging message from the network. To block UE_{test} from receiving the paging message, we rely on a prior attack called paging channel hijacking [65]. We also established a sniffer to pick up any paging message containing the victim's IMSI.

We observed that if we call UE_{test} but do not let the corresponding paging message in the VoLTE/packet switch domain (PS domain) to reach the UE_{test}, the offending network retries to send the paging messages in the PS domain twice. After two unsuccessful retries in the PS domain, it then sends a paging_imsi in the non-VoLTE/circuit switch domain (CS domain). We validated this by matching the IMSI with UE_{test}'s IMSI. We repeated this multiple times to observe the same consistent behavior. This led us to the complete attack design of PIERCER described below.

4.2.3 Attack Description

The threat model and PIERCER attack steps are given below.

Threat Model. For PIERCER, we assume an attacker who knows the victim's phone number, and can set up a paging message sniffer and a fake base station (with higher signal strength) in any cell including the victim's.

Description. An attacker initiates PIERCER by identifying the victim's paging occasion and current cell-level location with TORPEDO. The attacker then installs a paging message sniffer and a fake base station in the victim's cell. After which the attacker hijacks the victim's paging channel and then places a **single silent** phone call. As discussed above, vulnerable operators will send paging_imsi after several failed attempts with paging_tmsi (due to hijacked paging channel). The attacker's sniffer can capture the IMSI when paging_imsi is sent; completing the attack. The attacker may repeat the last step to gain higher confidence.

4.2.4 Discussion

Impact. PIERCER can also enhance the attacker capability to effectively mount some prior attacks that require the knowledge of the victim's IMSI [13, 16, 17, 65].

Defense. The defense for PIERCER is to ensure that the network operator never sends the paging_imsi message.

Observation. We attempted PIERCER with SMS or Twitter messages to no avail. We speculate that unlike phone calls SMS or Twitter does not have real-time requirements.

4.3 The IMSI Cracking Attack for 4G and 5G

We now present the bruteforce IMSI cracking attack, and also describe the oracles we have exploited for 4G and 5G paging protocols to decide whether a guessed IMSI belongs to the victim device. It is natural to question the rationale of designing a brute-force IMSI cracking attack for 4G where other legitimate means (e.g., identity_request) are available to retrieve the victim's IMSI in the clear. We wanted to demonstrate that the attack is feasible even when the IMSI is never released in the clear, as in 5G, where the IMSI (or, SUPI) is encrypted with the operators' public key. In fact, it is more efficient for 5G as one does not need to wait for the appropriate PFI.

Threat Model: For the cracking attack, we assume the adversary to have the same capabilities as described in the PIERCER attack in Section 4.2.3.

4.3.1 5G-SUPI/IMSI Representation and Information Leakage

Representation. The persistent SIM card-specific identity in 5G is called the Subscriber Permanent Identifier (SUPI). SUPI [69] can be either of the IMSI form or of the network access identifier (NAI) form. For our discussion, we focus on IMSI which

is not only used in 5G but also used in 4G to uniquely identify the subscriber for authentication.

IMSIs are represented as a 15-digit (14-digit for Europe) binary-coded decimal (BCD). The first 3 digits (resp., 2 digits for Europe) of an IMSI represent the mobile country code (MCC) whereas the next 3 digits (same in Europe) represent the mobile network code (MNC) identifying the specific network operator. The rest of the 9 BCD digits of IMSI, called mobile subscription identification number (MSIN), are unique to the subscriber.

Leakage. (1) Given a user's phone number, it is possible to look up the MCC and MNC (i.e., the first 5/6 BCD-digits) corresponding to that device using paid, Internet-based home location register lookup services [66]. This leaves 9 BCD-digits of the IMSI for the adversary to guess.

(2) Recall that, the last 10 bits of the IMSI are used for calculating the paging occasion of a device. In that calculation, however, the IMSI is considered to be a 14-/15-digit decimal number instead of a BCD number. Without loss of generality, if network operator base stations have T=nB=128 then calculating the victim's paging occasion will leak the last 7 bits of the victim's IMSI.

We will describe how these two forms of leakage can be combined by the adversary to decrease the search space of the brute-force search. For example, suppose that the IMSI the attacker intends to crack belongs to a US subscriber. The current maximum value of MCC for US subscribers is 316 whereas the maximum value of MNC is 990. If we consider the rest of the 9 digits of the IMSI to be 9, then the corresponding decimal number's (i.e., $316990[9]^9$) binary representation yields a 49-bit binary number whose leading 18 bits and the trailing 7 bits are known to the attacker, leaving only 24 bits for him to guess which would take the attacker 2^{24} (i.e., $\sim$ 16.77 million) guesses in the worst case.

4.3.2 The IMSI-Cracking Attack Against 4G

This section describes the `IMSI-Cracking` attack against 4G including the oracle that enables the attacker to check the correctness of his IMSI guesses.

Oracle for 4G. The main insight we use for designing the oracle for 4G is that the legitimate responses against a paging_imsi and a paging_tmsi are different. When a device receives paging_tmsi, it responds with a RRC layer connection request message which includes the device's TMSI. On the contrary, when a device receives a paging_imsi message, it invalidates its TMSI and the established security context (if any), and sends a RRC layer connection request followed by a NAS layer attach request. In this case, the RRC layer connection request message contains a random identity instead of its TMSI, which has been invalidated.

Recall that a paging message can contain up to 16 paging records each of which identifies a device for which there is a pending service. When a device wakes up to find a paging message, it goes through the paging records—in the order of their appearances—stopping at the first record whose identity field value matches the device's identity (i.e., IMSI/TMSI). We leverage this observation in the following insight. Suppose that the attacker knows the victim's TMSI T_{victim} but not his IMSI. The attacker makes a guess I_{guess} of the victim's IMSI and wants to check whether I_{guess} is the victim's IMSI. For this, the attacker can inject a fabricated paging message for the victim containing the following two paging records:

Paging record 1 containing I_{guess} in the identity field;

Paging record 2 containing T_{victim} in the identity field.

After receiving the above paging message, if the victim responds with a RRC layer connection request containing an identifier whose value is not equal to T_{victim}, then I_{guess} is the victim's IMSI as it is responding to paging record 1. If the victim, on the other hand, responds with a RRC layer connection request containing T_{victim} as the identifier, then it means that the attacker's guess is wrong because the victim is responding to the paging record 2.

The complete attack. The attacker starts off by using the ToRPEDO attack to identify the victim's coarse-grained location, paging occasion, and the current TMSI. Note that, the victim's paging occasion can be shared by multiple non-targeted users inducing an implicit K-anonymity set where (K-1) is the number of non-targeted users sharing the victim's paging occasion. The attacker then hijacks the victim's (and, also the other K-1 users') paging channel as described by prior work [65]. The attacker creates a fabricated paging message containing 16 paging records where the first 15 records contain different IMSI guesses from the adversary whereas the last paging record contains the victim's TMSI as the identifier.

For each fabricated paging message, if the attacker receives an RRC layer connection request with the victim's TMSI, then it means that none of the 15 IMSI guesses belong to the victim. On the other hand, if the attacker does not receive a RRC layer connection request with the victim's TMSI, it suggests that one of the 15 IMSI guesses belongs to the victim, although the attacker does not know which one it is. Also, as the victim received paging_imsi, it would invalidate the current TMSI. To narrow down which of the 15 guessed IMSIs belongs to the victim, the attacker stops the paging channel hijacking attack and lets the victim connect to the legitimate base station.

Then the attacker again uses ToRPEDO to identify the victim's current TMSI denoted by T^c_{victim}. Suppose the victim's IMSI belongs to the following set: $\mathcal{G} = \{I^i_{\text{guess}} | 1 \leq \text{i} \leq 15\}$ identified from the previous guess. Again, the attacker hijacks the paging channel of the victim including the other devices sharing the same paging occasion. Then the attacker sends a maximum of 15 paging messages each of which contains two paging records. For the first paging message, the first record contains $I^1_{\text{guess}} \in \mathcal{G}$ as the identifier whereas the second record contains T^c_{victim}. Similarly, for the second paging message, the first record contains $I^2_{\text{guess}} \in \mathcal{G}$ as the identifier whereas the second record contains T^c_{victim}, and so on. For the jth paging message where $1 \leq j \leq 15$, if the attacker receives an RRC layer connection request with a random identifier, then it suggests that the guess $\text{I}^{\text{j}}_{\text{guess}}$ belongs to the victim, concluding a

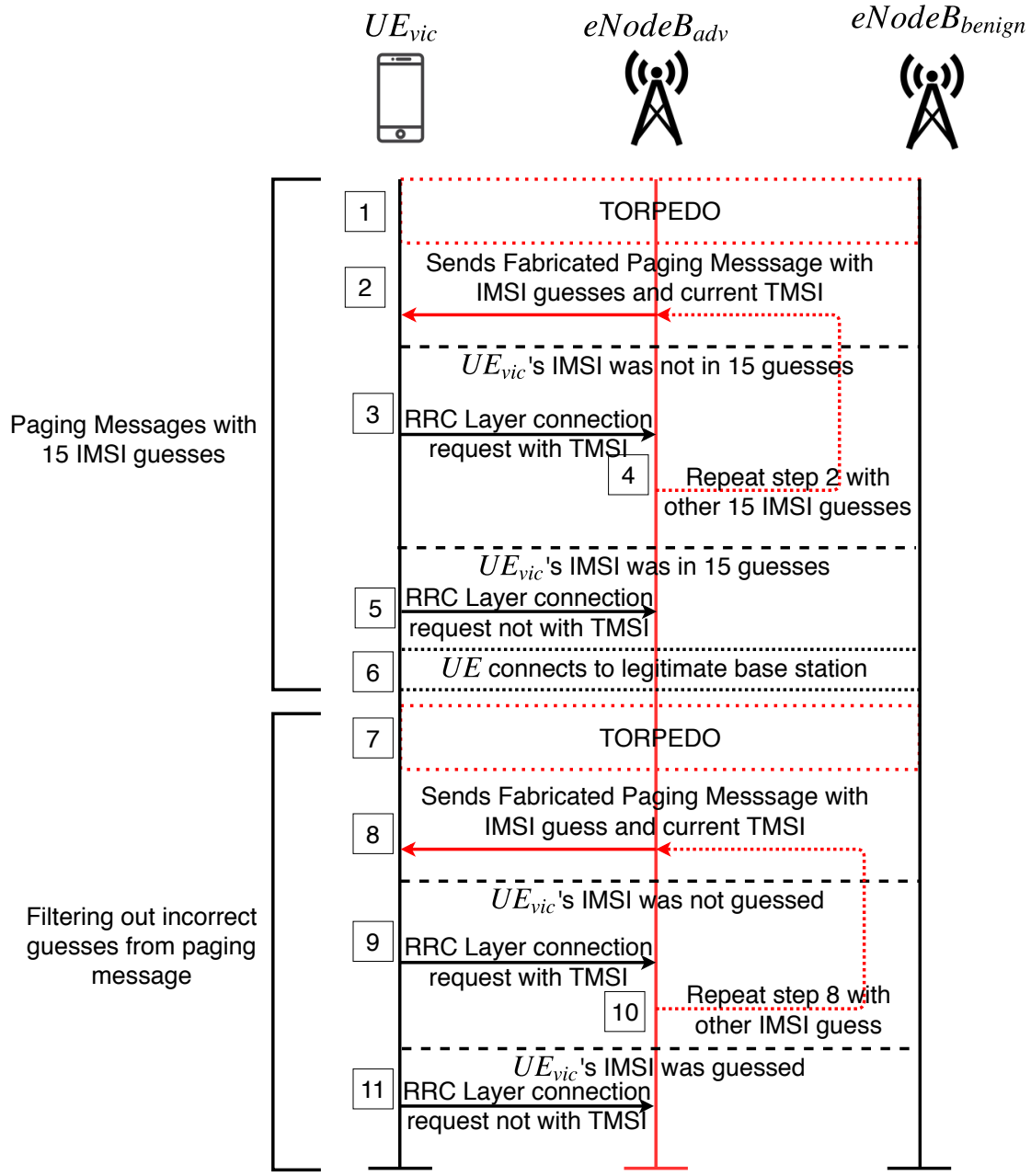

Figure 4.2.: `IMSI-Cracking` attack in 4G

successful attack. Figure 4.2 shows the detailed message flows for the `IMSI-Cracking` attack in 4G.

4.3.3 The IMSI-Cracking Attack Against 5G

This section presents the oracle needed for carrying out the `IMSI-Cracking` attack against 5G.

Oracle for 5G. We leverage three main insights to design the oracle for 5G. (i) The core network's responses to a registration_request message (resp., attach_request message in 4G) is different depending on whether the message contains a valid IMSI. If the core network receives a registration_request message with a non-existent/invalid IMSI, the network issues a registration_reject (cause #9: UE identity cannot be derived by the network) message (clause 5.5.1.2.5 of the 5G NAS standard [31]) to the device, whereas the network sends an auth_request message (*challenge*) in response to a registration_request message with an existent/valid IMSI. (ii) There is a one-to-one relationship between the cryptographic master key (K) and the IMSI of each device in the network which means that a device equipped with IMSI_i cannot solve an authentication challenge c_j derived from K_j of the device with IMSI_j, where $i \neq j$. (iii) A device's response to a valid auth_request message is different from the response to an invalid auth_request message. For an auth_request message, the device responds with an auth_response message if it can solve the challenge; otherwise, it responds with an auth_failure message with an indication to the message authentication code (MAC) or the sequence number verification failure.

If a device's initial registration_request message (containing MCC, MNC and the encrypted MSIN of the user) is not integrity protected, the network initiates an authentication procedure with the device (clause 6.4.6 of 5G Security Architecture [30]). The encrypted MSIN, also called concealed subscription identifier (SUCI), is a function of the home network's public key (CN_{pub_key}) and the MSIN of the user, i.e., $\text{SUCI} = f(CN_{pub\_key}, MSIN)$. We leverage this observation in the following insight. Suppose the attacker knows the core network's public key provisioned in the attacker-controlled SIM card/UE, and makes a guess I_{guess} of the victim's IMSI and wants to check whether I_{guess} is victim's IMSI. For this, the attacker calculates $SUCI_{\text{guess}}$ corresponding to the I_{guess} and sends a fabricated registration_request message to the

core network. Let $\mathcal{I}$ be set of all valid/active IMSIs for a test network. After receiving the registration_request message, if the network responds with a registration_reject message, it means that $I_{\text{guess}} \notin \mathcal{I}$. If the network, on the contrary, responds with a auth_request message, it signifies that $I_{\text{guess}} \in \mathcal{I}$ and the attacker considers I_{guess} as a potential candidate of the victim's IMSI. To validate such a guess, the attacker forwards the auth_request message to the victim's device. If the victim responds with an auth_failure message indicating a MAC verification failure, the attacker infers that the auth_request message generated by the network is not for the victim's IMSI and thus that I_{guess} is not the victim's IMSI. If the device, on the other hand, responds with an auth_response message, the attacker infers that the I_{guess} is the victim's IMSI.

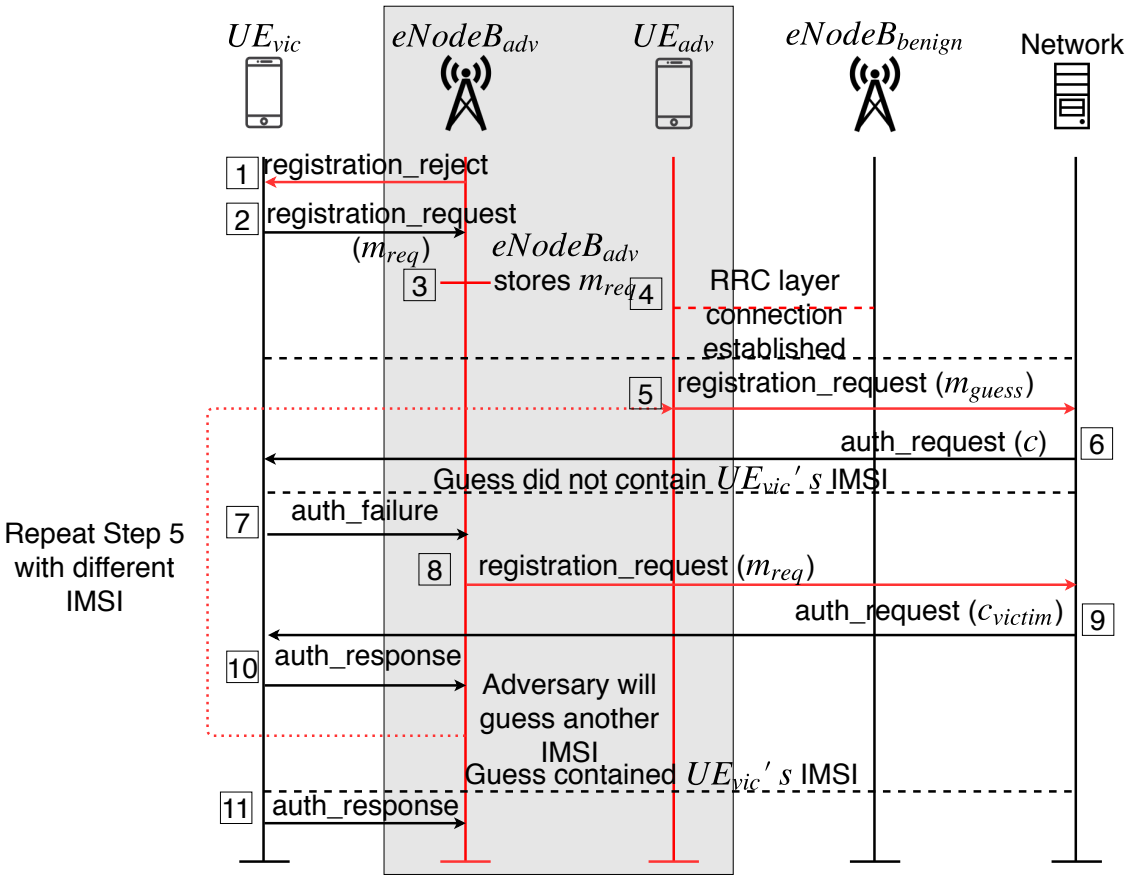

Figure 4.3.: IMSI-Cracking attack in 5G

The complete attack. Like the IMSI-Cracking attack in 4G, the attacker first identifies the victim's paging occasion. The attacker also sets up a *man-in-the-middle* type

relay [65, 70] between the victim device and the legitimate core network (as shown in Figure 4.3) to inject fabricated messages as well as to relay legitimate messages. Like in [65, 70], the relay consists of a malicious eNodeB, denoted by $\mathsf{eNodeB_{adv}}$, impersonating a legitimate eNodeB, denoted by $\mathsf{eNodeB_{benign}}$, towards the victim's device and a malicious UE, denoted by $\mathsf{UE_{adv}}$, impersonating victim's device towards the legitimate core network. In the following $\mathsf{UE_{vic}}$ denotes the victim legitimate UE. Without loss of generality, we use the term eNodeB to refer to a base station for both 4G and 5G.

Disconnect $\mathsf{UE_{vic}}$ *from the EPC*: For disconnecting $\mathsf{UE_{vic}}$ from the legitimate network, the attacker uses a registration_reject message sent by $\mathsf{eNodeB_{adv}}$.

Store $\mathsf{UE_{vic}}$*'s* registration_request*:* As $\mathsf{UE_{vic}}$ detaches itself from the EPC due to a registration_reject, it tries to attach to the eNodeB with the highest signal strength; which is $\mathsf{eNodeB_{adv}}$. $\mathsf{UE_{vic}}$ sends a registration_request message m_{req} to $\mathsf{eNodeB_{adv}}$ which $\mathsf{eNodeB_{adv}}$ stores for later use.

Send an initial registration_request *message containing* I_{guess} *to the EPC*: $\mathsf{UE_{adv}}$ establishes a RRC layer connection with $\mathsf{eNodeB_{benign}}$ and sends a non-integrity protected registration_request message m_{guess} containing I_{guess} to the core network.

Relay auth_request *to* $\mathsf{UE_{vic}}$: In response to m_{guess}, the network sends an auth_request (i.e., a challenge c) to $\mathsf{UE_{adv}}$ which $\mathsf{UE_{adv}}$ forwards to $\mathsf{UE_{vic}}$ through $\mathsf{eNodeB_{adv}}$. After $\mathsf{UE_{vic}}$ receives c, unaware that $\mathsf{eNodeB_{adv}}$ sent it, it tries to solve the challenge c to generate the correct response r. If $\mathsf{UE_{vic}}$ cannot solve the challenge, $\mathsf{UE_{vic}}$ sends an auth_failure message to $\mathsf{eNodeB_{adv}}$. By identifying an auth_failure message in response to c, the attacker infers that I_{guess} is not the victim's IMSI and then tries with $I_{\text{guess}}^{\text{next}}$.

For the attack to be successful, a challenge has to be addressed. We describe the challenge below and the steps taken to address it.

Addressing the challenge of two consecutive auth_failure *by* $\mathsf{UE_{vic}}$*:* If a device fails to verify the MAC or sequence number for two consecutive auth_request messages, the device downgrades to previous generations (e.g., 3G/2G) of cellular networks. This would prevent the attacker from being able to continue probing the network

and $\mathsf{UE}_{\mathsf{vic}}$ with two different IMSIs. We address this challenge by letting the attacker send a m_{req} message between two consecutive m_{guess} messages. After a trial with m_{req}, $\mathsf{UE}_{\mathsf{adv}}$, therefore, sends the m_{req} (obtained from $\mathsf{eNodeB}_{\mathsf{adv}}$) to the core network. In response to m_{req}, the network sends a valid auth_request message (c_{victim}) for $\mathsf{UE}_{\mathsf{vic}}$ which $\mathsf{eNodeB}_{\mathsf{adv}}$ and $\mathsf{UE}_{\mathsf{adv}}$ relay to $\mathsf{UE}_{\mathsf{vic}}$. $\mathsf{UE}_{\mathsf{vic}}$ solves the challenge and sends auth_response r to $\mathsf{eNodeB}_{\mathsf{adv}}$ which will not be relayed to the legitimate network.

$\mathsf{UE}_{\mathsf{vic}}$ then sends a new m_{guess} with another I_{guess} and repeats the above steps by interleaving m_{guess} and m_{req} messages. If $\mathsf{eNodeB}_{\mathsf{adv}}$ receives an auth_response message r for an I_{guess}, $\mathsf{eNodeB}_{\mathsf{adv}}$ is able to infer that I_{guess} belongs to the victim, concluding a successful attack.

4.4 Testbed setup

We now describe our testbed that we used for validating `ToRPEDO`, `PIERCER`, and `IMSI-Cracking` attacks in 4G.

Paging sniffer. For sniffing broadcast messages we set up a sniffer using a Universal Software-defined Radio Peripheral device, i.e., USRP B210 [54] (costs as low as $1300) connected to an Intel Core i7 machine running Ubuntu 16.04 as the hardware component and srsLTE [56], an open source LTE protocol stack implementation. We modified the srsLTE's `pdsch_ue` application to enable the sniffer to periodically ($\sim$ 10 minutes) switch its decoding mode between the master_info_block and the paging channels. Thus the sniffer periodically synchronizes the network time/frame similar to commercial-off-the-shelf (COTS) UEs and reliably computes the SFN value for a received paging message. We also use the sniffer to capture and decode the system_info_block_type_1 and system_info_block_type_2 messages and learn the parameters relevant for computing the victim UE's paging occasion (e.g., paging cycle and nB).

Malicious eNodeB. We use another USRP B210 [54]) connected to an Intel Core i7 machine running Ubuntu 16.04 as the hardware component and srsENB [56], an open source LTE protocol stack implementation for eNodeB, to set up a malicious

eNodeB. We modified the srsENB to allow the malicious eNodeB to broadcast paging messages without any paging_request from a legitimate MME. There are other more economial options for setting up a rogue eNodeB using LimeSDR [71] (costs as low as $200) which has also been shown to be effective [72].

4.5 ToRPEDO Evaluation

In this section, we validate and evaluate the *filtering*, *counting*, and *likelihood* variants of ToRPEDO.

Effectiveness metrics. For assessing the effectiveness of all variants of ToRPEDO, we use the following metrics: (1) **accuracy** (defined below), and (2) **number of trials** (i.e., calls/SMSs) required to correctly identify a victim UE's paging occasion. We also evaluate the same for the case when the victim is not present in a cell area.

$$\textbf{accuracy} = \frac{\text{total \# attacks - \# mis-identification}}{\text{total \# attacks}} * 100\%$$

4.5.1 Evaluation Setting

We evaluated the ToRPEDO variants in both peak (12:00 PM noon) and off-peak (12:00 AM midnight) times as the paging message distribution tends to vary with time of day [12, 34]. We also carried out the attacks in two different geographical locations, although we present results from one location due to space constraints. In the similar vein, we include results for only one major US network provider (i.e., **US-I**)[1] as we have mostly observed the same trends for the rest of the network providers in both US and Canada.

We have considered both VoLTE and CSFB phone calls while validating ToRPEDO variants. Similarly, we also considered paging in both PS and CS domains. We particularly considered paging with CS domain as our analysis of network traces from 34 different service providers [63] revealed that 14 of them use paging with CS

[1]To keep the four major US network operators anonymous, we use pseudonyms (i.e., **US-I**, **US-II**, **US-III**, **US-IV**) to identify them.

domain. Finally, we demonstrate ToRPEDO variants' effectiveness in identifying the victim's presence and also absence in a cell.

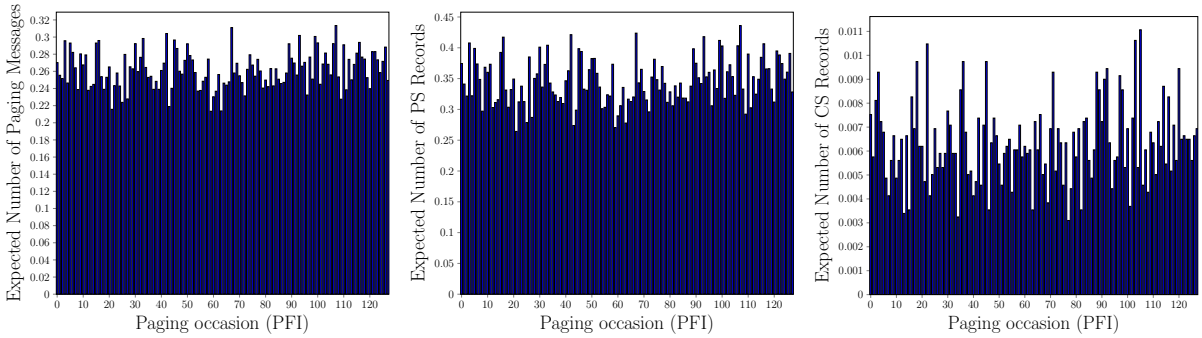

(a) Paging message base rate ($\lambda_{\mathrm{b}}^{\mathrm{paging}}$). (b) PS record base rate ($\lambda_{\mathrm{b}}^{\mathrm{ps}}$). (c) CS record base rate ($\lambda_{\mathrm{b}}^{\mathrm{cs}}$).

Figure 4.4.: Average number of paging message, PS record, and CS record arrivals in any PFI within one paging cycle during peak-time of a day.

4.5.2 Baseline for Likelihood Variant of ToRPEDO

Carrying out the likelihood variant of ToRPEDO requires the attacker to establish a baseline paging message (resp., records) distribution. For the baseline, the attacker first uses a sniffer to capture paging messages received at different PFIs for 15 minutes. The adversary then computes the following Poisson distribution parameters: (i) $\lambda_b^{\mathrm{paging}}$ = average number of paging message arrivals for any PFI within one paging cycle (T); (ii) λ_b^{PS} average number of PS record arrivals for any PFI within one paging cycle; and (iii) λ_b^{CS} = average number of CS record arrivals for any PFI within one paging cycle. Figures 4.4(a), 4.4(b), and 4.4(c) show the average number of paging message, PS record and CS record arrivals, respectively, in any PFI within one paging cycle during peak time. For the rest of this section, we will use: $\lambda_b^{\mathrm{paging}} = 0.26$, $\lambda_b^{\mathrm{PS}} = 0.34$, and $\lambda_b^{\mathrm{CS}} = \mathbf{0.0065}$ which we observed in our testing location.

4.5.3 Identifying Victim's Presence with ToRPEDO

We now describe validation results of ToRPEDO variants with different trial types (e.g., VoLTE phone call, SMS).

VoLTE Call

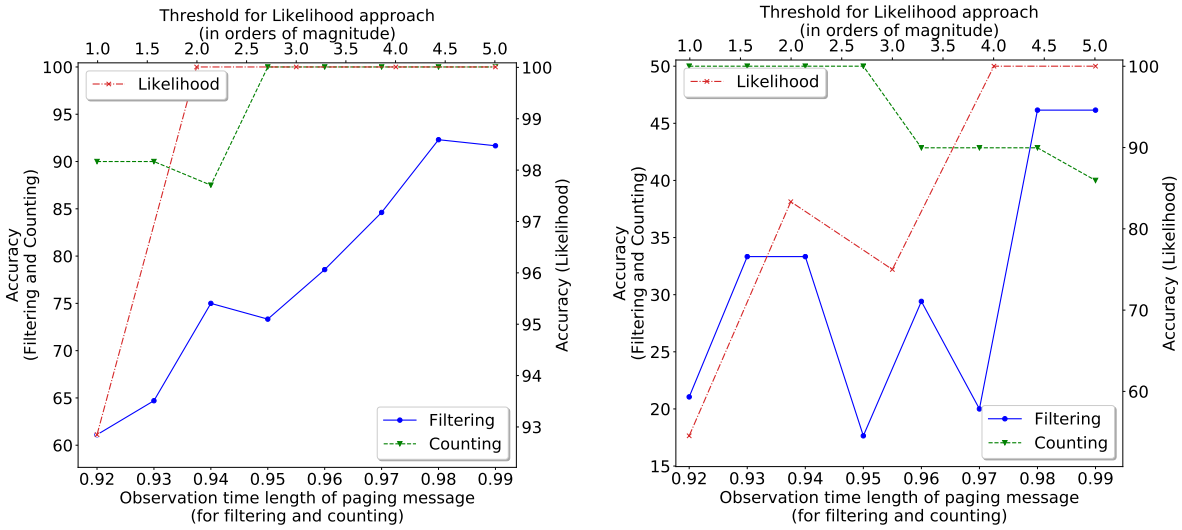

(a) No missing paging.

(b) 15% missing paging

Figure 4.5.: Accuracy and number of trials against thresholds for ToRPEDO using VoLTE calls during the peak hour (around noon) of a day.

Parameter selection. Carrying out ToRPEDO variants requires fixing few parameters. For the filtering and counting variants the important parameter is the *observation interval*. Given a time period, an observation interval of 0.95 means that 95% of the observed paging messages arrived within the considered time period. The observation interval can be computed from the histogram of the paging delay similar to ones in Figure 4.1(a). In the similar vein, the necessary parameter for likelihood variant of ToRPEDO is the threshold value τ. τ is used to compare the likelihood of the two PFIs with highest likelihood values.

Figure 4.5(a) shows the accuracy of three approaches for different observation intervals and thresholds. Note that the scale of Y-axis for likelihood based approach is different from that of the filtering and counting based approaches. As we increase the observation interval, the accuracy for the filtering and counting based approaches improve whereas the accuracy of the likelihood approach improves with increasing value of threshold (τ).

One can then choose the parameter values for each ToRPEDO variant that results in the highest accuracy by consulting the Figure 4.5(b). Precisely, we set the observation intervals for *filtering* and *counting* to 0.98 and 0.95, respectively, whereas we set the threshold for *likelihood* to $\tau = 4$. We omit the parameter selection process for the latter trial types as they are similar to the VoLTE case.

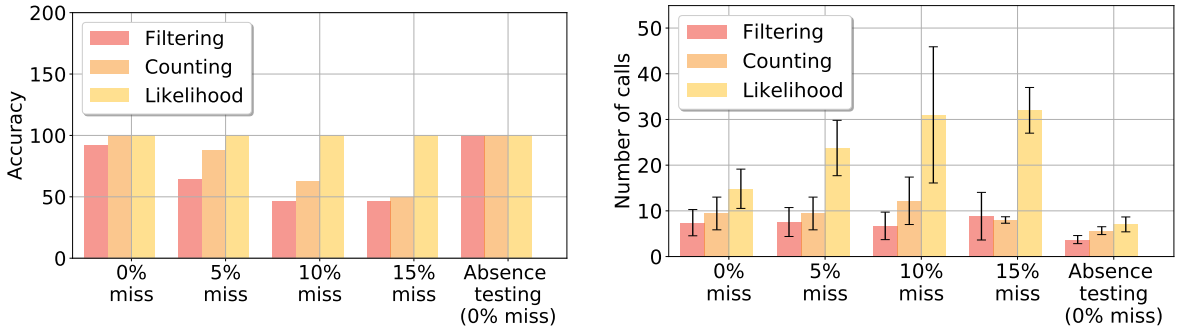

(a) Accuracy (at peak hour)

(b) Number of calls (at peak hour)

Figure 4.6.: Accuracy and number of trials against the selected observation intervals and threshold value (in order of magnitude) for ToRPEDO using VoLTE calls during the **peak** hour of a day. Observation interval for filtering = 98 %, observation interval for counting = 95 %, threshold (in orders of magnitude) for likelihood = 4.

Accuracy for VoLTE calls. Figure 4.6(a) and Figure 4.7(a) show the accuracy of *filtering*, *counting*, and *likelihood* based approaches in the peak and off-peak hours of a day for different paging missing rates. The accuracy drops for filtering and counting with increasing paging missing rates. For instance, the accuracy for counting drops from 100% to 48% (Figure 4.6(a)) as the paging missing rate increases from 0% to

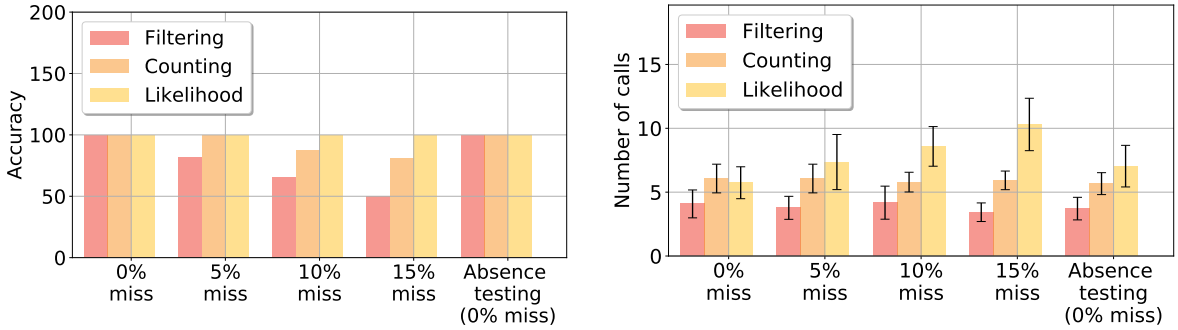

(a) Accuracy (at off-peak hour)

(b) Number of trials (at off-peak hour)

Figure 4.7.: Accuracy and number of trials against the selected observation intervals and threshold value (in order of magnitude) for ToRPEDO using VoLTE calls during the **off-peak** time of a day. Observation interval for filtering = 98%, observation interval for filtering = 98%, threshold (in orders of magnitude) for likelihood= 3.

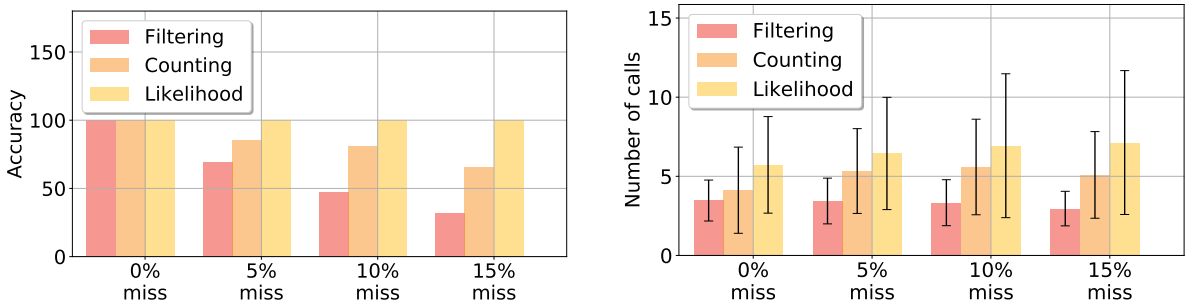

(a) Accuracy (at off-peak hour)

(b) Number of calls (at off-peak hour)

Figure 4.8.: Accuracy and number of trials against the selected observation intervals and threshold value (in order of magnitude) for ToRPEDO using **CSFB** calls during the **off-peak** time of a day. Observation interval for filtering = 98%, observation interval for filtering = 98%, threshold (in orders of magnitude) for likelihood= 2.

15% whereas the accuracy for likelihood approach remains 100% for all paging missing rates.

Number of VoLTE calls required. Figure 4.6(b) and Figure 4.7(b) show the number of silent VoLTE phone calls that an adversary requires in the peak and off-peak hours of a day for successful identification of victim's PFI using *filtering*, *counting*, and *likelihood* based approaches for different paging missing rates. The number of silent

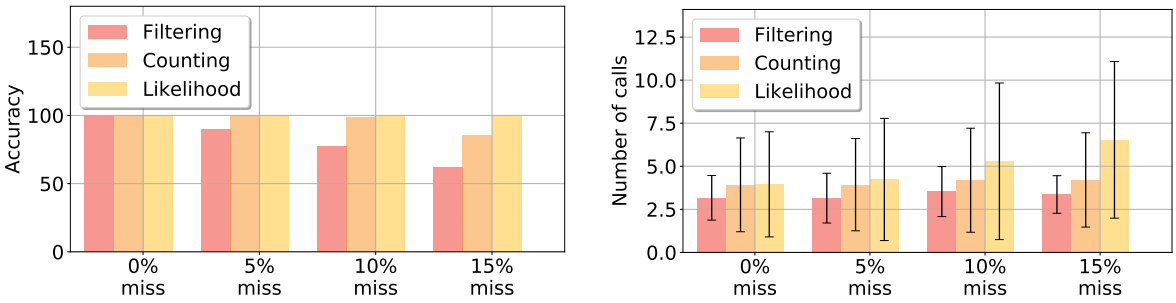

(a) Accuracy (at off-peak hour)

(b) Number of trials (at off-peak hour)

Figure 4.9.: Accuracy and number of trials against the selected observation intervals and threshold value (in order of magnitude) for ToRPEDO using **CSFB** calls during the **off-peak** time of a day. Observation interval for filtering = 98%, observation interval for filtering = 98%, threshold (in orders of magnitude) for likelihood= 2.

phone calls for likelihood increases with increasing paging missing rates whereas the number of silent calls for filtering and counting remains consistently low for all paging missing rates. This is because both the filtering and counting approach removes the victim's PFI from the set of candidate PFIs (as discussed in Section 4.1) if the paging is missed for a silent call or a couple of silent calls. In contrast, likelihood based approaches take the error rate into account and thus require additional silent phone calls to reach the threshold (e.g., $\tau = 4$ for likelihood) in the case where paging messages are missed. Note that, since the base paging rate during off-peak hours is significantly lower than that of the peak hours, the adversary requires less number of phone calls at off-peak hours as shown in Figure 4.7(b). For instance, the adversary requires only $\sim$5 silent phone calls with likelihood approach (for no missing paging rate) at off-peak hours which increases to $\sim$13 calls at peak hours.

CSFB Phone Call

For the network operators which choose to generate mobile terminated CSFB call for the callee based on VoLTE capability of the callee device and the network, the adversary takes into account both the PS and CS records in the paging messages

after a silent phone call for *filtering*, *counting*, and *likelihood* based approaches. In contrast, for other types of network the adversary considers only the CS records for inferring victim's PFI.

Accuracy for CSFB calls. Figure 4.8(a) and Figure 4.9(a) show the accuracy of *filtering*, *counting*, and *likelihood* based approaches during peak and off-peak time for different paging missing rates. In general, the accuracy trend for CSFB calls is similar to that for the VoLTE calls as shown in Figure 4.6(a) and Figure 4.7(a).

Number of CSFB calls required. Figure 4.8(b) and Figure 4.8(b)show the number of silent VoLTE phone calls that an adversary requires at peak and off-peak time for successfully identifying victim's PFI using *filtering*, *counting*, and *likelihood* based approaches for different paging missing rates. Since the base rate of CS domain records significantly lower (as low as 0.0065 for any PFI within one paging cycle), the number of silent CSFB phone calls using all three approaches is significantly lower than that of the VoLTE phone calls as shown in Figure 4.6(b) and Figure 4.7(b). The results signify that it is easier to identify the victim's PFI and its presence if the victim UE or the serving eNodeB are not VoLTE capable. One implication could be that for locations where eNodeBs are not VoLTE capable, it may be easier to identify a particular user's presence with only a small number of phone calls.

SMS and Tweets

We successfully validated `ToRPEDO` using SMS and tweets (by mentioning victim's Twitter handle). The accuracy for SMS and Tweets follow the similar trend of phone calls. The number of required trials, however, was much lower because of a smaller paging delay (3-5 seconds as shown in Figure 4.1(a)). We omit the results for space constraints.

4.5.4 Sensing Victim's Absence with ToRPEDO

We also perform the ToRPEDO attack when the victim device and the adversary's sniffer are not in the same tracking area and evaluate the accuracy and the number of silent calls required for identifying victim's absence during the peak and off-peak hours of a day. The accuracy of filtering, counting, and likelihood based approaches follow a trend similar to identifying victim's PFI (i.e., presence) as shown in Figure 4.6(a) and Figure 4.7(a). Figure 4.6(b) and Figure 4.7(b) show that the adversary with likelihood based approach requires slightly less number of calls (8 calls for threshold, $\tau = 4$) during peak hours for identifying victim's absence whereas it requires $\sim$13 calls for identifying victim's PFI (i.e., presence) as shown in Figure 4.6.

4.6 Validating PIERCER and IMSI-Cracking Attacks

In this section, we describe our validation process of PIERCER and IMSI-Cracking attacks for 4G.

4.6.1 PIERCER Evaluation

The goal of our PIERCER validation is to determine how many calls the adversary needs to reliably retrieve the victim UE's IMSI given its phone number and PFI (assumed to be obtained with ToRPEDO attack). We describe the validation process for **US-I** only, although similar behavior was observed for three other network operators of a South Asian country.

Paging channel hijacking. After identifying the victim's PFI, we carried out the paging channel hijacking attack by faithfully following the steps described in Chapter 3.3.

The attack. Once the victim's paging channel was hijacked, we made a single phone call to the victim's phone number which caused the legitimate eNodeB/MME to first send a paging_tmsi in the PS domain for the victim UE. Once a paging_tmsi

is issued, we observed that the US-I network sets a timer for the response and the maximum_paging_attempt to 2. Since the victim is unaware of the actual paging_tmsi message, the timer at MME expires because of UE's unresponsiveness. We then observed that the MME initiates another paging_tmsi in the PS domain and continues to do so until it reaches the maximum_paging_attempt. Upon expiration of retries, the MME of US-I first sends paging_tmsi in the CS domain and then, when its timer expires, it broadcasts the paging_imsi in the CS domain. If the adversary now makes a second phone call, the MME initiates another paging_tmsi in the CS domain without trying with the PS domain first, and then, upon expiration of the timer, the MME broadcasts paging_imsi again validating our attack.

Total call trials. Excluding the phone calls needed for the prerequisite `ToRPEDO` attack, we validated that indeed a single phone call was sufficient to expose the victim's IMSI.

4.6.2 `IMSI-Cracking` Evaluation

The goal of our `IMSI-Cracking` attack's evaluation is to determine the time and the number of paging messages that an adversary needs to make to identify the victim's IMSI given that the adversary knows the victim's phone number (in our case, MCC=310 and MNC=260 retrieved from [66]), PFI (in our case, 21), and TMSI (using techniques from [12, 17]).

The adversary faithfully follows the paging channel hijacking attack as demonstrated in Chapter 3.3, and computes the $I^{\max}_{\text{guess}}$ and $I^{\min}_{\text{guess}}$, i.e, the maximum and minimum possible IMSI values (in binary) that have the value 310260 in 18-bits MSB and the value 21 in 8-bits LSB. We found $I^{\max}_{\text{guess}} = 310260999999381$ and $I^{\min}_{\text{guess}} = 310260000000021$ for the given PFI, MCC, and MNC. We started with $I^{\max}_{\text{guess}}$ in descending order and fabricated paging messages with 14 I_{guess}s each. Note that, though the standard specifies that up to 16 paging records can be accommodated into a single paging message, we observed that our test UE device accepts paging

messages containing at most 15 paging records which indicates a deviation from the standard and an interoperability issue.

Number of paging messages. To identify the victim's IMSI (=310260628687893), the attacker needed to try a total of 2900876 IMSIs and thus sent 207206+14 = 207220 paging messages through the malicious eNodeB.

Time requirement. We set the values of paging cycle T and nB to 128 for hijacking paging channel and therefore, sent one paging message every 1.28 seconds. The total time required to crack the victim's IMSI was 74 hours. We performed this experiment for 7 days in the off-peak hours. Note that the attack can be expedited by at most 32 times by setting the value of nB = $\frac{T}{32}$.

4.7 Discussion

Threat to validity. The empirical evaluations reported in this chapter were carried out in multiple locations during both peak and off-peak hours. As cellular network behavior is highly dependent on the cell area, load, and equipment, some of the numbers (or, findings) reported here may not exactly match up when reproduced in other locations with different equipment.

Limitations. For `ToRPEDO` to be successful, an attacker needs to have a sniffer in the same cellular area as the victim. If the number of possible locations that the victim can be in is large, the expense of installing sniffers (i.e., $200 each) could be an impediment to carrying out a success attack. In a similar vein, for a successful `PIERCER`, the attacker needs to have a paging message sniffer and also a fake base station which would cost around $400. The `IMSI-Cracking` attack for 4G will be feasible only in cases where the attacker can carry out his attack without the victim noticing that his device is not receiving any notifications, for instance, when the victim is sleeping at night. `ToRPEDO` and `IMSI-Cracking` attacks on 5G were not validated due to the lack of deployed networks.

Responsible disclosure. We are in the process of reaching out to the affected network operators that are verifiably vulnerable to `PIERCER`. We are also reaching out to

3GPP standard's committee for responsibly disclosing the ToRPEDO and IMSI-Cracking attacks.

4.8 Summary

This chapter sheds light on an inherent design weakness of the 4G/5G cellular paging protocol which can be exploited by an attacker to not only obtain the victim's paging occasion but also to identify the victim's presence in a particular cell area just from the victim's soft-identity (e.g., phone number, Twitter handle) with a novel attack called ToRPEDO. We also demonstrate that ToRPEDO can enable an attacker to exploit a deployment oversight of several network operators to retrieve a victim's IMSI from his phone number using the PIERCER attack. To further provide evidence of ToRPEDO's potency, we show that it empowers an attacker to launch a brute-force IMSI-Cracking attack through the use of two novels oracles we designed for 4G and 5G, respectively. Each of these attacks can also be leveraged to enhance prior attacks. All of our attacks have been validated in realistic setting for 4G using cheap software-defined radio and open-source protocol stack.

We leverage the findings in Chapter 3 and Chapter 4 and investigate plausible countermeasures in the next chapter addressing broadcast authentication for ripping out the root cause of many active attacks identified in the previous chapters.

5. INSECURE CONNECTION BOOTSTRAPPING IN CELLULAR NETWORKS: THE ROOT OF ALL EVIL

5.1 Introduction

A cellular device's connection to the operator's network starts off by the device scanning for appropriate signals broadcast by nearby base stations. Among the available base stations, the device selects to initiate the connection to the one that emits signals with the highest strength. Once the device connects to the base station, the base station then plays the role of a trusted intermediary enabling the device to seamlessly communicate with the core network. Unfortunately, no mechanism currently exists with which a device can verify the legitimacy of the base station. This lack of authentication allows adversaries to install rogue base stations which lure unsuspecting devices to connect to them [17, 73]. Forcing devices to establish a connection with a rogue (or, fake) base station is often the necessary first step for the adversary to carry out other destructive attacks [9, 11, 13, 14, 16, 17, 65, 70]. Although this fundamental connection bootstrapping weakness is widely acknowledged, there does not seem to be a conscious effort in mitigating this even in the new 5G standard [29]. *This work aims to fill this gap by proposing an authentication mechanism for enhancing the security of connection bootstrapping.*

Existing work: Unlike the majority of the existing research [14, 15, 19, 53, 65, 70, 74, 75], which focuses on identifying security weaknesses of cellular networks, there are only a few proposals that focus on misbehaving base stations [18, 76–78]. The most relevant to our work is the proposal by Li et al. [76], named FBS-Radar, which collects spam messages (and, its accompanying meta-data) received by end-users to identify the location of base stations. On the other hand, Zhuang et al. [77] developed FBSleuth which uses Radio Frequency Fingerprinting to establish forensic evidence of

a base station's misbehavior. These prior efforts, however, cannot alleviate the root cause that allows adversaries to lure devices into connecting to fake base stations to begin with: *insecure bootstrapping*.

Challenges: To ensure the effectiveness and feasibility of any retrospective authentication mechanism that addresses the insecure bootstrapping problem, it is crucial that such mechanism maintains backward compatibility without requiring a major overhaul of the cellular protocol or infrastructure. More concretely, any effective mechanism has to decide for which bootstrapping signals of the base station it will provide authentication guarantees while taking into consideration the quality of service guarantees, overhead of the base stations and cellular devices, bandwidth overhead, scheduling restrictions, and maximum transmission unit (MTU).

Approach: Conceptually, one can consider the following two possible approaches for providing bootstrapping authentication: one based on the *TESLA* [79] protocol and the another based on *Public Key Infrastructure* (PKI). TESLA is a broadcast authentication protocol in which multiple time-synchronized receivers (i.e., cellular devices) must authenticate messages periodically broadcast by a sender (i.e., base station). TESLA uses symmetric cryptographic functions (MAC) to achieve asymmetric properties using delayed key disclosure and one-way key chains. TESLA, however, relies on a pre-existing authenticated channel for its own bootstrapping which is not available in our context, making it ineffective.

In the PKI-based approach, each base station will be equipped with a public and private key pair. Any broadcast signal emitted by a specific base station will be digitally signed by its private key. Any cellular device that has access to the base station's public key can then verify that the bootstrapping signal is indeed emitted by the claimed base station. To realize such an approach, the cellular device is required to verify the authenticity of a base station's public key. This is achieved by the base station sending a public-key certificate chain (e.g., X.509 [80]) to prove its public-key's authenticity. In our context, we consider a 3-length public-key certificate chain where only two of them are transmitted during bootstrapping. The first certificate of the

chain (i.e., trust anchor) is self-signed by the network operator's private key and is stored in the device's subscriber identity module (SIM) card. The second certificate in the chain—signed by the network operator's private key—belongs to the mobility management entity or MME [4] (resp., Access and Mobility Management Function or AMF in 5G [29]) which is responsible for a set of base stations in a designated tracking area. The final certificate in the chain belongs to the base station and is digitally signed by the MME's private key.

At face value, implementing the PKI-based authentication mechanism seems like a straightforward proposition. In reality, however, realizing an implementation of the authentication mechanism requires addressing several deployment constraints. Due to the restriction on the broadcast packet size, we observed that even a single vanilla X.509 certificate does not fit into a packet. Similarly, another relevant issue one needs to consider for a successful deployment is the revocation of a base station's public key prior to its expiration date, especially, in exceptional cases (e.g., private key leak). This is a relevant threat as the adversary can gain physical access to the base stations which are often left unguarded. Typical revocation mechanisms (e.g., certificate revocation list and online certificate status protocol) are ineffective in our context as they require connectivity which the device is attempting to gain in the first place. The final challenge one would have to address is to protect against relay or replay attacks which have been shown to be extremely effective in case of cellular networks [65, 70]. We address these challenges in the following manner.

Certificate size: To overcome the packet size constraint, we construct a very lightweight certificate containing only the fields necessary in our context (e.g., identity, public-key, expiration date, the digital signature, location of the base station).

Revocation: We avoid an explicit revocation mechanism by proposing base station certificates to have a small expiration (e.g., <10 minutes). This can severely limit the attack window with which an adversary can exploit the leakage of a base station's private key.

Relay-/replay-attack protection: For preventing relay-/replay-attacks, we introduce a location-dependent, configurable parameter that influences the validity period of a given broadcast message and in turn can control the exploitation window.

The final issue we need to address for the realization of an effective and secure authentication mechanism is the choice of digital signature scheme. Our choice of a digital signature impacts three different aspects: (a) Signature size; (b) Signature generation time; (c) Signature verification time. This is also known as the trilemma of digital signatures and a scheme can only optimize (i.e., minimize) two of these aspects. In our instantiation, we choose to optimize aspects (a) and (b) while sacrificing (c). The rationale of optimizing aspect (a) is clear as this will minimize the overhead of the packet size. We optimize aspect (b) instead of aspect (c) because a device typically will verify signatures for one session whereas the base station keeps generating signatures for the bootstrapping signals based on its schedule (e.g., ∼80 milliseconds). Optimizing aspect (b) will decrease the computation and energy overhead for the base station significantly.

Implementation: We implemented our PKI-based broadcast authentication for 4G LTE (since no open-source 5G implementation is available) in a real test-bed using software-defined radios and open-source 4G LTE protocol stack [54, 56]. For digital signature schemes, we consider ECDSA [81], BGLS [82], and SCRA-BGLS [83] (BGLS signature generation optimized with offline pre-computation). In our evaluation, we observed that our mechanism imposes only moderate overhead with respect to additionally transmitted bytes (e.g., ∼**220** bytes) and connection time (e.g., ∼**28** milliseconds).

Impact: In the recent 5G proposal, a PKI is already introduced for protecting against IMSI catching attacks [17, 73, 84] by requiring devices to encrypt their IMSIs/IMEIs with the network operator's public key during communication. The current work goes a step further by extending the existing 5G PKI to allow devices to authenticate base stations and in the process preventing a substantial amount of existing attacks—also applicable to 5G—which stem from the insecure bootstrapping process. As 5G is still

awaiting deployment, incorporating a defense such as ours is feasible and can go a long way in securing the cellular ecosystem.

Contributions. In summary, the work makes the following contributions.

- We propose an optimized PKI-based authentication mechanism that enables a cellular device to authenticate a base station during connection bootstrapping. Our defense can protect against many high-profile attacks against the cellular network including the notorious IMSI-catching attack and DNS redirection through man-in-the-middle relays.
- We implemented our scheme on a real test-bed using software-defined radios and open-source protocol stack.
- Our evaluation on the real test-bed shows that our approach only has a moderate overhead with respect to the number of transmitted bytes, signature generation time for the base station, and the connection establishment overhead for the device. From a purely technical point-of-view, it is feasible to incorporate our scheme in a real network.

5.2 Problem Description

In this section, we first present our adversary model, then identify the constraints imposed by both the stakeholders and the cellular ecosystems that need to be respected by a defense, and finally formulate the problem we address in this work.

5.2.1 Threat Model

In our threat model, the adversary has the following capabilities:

Eavesdropping or tampering with protocol messages. We consider the adversary to have the capability of establishing a man-in-the-middle relay [65, 70] which in turn may allow him to drop, modify, eavesdrop, and forward messages transmitted between benign protocol participants (e.g., legitimate devices and base stations) in the public channel while respecting cryptographic assumptions.

Impersonating a legitimate base station. We also consider an active adversary who can install and run its own base station with the same capabilities as a legitimate one. In addition, the fake base station can impersonate a legitimate base station and thus can force a victim device to connect to it by broadcasting MIB and SIB messages in the victim UE's frequency with a higher signal strength than the legitimate base station. We make the assumption that the adversary can learn legitimate values for MIB and SIB messages by eavesdropping the public channels where these are broadcast.

Other assumptions. We assume that the adversary cannot physically tamper with the SIM card, base station, or the core network to obtain the sensitive information, e.g., cryptographic keys. Side-channel attacks and denial-of-service (DoS) attacks due to wireless signal jamming are considered out of the scope of this work.

5.2.2 Deployment Constraints

For a defense to be deemed deployable and feasible, there are certain constraints which it must respect. These constraints are imposed by both the cellular protocol/ecosystem and its stakeholders (e.g., network operators), and are discussed below.

Cellular protocol/ecosystem. For a solution to be viable in the perspective of the ecosystem itself, the following constraints must be met: **(CE1)** Additional bytes added for supporting authentication must not exceed the MTU; **(CE2)** Backward compatibility should not be compromised, that is, legacy devices should be able to connect to the base station without authentication; **(CE3)** The computational overhead must not introduce delays in the message broadcast schedule; **(CE4)** The authentication mechanism must not rely on a pre-existing authenticated channel.

Cellular stakeholder. Unlike the cellular network ecosystem constraints, the following constraints imposed by cellular stakeholders are directly/indirectly related to revenues and are expected to be fulfilled by any potential defense: **(CS1)** The additional bytes added in the control-plane messages due to authentication must be minimized; **(CS2)** The authentication verification (resp., authentication material

generation) overhead must not cause downtime or delays; **(CS3)** The defense must not require major overhauls in the protocol/infrastructure.

5.2.3 Scope and Problem Statement

Lack of authentication of the MIB and SIB messages enables the adversary to spoof a legitimate base station. The adversary exploiting this deeply rooted vulnerability can lure an unsuspecting cellular device to connect to it and then carry out specific attacks using unauthenticated messages exclusively sent to the victim device. We identify the following two types of defense mechanisms that could prevent such attacks. (i) *Attack-specific defenses* attempt to thwart a particular discovered vulnerability. For instance, ignoring unauthenticated and out-of-order auth_reject messages can protect devices from denial-of-service attacks as demonstrated in Chapter 3. (ii) *Generic defenses*, on the contrary, prevents the root cause of a vulnerability which may be exploited by multiple attacks. In our context, such a defense would be to prevent adversaries from forcing the UE to connect to the fake base station in the first place by making possible for the UE to authenticate base stations. Naturally, the former types of defenses protect devices only from a very specific set of *discovered* attacks due to adversary's use of fake base stations. There are, however, many other attacks that exploit the capability of setting up a fake base station [65]; such an attack-specific defense cannot thwart these and hence such a case-by-case defense cannot be a practical solution. It is thus clear that, because to its wider applicability, a generic defense mechanism is critical for the security of the cellular networks. Designing such a mechanism is the focus of the current work.

Protocol versions. Our discussion, although mainly focusing on the 4G LTE and 5G versions of the cellular protocol, is generalizable to older protocol versions (e.g., 3G/2G).

Which messages to authenticate? A cellular device may authenticate either (i) the broadcast MIB and SIB messages, or (ii) the exclusive connection setup message (i.e., the rrc_connection_setup message in step 5 of Figure 2.3) to connect to a

legitimate base station. When the device is in the idle mode (i.e., no radio activity), however, it only captures the MIB and SIB messages and camps on a cell for receiving paging messages without setting up any explicit connection with the base station. Since paging messages along with MIB and SIB messages do not have any integrity/authenticity protection, the adversary can inject fake emergency alerts using fabricated SIB and paging messages [65]. Such attacks in device's idle mode are hard to prevent without ensuring the authenticity of MIB and SIB messages. Authenticating the rrc_connection_setup message, on the other hand, implicitly requires authenticating the SIB messages (through MAC) received before. Since at bootstrapping time the UE and the base station do not share a session key, it is not clear which key to use for generating the MAC. In light of the above discussion, it is therefore clear that broadcast (i.e., MIB, SIBs) messages are the natural choice for authenticating a base station and the root of trust for establishing a secure connection to the base station and consequently with the core network.

Problem Statement. Formally, in this work, we aim to design and evaluate a secure connection bootstrapping mechanism for cellular devices by providing authentication guarantee and integrity protection to MIB and SIB broadcast-messages while conforming to the aforementioned constraints (i.e., **CE1-CE4** and **CS1-CS3**).

5.3 Potential Solutions for Broadcast Authentication

In this section, we discuss two candidate mechanisms that can possibly provide the authenticity and integrity protection for bootstrapping signals/messages transmitted by the base stations. One of these mechanisms is based on symmetric key cryptography whereas the other is based on public key cryptography. Conceptually, both mechanisms are capable of providing cellular devices the necessary method for authenticating base stations. We discuss their relative merits and demerits in the context of deployment.

5.3.1 Infeasible Symmetric Key-based Broadcast Authentication Mechanisms

One infeasible but straightforward symmetric key based approach for providing broadcast authentication is to use Message Authentication Codes (MAC) [85]. At its core, a MAC-based authentication mechanism can provide the integrity protection for the broadcast messages without incurring substantial computational or space overhead. Having an effective MAC-based authentication mechanism, however, boils down to effective key management. Sharing a single symmetric key between all devices and base stations is not viable as the adversary can extract the key and subsequently bypass the security. Having a pre-shared key between each pair of device and base station, on the other hand, is infeasible with respect to key management and storage requirements.

Another promising symmetric key based (i.e., MAC-based) authentication mechanism is the TESLA protocol [79]. It has particularly been shown to be effective for sensor networks. It addresses the broadcast authentication problem, for a setting in which there is a single sender but multiple receivers, through the use of delayed key disclosure and one-way key chains. Due to its promised security guarantees, we qualitatively analyze its feasibility with respect to the deployment constraints of cellular networks.

TESLA Protocol Description.

In TESLA, the sender and the receivers are considered to be loosely time-synchronized. The sender uses the elements of a hash chain (in the reverse order) and a pseudo-random function to create a one-time symmetric key to generate a MAC for the broadcast signals. Each key for verification is released at a stipulated later point of time until which the message in need of authentication is required to be buffered on the receiver side. Note that, for receivers and the sender to go through a loose time synchronization procedure, *an authenticated channel* is assumed to exist apriori

through which the sender sends the key disclosure schedule that allows the receivers to estimate when a certain key will be disclosed.

TESLA for Cellular Networks.

For applying TESLA in our context, we have to first accomplish the required time synchronization between the sender and receivers. Fortunately, time synchronization is inherently provided by cellular networks through the use of MIB messages. The next challenge of applying TESLA is to satisfy its assumption of a pre-existing authenticated channel to share the disclosure delay and initial key commitment with the receivers. This suggests that the base station should include this information inside a MIB message while ensuring its authenticity and integrity. Without such guarantees, a fake base station can simply broadcast its own TESLA protocol parameters, which a cellular device will not be able to distinguish from a legitimate one. One possible approach of addressing this challenge is to use some form of digital signatures. This would require the base station to have a public-key whose authenticity can be verified by the device with the use of a PKI and a trust anchor stored in the device. The use of digital signatures and PKI, however, undermines the actual purpose of using a symmetric key based approach. Moreover, for TESLA to work, the base station always needs to send an additional message (e.g., SIB3) that discloses the key used for generating MAC of the previous messages (e.g., SIB2). In addition, due to its delayed key disclosure, cellular devices have to wait for other key disclosing SIB messages before establishing the connection inducing a substantial delay in the initial connection setup with the core network. In summary, due to its latency overhead and reliance on a PKI, we conclude that TESLA is an infeasible mechanism for our domain.

5.3.2 Asymmetric Key-based Broadcast Authentication (PKI)

In this section, we briefly present a high-level overview of a PKI-based secure bootstrapping mechanism that we envision and then outline the challenges one has

to address for achieving an optimal PKI-based broadcast authentication scheme for cellular networks.

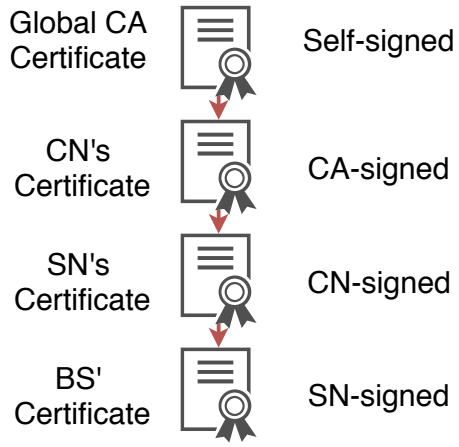

Figure 5.1.: Initial PKI Scheme.

High-level Overview of PKI-based Solution

In our initial attempt at developing a PKI-based solution, we consider the following stakeholders: the core network/network operator (denoted with CN); the serving network or MME (denoted with SN); the base station (denoted with BS). We consider each of these entities to possess a public-key, secret-key pair of the form $\langle P, S \rangle$. Each of these entities also has a public-key certificate (e.g., X.509 certificate) which maps its identity to the public-key (See Figure 5.1). The BS' certificate is digitally signed by the secret key of the serving network (i.e., S_{SN}). Similarly, the serving network's certificate is digitally signed by the CN's private key (i.e., S_{CN}). We also consider a global certificate authority (CA) which also has a self-signed certificate which will be stored in the device's memory and will be used as the trust anchor, that is, the CA's secret key will be used to digitally sign the CN's certificate. Once such a PKI is established, it is possible to provide a mechanism through which a device can authenticate a base station.

In such a mechanism (see Figure 5.2), for authenticating a specific bootstrapping message m, the base station (i.e., BS_j) using its secret key $\mathsf{S}_{\mathsf{BS_j}}$ will generate the

signature $\mathsf{sig_m}$ of m and will append the signature (e.g., $\mathsf{sig_{SIB}}$ for a SIB message) and the certificate-chain $\langle \mathsf{sig_m}, \mathsf{cert_{BS_j}}, \mathsf{cert_{SN_i}}, \mathsf{cert_{CN}} \rangle$ to m. Once the device receives m, its digital signature, and the certificate chain, it will first verify the certificate chain and then will verify m's digital signature. Legacy devices in which signature verification mechanisms are not present or will be too demanding, on the other hand, can safely ignore both the signature and certificate chain.

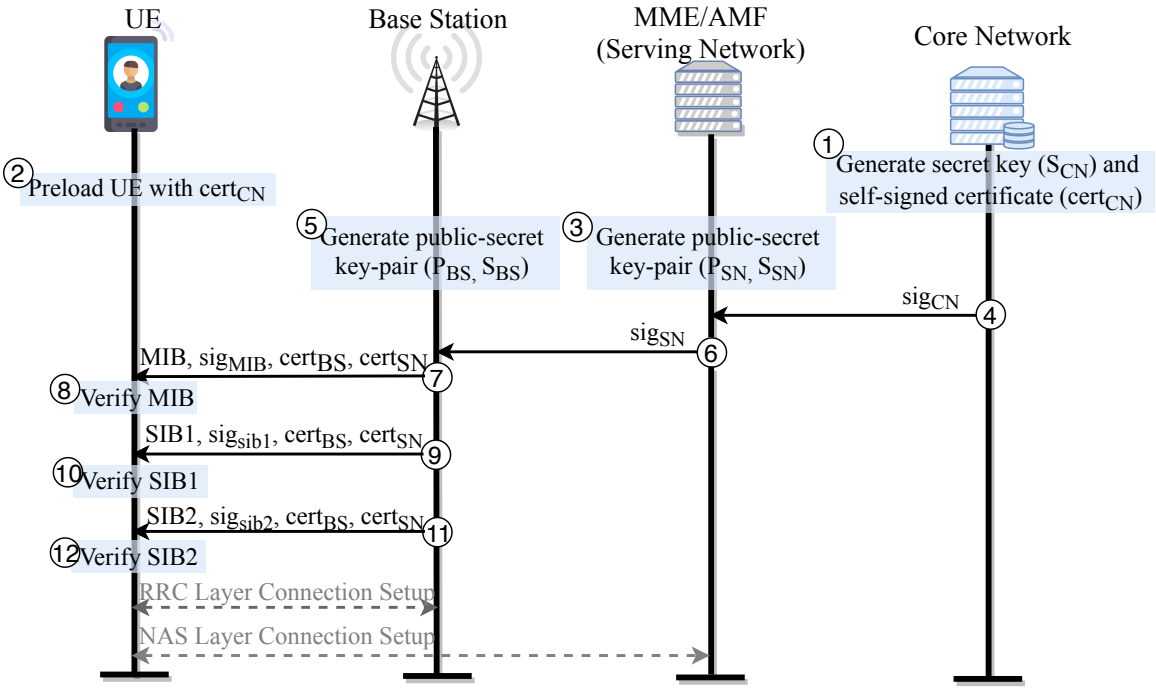

Figure 5.2.: Proposed PKI Scheme.

Deployment challenges. Realizing the above straightforward mechanism in practice, however, requires us to address the following challenges. (i) There is an upper-limit on the size of MIB and SIB messages which imposes an upper-limit on the size of the certificate chain. Since the size of a X.509-based certificate [80] is prohibitively large, it is nearly impossible to fit the X.509 certificate-chain in a single MIB/SIB message. We have empirically validated this claim. (ii) It is not clear how would one facilitate certificate revocation in our setting. (iii) The broadcast signals along with the digital signature can be relayed/replayed by a Man-in-the-Middle (MitM) relay attacker possibly luring devices to connect to a fake base station. (iv)

The base station frequently broadcasts the MIB and SIB messages (e.g., SIB is sent every 80 ms) and hence to maintain this transmission schedule the packet construction overhead including the signature generation time should be minimized.

5.4 Optimized PKI Scheme

In this section, we discuss how we address the above challenges by optimizing the proposed scheme from three dimensions: (1) PKI-level, (2) protocol-level, and (3) cryptographic scheme-level.

5.4.1 PKI-level Optimizations

Realigning trust anchor. As the device inherently has to trust the core network, one can provision the SIM card to use the core network's certificate as the trust anchor instead of the glocal CA's certificate. This has the added benefit of decreasing the certificate chain length which in turn reduces the message size and computation time for verifying the chain. In case of roaming, the SIM card can be equipped with (or, delivered over-the-air) the certificates belonging to the roaming network operators. This is particularly feasible due to the recent introduction of eSIM cards [86].

A Lightweight Design of Certificate. A general X.509 certificate is equipped with many different fields and extensions which are not particularly relevant to our context and hence can easily be omitted. We, therefore, propose a specialized certificate format only containing the following necessary fields:

$$\mathsf{cert_{CN}} = \mathsf{P_{CN}}, \mathsf{MCC}, \mathsf{MNC}, \mathsf{ext_{cert_{CN}}}$$

$$\mathsf{cert_{SN_i}} = \mathsf{P_{SN_i}}, \mathsf{SN\_ID}, \mathsf{ext_{cert_{SN_i}}}, \mathsf{sig_{CN}}$$

$$\mathsf{cert_{BS_j}} = \mathsf{P_{BS_j}}, \mathsf{CELL\_ID}, \mathsf{loc_{BS_j}}, \mathsf{ext_{cert_{BS_j}}}, \mathsf{sig_{SN_i}}$$

where, MCC and MNC form the unique network ID, $\mathsf{SN\_ID}$ and $\mathsf{CELL\_ID}$ respectively represent the unique identities of $\mathsf{SN_i}$ and $\mathsf{BS_j}$, $\mathsf{loc_{BS_j}}$ denotes the physical location (i.e., latitude and longitude) of $\mathsf{BS_j}$, and $\mathsf{ext_{cert_{CN}}}$and $\mathsf{ext_{cert_{SN_i}}}$indicate the certificate

expiration time for CN and $\mathsf{SN_i}$, respectively. The core network's signature for $\mathsf{SN_i}$ (i.e., $\mathsf{sig_{CN}}$), and the $\mathsf{SN_i}$'s signature for $\mathsf{BS_j}$ (i.e., $\mathsf{sig_{SN_i}}$) are computed as follows:

$$\mathsf{sig_{CN}} = sign(\langle \mathsf{P_{SN_i}}, \mathsf{SN\_ID}, \mathsf{ext_{cert_{SN_i}}} \rangle, \mathsf{S_{CN}})$$
$$\mathsf{sig_{SN_i}} = sign(\langle \mathsf{P_{BS_j}}, \mathsf{CELL\_ID}, \mathsf{loc_{BS_j}}, \mathsf{ext_{cert_{BS_j}}} \rangle, \mathsf{S_{SN_i}})$$

where $sign(m, K)$ function generates the digital signature of a given message m with respect to a secret key K.

Certificate revocation. Instead of an explicit revocation mechanism (e.g., CRL, OCSP), we rely on short-lived certificates (e.g., <10 minutes) for the base stations. The exact validity period of base station certificates is left as an implementation parameter and its value directly influences the exploitation window size when base stations are compromised.

5.4.2 Protocol-level Optimizations

Since including authentication material increases both the packet size and computational time on the base station and device sides, we minimize the overhead by: (a) Providing authentication guarantees for only critical messages; (b) Aggregating authentication of multiple messages; (c) Limiting the certificate chain transmission.

Authenticating Critical Broadcast Signals

Ideally, all broadcast messages should be authenticated, however, such an approach can be impractical due to its substantial communication and computational overhead requirement. We thus only provide authentication guarantees for a limited number of bootstrapping messages.

Messages requiring authentication. During bootstrapping, frame synchronization signals and MIB provide instructions on how to decode subsequent SIB messages and thus enable devices to achieve current system frame time synchronization with the base station. The SIB messages, on the other hand, provide information neces-

sary for connection establishment. Therefore, if only SIB messages are authenticated instead of frame synchronization and MIB messages, an adversary may only achieve a DoS attack by jamming the network through desynchronizing the frames, which, as mentioned earlier, is out of the scope of this work. Thus, we do not provide authentication for frame synchronization and MIB messages.

Which SIBs to authenticate?. According to the 3GPP standard, there are 13 System Information Block (SIB) messages (i.e., SIB1-13) characterized by the type of information they carry. SIB1 provides the essential information regarding the radio access network (RAN) and includes a broadcast schedule for subsequent SIB messages. Authenticating SIB1 thus guarantees that devices will obtain legitimate access information along with a legitimate broadcast schedule. Otherwise, the adversary could inject fake scheduling information as well as fake SIBs which would enable him to broadcast fake emergency alerts using SIB1 and SIB10-11 messages. Therefore, SIB1 requires authentication and integrity protection.

SIB2 immediately follows SIB1 and provides the necessary information for initiating the attach procedure (i.e., initial connection with the base station and the core network). Since SIB2 contains critical information for connecting to the base station, we provide authentication for this message. Protection for the other SIBs is not mandatory as they are not critical to connection bootstrapping.

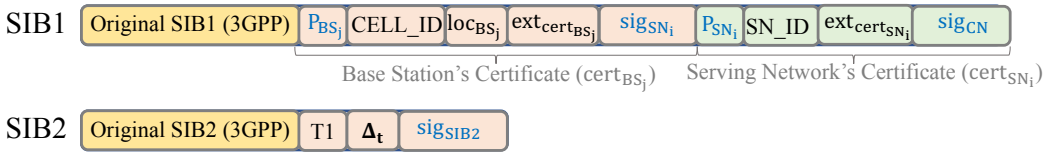

Figure 5.3.: Content of SIB1 and SIB2 after protocol-level optimization for secure broadcast authentication

Minimizing certificate chain transmission

Since SIB1 and SIB2 are sent in the same radio frame, the probability of one of the certificates in the chain getting revoked between SIB1 and SIB2 is negligible. The

base station thus transmits the certificate chain with SIB1 message only, and expects the device to use the same base station public key for authenticating SIB2 signature. In the extreme case, revocation happens between SIB1 and SIB2, the base station can include the new certificate chain in SIB2 and its presence can be indicated by a single bit.

Aggregating authentication

Since a base station broadcasts SIB1 and SIB2 in the same radio frame (1 radio frame = 10 ms) but in a different subframe (1 subframe = 1 ms), and the cellular device does not initiate the connection with the base station before receiving SIB2, we propose to authenticate SIB1 and SIB2 messages together instead of authenticating them individually. Thus, the base station includes the certificate-chain in the SIB1 message whereas the digital signature authenticating SIB1 and SIB2 (i.e., $\mathsf{sig}_{\mathsf{SIB2}}$) is included in the SIB2 message. Precisely, $\mathsf{sig}_{\mathsf{SIB2}} = sign(\langle \mathsf{SIB1} \mid\mid \mathsf{SIB2} \rangle, \mathsf{S}_{\mathsf{BS_j}})$ (See Figure 5.3).

The device, therefore, should buffer the SIB1 message and verify both messages only after the reception of the SIB2 message. The device is also required to verify the certificate-chain included in the SIB1 message using $\mathsf{cert}_{\mathsf{CN}}$ provisioned in the SIM card. This aggregated authentication of SIB1 and SIB2 reduces the time, computational resources, and communication overhead otherwise incurred by individual authentications of SIB1 and SIB2 messages.

5.4.3 Cryptographic scheme-level Optimization

The choice of digital signature schemes can not only influence the security provided by a mechanism but also the overhead incurred due to the size of the signature, time to generate and verify a signature. As mentioned before, we aim to maintain respectable security (i.e., 112-bit) while optimizing for signature sizes and signature generation

time. In what follows, we discuss possible signatures schemes and their effectiveness in our context.

RSA and ECDSA. RSA [87] is one of the most widely used signature schemes in the wild. In our context, however, RSA is inappropriate as it requires a large key and generates a large signature when maintaining our desired 112-bit of security. In our evaluation, we observed that RSA keys and signatures are too large to fit in either SIB1 or SIB2 messages. Elliptic Curve Digital Signature Algorithm (ECDSA) [88] scheme, on the other hand, is a viable replacement of RSA as it can provide the same level of security with a smaller key and signature size compared to RSA. ECDSA signature generation and verification, however, incur a significant computational overhead due to its inherent expensive cryptographic operations.

BGLS. We also considered BGLS [89] which has two desired properties: (1) It generates fairly small signatures while maintaining the desired level of security; (2) It allows the aggregation of multiple digital signatures—generated from different private keys—into a single short signature. Property (2) of BGLS especially comes in handy for aggregating the signatures in the certificate chain (See Figure 5.4) which consequently reduces the communication overhead (in bytes). BGLS, however, incurs a substantial overhead on the verifier side due to expensive cryptographic pairing operations.

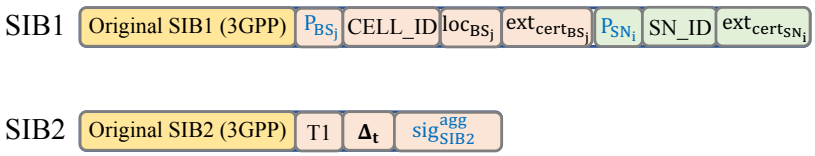

Figure 5.4.: Content of SIB1 and SIB2 after cryptographic scheme-level optimization for secure broadcast authentication

SCRA-BGLS: To further reduce the computation overhead of BGLS signature generation, we leverage the *Structure-free and Compact Real-time Authentication* (SCRA) framework [90] which divides the message signing operation into offline and online stages. It shifts the expensive parts of the signature generation algorithm to

the offline key-generation phase. The online signature generation phase leverages the pre-computed values from the offline phase and lightweight cryptographic operations.

In what follows, we briefly discuss how the SCRA algorithm works for generating SIB2's signature (i.e., $\mathsf{sig}^{\mathsf{agg}}_{\mathsf{SIB2}}$).

1) Key Generation (Offline): The offline stage is executed just once when the base station starts. A d-bit hash of $\mathsf{SIB1} \,||\, \mathsf{SIB2}$ can be thought of as L equal chunks of b bits each such that $b \cdot L = d$. A signature is computed for each b-bit integer concatenated with its corresponding index i and a predefined padding using the base station's secret-key $\mathsf{S}_{\mathsf{BS_j}}$. A pre-computed sub-message/signature table Γ is generated and stored at the sender's side.

2) Signature Generation: For the SIB2 message, the sender computes the cryptographic hash of $\mathsf{SIB1} \,||\, \mathsf{SIB2}$ and divides it into L chunks. It then fetches the corresponding signatures from the table Γ. Finally, it combines the signatures from the pre-computed table efficiently according to the base scheme.

3) Signature Verification: Upon reception of SIB1 and SIB2, the cellular device computes the hash of $\mathsf{SIB1} \,||\, \mathsf{SIB2}$ and runs the verification algorithm on the signature and the hash using the public keys $\mathsf{P}_{\mathsf{BS_j}}$, $\mathsf{P}_{\mathsf{SN_i}}$, and P_{CN} among which $\mathsf{P}_{\mathsf{BS_j}}$ and $\mathsf{P}_{\mathsf{SN_i}}$ are included in SIB1 message and P_{CN} is provisioned in the SIM card.

5.4.4 Countermeasure for Relay Attacks

Since not all control-plane cellular protocol messages are cryptographically protected, a fake base station f_{BS} relaying/replaying bootstrapping messages from a legitimate base station can lure devices to connect to f_{BS} and then can launch different attacks [65, 70]. Digital signatures alone cannot protect against such threats. For thwarting relay attack, one would ideally need to deploy a distance-bounding protocol which, however, has been shown to be difficult to realize in practice [64]. *To address such issue, we coarsely approximate a distance-bounding protocol by allowing each bootstrapping message to be valid for only a short period of time severely limiting the attack opportunity.*

In our approximation, we consider each SIB2 message to contain the following three additional fields: T_{gen} specifying the time which the SIB2 message was constructed; a location-dependent parameter Δ_t; $\mathsf{loc}_{\mathsf{BS_j}}$ denoting the latitude and longitude of the base station. If a device receives an SIB2 message at time $\mathsf{T_i}$, it would consider it valid if and only if $\mathsf{T_i} - \mathsf{T}_{\text{gen}} < \Delta_t$. A fake base station can only successfully relay a legitimate SIB2 if it can ensure that the relayed SIB2 message reaches the device within Δ_t time of T_{gen}. Under an appropriate Δ_t value, due to triangle inequality, one can avoid the threat of a relay attack (See Figure 5.5(b)).

Computing an exact value for Δ_t is non-trivial as it requires taking location-dependent signal interference into consideration which is very hard to approximate due to environment dynamics. We, however, show how to approximate lower and upper bounds of Δ_t which we envision a base station would calculate periodically. Our bound calculation requires the following constants.

- $\mathsf{C_{BS}}$: The time difference between when an SIB2 is generated (T_{gen}) and transmitted. A significant portion of this time will likely be spent on signature generation.
- $\mathsf{C_S}$: Transmission time of SIB2 from memory to network.
- $\mathsf{C_R}$: Time required by the device to receive and store an SIB2 message.
- R : Base station's broadcast radius in some unit d.
- S : Time required to cover one unit of distance ($d = 1$) at the speed of light.

Lower bound: The lower bound of Δ_t (denoted by Δ_{TL}) can be approximated by the maximum time required by an SIB2 message to travel from a legitimate base station to a device. This would require the device to be located at the farthest point from the legitimate base station within the cell. Figure 5.5(a) represents the scenario described above. In such a case, the network delay can be computed as $(\mathsf{R} * \mathsf{S})$; note that, S is not the speed of light. Hence, $\Delta_{TL} = C_{BS} + (R * S) + C_S + C_R$.

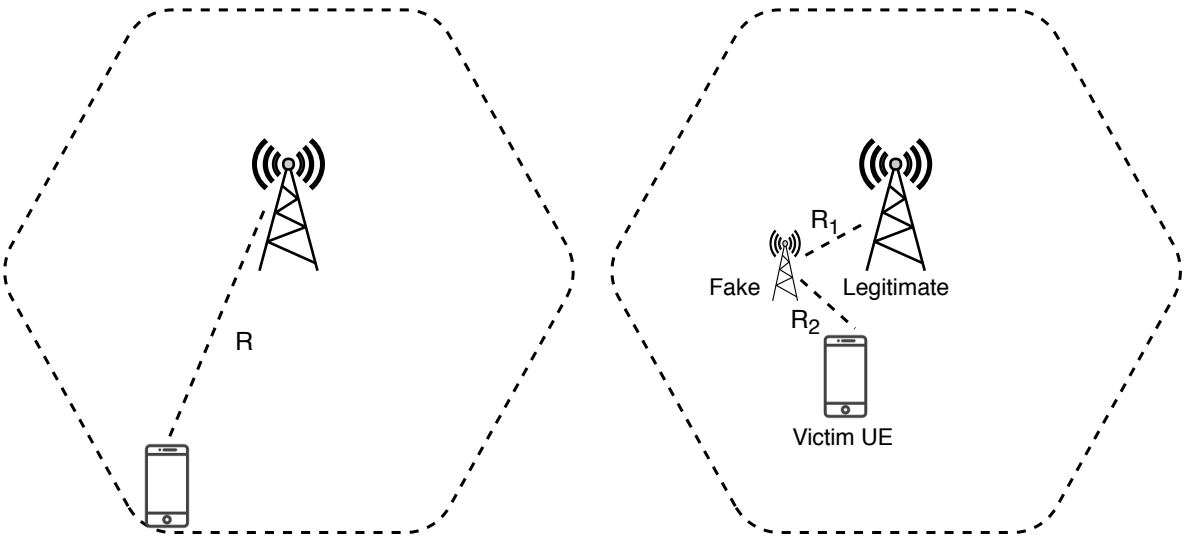

(a) Illustration for calculating the lower bound of Δ_t

(b) Illustration for calculating the upper bound of Δ_t.

Figure 5.5.: Computation of Δ_t bounds

Upper bound: The upper bound of Δ_t (denoted by Δ_{TU}) can be approximated by the minimum time required by a fake base station to successfully relay/replay a legitimate SIB2 message to a device. This scenario is shown in Figure 5.5(b). In this case, suppose that the distance between the legitimate and fake base station is $\mathsf{R_1}$ whereas the distance between the fake base station and the device is $\mathsf{R_2}$. As the SIB2 message is sent twice (once by the legitimate base station and then by the fake base station requiring a time of $2\mathsf{C_S}$) and also, received twice (once by the fake base station and then by the cellular device requiring a time of $2\mathsf{C_R}$). Therefore, the total time required for the SIB2 message to travel from a legitimate base station to the device through the fake base station can be computed as: $\Delta_{TU} = C_{BS} + ((R_1 + R_2) * S) + 2(C_S + C_R)$.

Selecting a value for Δ_t: Ideally, the total distance from the legitimate base station to the fake base station ($\mathsf{R_1}$) and from the fake base station to the victim device ($\mathsf{R_2}$) cannot be less than R, i.e., ($\mathsf{R_1}$+$\mathsf{R_2}$) $\geq \mathsf{R}$ due to triangle inequality. Moreover, the scenario in Figure 5.5(b) requires an extra round of message transmission and

reception incurring a cost of $2(\mathsf{C_S} + \mathsf{C_R})$ unit of time. Therefore, it is evident that $\Delta_{\mathsf{TL}} << \Delta_{\mathsf{TU}}$, and we need to select a value for Δ_t such that the following condition is satisfied: $\Delta_{TL} < \Delta_t < \Delta_{TU}$.

5.5 Evaluation

This section starts by describing our testbed setup, followed by the results of four sets of experiments used to evaluate and compare the proposed signature schemes in our PKI-based defense: 1) Overhead in bytes for SIB1 and SIB2; 2) End-to-end delay; 3) Signature generation time; 4) Signature verification time. We conclude by analyzing the time and storage requirements for the offline phase of SCRA-BGLS scheme.

5.5.1 Testbed Setup

Setup with 4G LTE (Why not 5G?). We chose to set up the testbed for 4G LTE mainly due to the following reasons: (1) there are currently no open-source implementations of 5G UE, base station, and core network available; and (2) the bootstrapping broadcast signals (i.e., the frame synchronization, MIB, and SIB signals) and the initial connection setup procedures for both 4G and 5G are identical. Hence, the overhead and security guarantees induced by our optimized PKI scheme in 4G LTE will likely transfer to 5G.

Base station and core network setup. We use a USRP B210 [54]) as the hardware component connected to an Intel Core i7 machine running Ubuntu 16.04. We used srsLTE [56], an open-source LTE protocol stack implementation, for establishing the base station and core network. We set up the base station and the core network in the same machine with srsENB [56] and srsEPC, respectively. We enhanced srsENB to allow signatures, public keys, and other necessary fields in SIB1 and SIB2 as non-critical extensions. By loading them as non-critical extensions, next-generation

UEs can adopt our defense while legacy devices simply ignore such fields, thereby maintaining backward compatibility.

UE setup. We use a similar USRP B210 [54] connected to an Intel Core i7 machine running srsUE [58] (open-source protocol stack implementation for UE) as the next generation UE which costs around $1300. We enhanced srsUE to follow our mechanism.

Why not actual UE? Since commercial 4G LTE modems' firmware are closed source, sending a patch containing our proposed solution is unachievable. To verify the backward compatibility of our solution, we use commercial off the shelf (COTS) phones which do not process the signatures and other critical fields in the SIB1 and SIB2 messages and thus are not affected by our proposed scheme.

Table 5.1.: Overhead in bytes per field in SIB1 message due to extra bytes added for authentication. N/A denotes that the field is not broadcast in SIB1 when using the given scheme.

SIB1				
Field	**ECDSA-192**	**ECDSA-224**	**BGLS**	**SCRA-BGLS**
MME Public Key	49	57	85	85
MME Public Key Expiration	4	4	4	4
MMEI	3	3	3	3
eNodeB Public Key	49	57	85	85
eNodeB Public Key Expiration	4	4	4	4
MME Signature	56	64	N/A	N/A
CN Signature	56	64	N/A	N/A
Total	221	253	181	181

5.5.2 Evaluation Results

We evaluate the effectiveness of our proposed defense with respect to the following metrics. We consider four digital signature schemes: (i) ECDSA-192, (ii) ECDSA-

Table 5.2.: Overhead in bytes per field in SIB2 message due to extra bytes added for authentication. N/A denotes that the field is not broadcast in SIB2 when using the given scheme.

SIB2				
Field	**ECDSA-192**	**ECDSA-224**	**BGLS**	**SCRA-BGLS**
Timestamp	4	4	4	4
Delta	2	2	2	2
Longitude	2	2	2	2
Latitude	2	2	2	2
SIB1+SIB2 Signature	56	64	N/A	N/A
Aggregated Signatures	N/A	N/A	29	29
Total	66	74	39	39

224, (iii) BGLS, and (iv) SCRA-BGLS for comparing our proposed PKI scheme with the baseline implementation which does not include broadcast authentication.

(I) Overhead in bytes. Table 5.1 and Table 5.2 show the byte overhead per field in SIB1 and SIB2 messages for ECDSA-192, ECDSA-224, BGLS, and SCRA-BGLS digital signature schemes. Table 5.1 shows that ECDSA-192 and ECDSA-224 require SIB1 to include two 56-byte and two 64-byte signatures of CN and MME, respectively, whereas the BGLS and SCRA-BGLS calls for no signature at all in SIB1 message. Since the base station with BGLS and SCRA-BGLS schemes aggergate CN's signature ($\mathsf{sig}_{\mathsf{CN}}$) and MME's signature ($\mathsf{sig}_{\mathsf{SN_i}}$) with SIB2's signature, SIB1 message does not induce additional overhead resulting from signatures.

Table 5.2 shows that SIB2 message with ECDSA-192 and ECDSA-224 schemes include one 56-byte and one 64-byte signatures, respectively, whereas both BGLS and SCRA-BGLS add only a small signature of size 29-byte to SIB2. This can be attributed to the capability of BGLS to generate compact signatures as well as to aggregate them into just one small signature. This means that BGLS and SCRA-

BGLS induce significantly smaller communication overhead than ECDSA-192 and ECDSA-224.

(II) Signature generation time. Two of the three signatures (i.e., CN Signature, MME Signature) in our optimized PKI scheme are computed by CN and MME offline and are shared with the base station at base station boot up time. These signatures can be used until the expiration time for each key is reached.

Table 5.3 shows the computation overhead, i.e., the time required for generating CN's and MME's signature offline with four different signature schemes and the corresponding time required for generating base station's signature at runtime. Since SCRA-BGLS takes lowest signature generation time (0.084 ms) and results in the smallest signature size (29-bytes) among four different schemes, we arguably prefer SCRA-BGLS over other schemes for computing CN's and MME's signatures offline.

Table 5.3.: The time it takes by the CN, MME, and base station to generate the required signatures. Note that CN's Signature and MME's signature are generated at offline whereas only eNodeB's signature is generated at runtime/online.

Algorithm	**CN Signature**		**MME Signature**		**eNodeB Signature**	
	Avg. (ms)	SD (ms)	Avg. (ms)	SD (ms)	Avg. (ms)	SD (ms)
ECDSA-192	1.14	0.24	0.83	0.139	0.48	0.7
ECDSA-224	1.20	0.01	1.19	0.02	1.21	0.02
BGLS	1.74	0.49	1.92	0.54	3.08	1.08
SCRA-BGLS	0.084	0.007	0.082	0.004	0.084	0.006

Due to the relay/replay protection, the timestamp and the signature of eNodeB for authenticating SIB1 and SIB2 have to be recomputed prior to every broadcast. Table 5.3 demonstrates that ECDSA-224 with larger key size induces longer latency (1.21 ms) than ECDSA-192 (0.48 ms) for generating eNodeB's signature on SIB1 and SIB2 whereas SCRA-BGLS induces significantly smaller (shortest among all) latency (0.084 ms) than BGLS (3.08 ms) because SCRA-BGLS minimizes the number of expensive cryptographic operations at runtime by offloading them to the offline

phase. Since the base station using BGLS aggregates the signatures of CN, MME, and eNodeB into one signature in SIB2 without leveraging the pre-computed signatures of small chunks, the time required to generate the aggregated signature using BGLS is higher than the rest.

Table 5.4.: The time taken by a UE to verify each individual signature when using ECDSA-192 and ECDSA-224.

Algorithm	**Verify CN Signature**		**Verify MME Signature**		**Verify eNodeB Signature**	
	Avg. (ms)	SD (ms)	Avg. (ms)	SD (ms)	Avg. (ms)	SD (ms)
ECDSA-192	1.26	0.15	1.31	0.18	1.32	0.16
ECDSA-224	2.27	0.19	2.26	0.21	2.27	0.23

(III) Signature verification time. With both ECDSA-192 and ECDSA-224, the UE verifies the signatures of CN, MME, and eNodeB individually. Table 5.4 shows the time individual signature verification takes for ECDSA-192 and ECDSA-224. Owing to higher key size, ECDSA-224 induces two times higher verification time ($\sim$2.25 ms) than ECDSA-192 does ($\sim$1.30 ms) for a single signature.

Table 5.5 shows the total time taken by a UE to verify the signatures when using different schemes. The signature verification time at UE, however, is significantly higher than the signature generation time (Table 5.3) at the base station due to the fact that the base station can reuse precomputed signatures whereas the UE must verify all three signatures separately. To avoid this, when using ECDSA-192, the UE could maintain pairing of signatures and the public keys of base station and MME in memory so that once these are verified, the UE can look them up on a table and avoid signature verification for subsequent messages.

Since, in both BGLS and SCRA-BGLS, a UE has to perform expensive bilinear pairing checks for verifying a signature, they both have significantly higher verification time (17.81 ms and 119.19 ms, respectively) than ECDSA-192 (3.81 ms) and ECDSA-224 (6.81 ms). Note that in BGLS there are only two pairing calculations whereas in SCRA-BGLS there are 32 pairing calculations for which SCRA-BGLS induces the

highest verification time among the four schemes. Since a device typically verifies signatures for one session whereas the base station keeps generating signatures for the bootstrapping signals based on its schedule (e.g., $\sim$80 milliseconds), we have chosen to minimize the overhead of the packet size and signature generation time at the base stations than the signature verification time at the UE. *Considering all these trade-offs, we argue that BGLS and SCRA-BGLS are more effective digital signature schemes than ECDSAs in the context of cellular ecosystems.*

Table 5.5.: The total time taken by a UE to verify the authenticity of the base station, i.e., to verify the signatures included in SIB1 and SIB2 messages for different signature schemes.

Algorithm	**Verify**	
	Avg. (ms)	SD (ms)
ECDSA-192	3.81	.01
ECDSA-224	6.81	0.33
BGLS	17.81	6.0
SCRA-BGLS	119.19	0.9

(IV) SCRA-BGLS pre-computation overhead. With SCRA-BGLS, the time required to pre-compute the signature table is 5729.36 ± 8.2 seconds and the space required to store that table is 160 KB when the total number of chunks is 32 and each chunk is 8-bits long.

(V) End-to-end delay. We define end-to-end delay (computed at the UE side) as the time between when an SIB1 message is received at UE and when the UE completes setting up the RRC layer connection with the base station. Figure 5.6 compares the baseline and four digital signature schemes with respect to end-to-end delay for a UE to connect with the legitimate base station. Each stacked bar in Figure 5.6 shows the transmission overhead (in times), signature generation, and verification times with three different individual segments. Due to large public key

Figure 5.6.: End-to-end delay induced by different digital signature schemes against baseline. For ease of comparison, Y-axis represents the log of the delay in milliseconds.

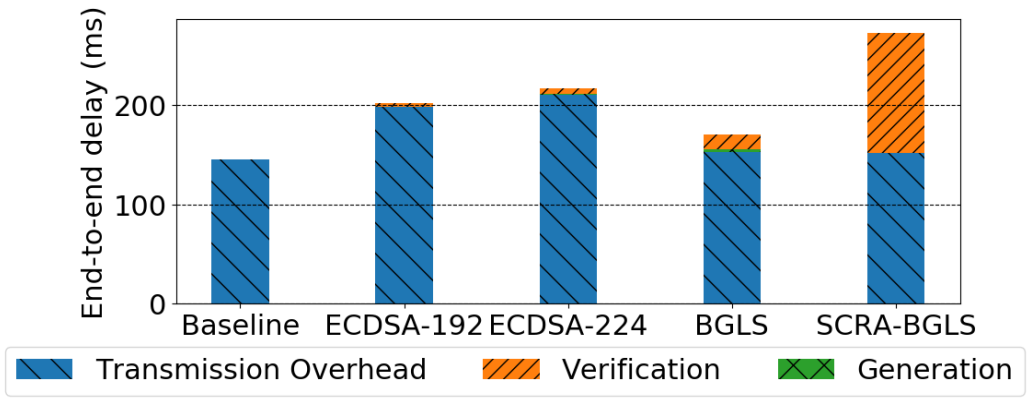

and signature, ECDSA-224 induces the highest transmission overhead ($\sim$210 ms) which naturally boils down our choice to BGLS and SCRA-BGLS that add negligible transmission overhead compared to the baseline.

5.6 Security Analysis

In this section, we analyze the security and privacy of our proposed PKI-based countermeasure with respect to the adversary model discussed in Section 5.2.1. We show that the adversary with the given capability cannot force a UE to connect to its fake base station when our proposed defense mechanism is in use.

- *The adversary cannot inject or modify SIB messages.* Since the adversary does not know the legitimate base station's private key, it will not be able to generate a valid signature of a fake SIB message. Thus the UE would not authenticate the SIB messages by the fake base stations. Similarly, the authentication will fail with our solution in place if an on-path attacker using man-in-the-middle relay modifies the contents of a legitimate SIB1 message. Since the UE eventually verifies SIB1 along SIB2 sent/received in the same radio frame, it rejects fabricated SIB messages and refrains from connecting to the fake base station.

- *The adversary cannot replay/relay SIB2 messages.* Since most of the parameters in the SIB1 and SIB2 messages are constant, our proposed solution uses the timestamp t as a nonce for generating non-deterministic signatures. The UE identifies the freshness of any SIB2 message using the t and the Δ_t parameters of the message. Computing freshness in this way would give the UE a performance edge since the UE will neither require storing previous SIB1 messages nor checking the signatures associated with the messages. With the relay/replay protection incorporated into our proposed PKI cheme, the UE will be able to prevent DNS redirection and phishing attacks [70].

- *The adversary cannot inject other control-plane protocol messages usually sent after MIB and SIB.* With our proposed solution a UE is able to identify fake base stations by verifying the authenticity of the SIB messages, it never establishes the RRC layer connection to the fake base station. This thwarts the fake base station from injecting unauthenticated malicious messages. The UE, therefore, with our solution in place will not expose its IMSI, or downgrade to 3G/2G or enable its location tracking by attackers.

However, the adversary can still sniff messages sent by the legitimate parties and can overhear IMSI in the attach_request and the identity_response messages. This type of IMSI catching attack is very hard to detect since the adversary does not leave any footprints. The upcoming 5G, however, solves this problem by enabling a UE to encrypt its IMSI while sending attach_request or identity_request message to the core network.

5.7 Discussion

In this section, we discuss two salient aspects of our proposed countermeasure.

GPS Time. One important limitation with our proposed solution is the requirement for precise time synchronization without the usage of SIB messages which essentially leads to the requirement of GPS time capability for cellular devices.

Asymmetric cryptography in 5G. In 5G, the cellular device is already provisioned with the public key of the core network using which the device encrypts its IMSI while sending the IMSI in an over-the-air (OTA) message. This prevents devices' IMSIs from getting exposed to the IMSI-Catchers [18]. Such PKI for 5G already in place should enable the cellular ecosystem to seamlessly adopt our proposed PKI scheme for achieving secure connection bootstrapping that protects cellular devices from most of the active attacks including IMSI-Catching attacks.

5.8 Summary

In this work, we investigate cryptography-backed authentication mechanisms to prevent adversaries, from luring unsuspecting cellular devices to connect to malicious base stations. We accomplish this by enabling next generation cellular devices to authenticate the legitimacy of a base station, prior to connection. We overcome the constraints imposed by both the ecosystem and stakeholders, and design an optimized PKI scheme. We leverage precomputation-based digital signature generation algorithms and employ different domain-specific optimizations to address the trilemma imposed by digital signatures. We then implement our mechanism and observe that our authentication scheme with the best performing digital signature algorithm imposes moderate overhead in bytes ($\sim$**220** bytes) and minimal overhead connection time wise ($\sim$**28** ms), all while maintaining backwards compatibility.

Even with a PKI-based countermeasure in place, the adversary can still circumvent such defenses to perform `ToRPEDO` attack for which we continue our investigation of countermeasures against the side-channel attacks in the following chapter.

6. HARDENING AGAINST PRIVACY ATTACKS EXPLOITING SIDE-CHANNEL INFORMATION

Rreceiving and transmitting radio packets as part of the cellular communication protocol are arguably two of the most demanding functions of a cellular device with respect to energy consumption. Therefore, to save device energy, the cellular protocols allow a device to transition to a low-power, idle state when the network detects a predefined period of cellular inactivity from the device. It is, however, crucial to ensure that when the device is in such an idle state, it does not overlook any pending network services (e.g., phone call). This is where the cellular paging protocol comes into play. The paging protocol strives to achieve the right balance between the device's energy consumption and quality-of-service (e.g., timely delivery of services such as phone calls). When a device is in idle state, paging messages are used to notify a device for incoming phone calls, SMS, or data services. The device in idle state, therefore, wakes up periodically to poll for paging messages. For a given cellular device and the serving network, the exact time periods (i.e., the paging occasions) when the device polls for incoming paging messages are fixed. As we observed in Chapter 5 that this fixed nature of paging occasions is a fundamental weakness in both 4G and 5G which the adversary may exploit to associate a victim's soft identity, e.g., phone number or Twitter Handle with its paging occasion. This further enables the adversary to perform `ToRPEDO` attack through which the adversary can infer a victim's coarse-grained location information, inject fabricated paging messages, and mount denial-of-service attacks.

Existing efforts against location tracking attacks that exploit paging protocol. Recent studies [12, 17] exploit the deployment weakness of infrequent and predictable changes in the device's TMSI [34] which would allow an adversary to identify a user's presence in a geographical area. To achieve that the adversary places

multiple phone calls to victim's phone number which forces the network to expose the victim's TMSI in the broadcast paging messages. Though [12, 17] have suggested frequent reallocation of TMSI as a possible mitigation technique, the adversary can still identify a user's presence by circumventing the proposed countermeasure with our ToRPEDO attack. Even encrypted/anonymized TMSI or changing victim's TMSI after every VoLTE call cannot circumvent the ToRPEDO attack.

Challenges. The sheer mitigation of such side-channel attack requires a concerted effort from all cellular stakeholders as it warrants for changes in the standard. However, the vulnerability is so deeply rooted in the protocol that designing a clean-slate solution against such attack would pose the following requirements— (1) change other procedures of the protocol, (2) break the backward compatibility, and (3) induce performance loss— which would undermine the actual motivation of the paging procedure. Therefore, any countermeasure to prevent such side-channel attacks needs to address the following challenges: (a) *backward compatibility for legacy devices*, and (b) *overhead induced due to enhanced security.*

Our work. With the challenges in mind, we first explore the solution space against ToRPEDO attack in two dimensions— (1) protocol-level defense that remove the root cause of the attack, and (2) detection of the attack's (behavioral) signature. Our clean-slate design of the protocol-level countermeasure aims to make the paging occasions and the identities in the paging messages unpredictable for any device. However, this solution requires to change the protocol which in turn breaks the backward compatibility. In addition, changing paging occasions and identifiers after every paging message turns out to be practically unrealizable since it incurs prohibitive computational and memory overhead and unreasonable energy cost. All these limitations induce to shift our focus to a more practical approach based on noises by which a legitimate base station carefully injects fake paging messages containing legitimate devices' TMSIs. We evaluated its efficacy with real network traces for different operators. In our evaluation, we observed that with ~ 600 fake paging messages injected

within $\sim$ 40 seconds interval can prevent the adversary to perform the ToRPEDO attack with as many as $\sim$ 500 phone calls.

Contribution. To summarize, this work makes the following contributions.

- We propose a lightweight and noise-based countermeasure that raises the bar for the attackers without changing the protocol or breaking the backward compatibility.
- We implement and evaluate our proposed countermeasure with real network traces and demonstrate the efficacy of the countermeasure with respect to resiliency against the ToRPEDO attack and overhead due to added security.

6.1 Solution Space Exploration for ToRPEDO

It is only natural to consider countermeasures that primarily focus on either thwarting the root cause (i.e., fixed paging occasion) of ToRPEDO or defending against ToRPEDO through the detection of its (behavioral) signature. Such a view induces the following two categories of defenses, referred to as *Protocol-level* and *Signature-based* countermeasures. However, as we discuss below, these categories of countermeasures are ineffective due to deployment constraints. This inspired us to design a countermeasure which prevents the adversary from retrieving accurate side channel information through the addition of noise. We call this the *Noise-based* countermeasure and demonstrate that it can effectively thwart ToRPEDO without incurring substantial overhead.

6.1.1 Protocol-level Defenses

The main philosophy of protocol-level defenses is thwarting the root cause of ToRPEDO, that is, to ensure that a UE's paging occasion does not remain fixed in a particular cell area. Having the paging occasion rely on the TMSI instead of the IMSI can be a plausible solution. At a first glance, it seems that this solution would

work, but a recent study [17] has shown that network operators do not change TMSI frequently and even when they do, the TMSI remains predictable [34]. As most network operators reallocate the TMSI only after the CSFB, a TMSI would remain fixed for a device until a CSFB is executed. This may give the adversary ample time to launch ToRPEDO using VoLTE calls, SMS, or data services. Another naive solution would be to ensure that a device's TMSI is reallocated after it receives a paging message. Such a solution, however, is infeasible in practice due to its high energy demand for a device and high protocol overhead.

Another effective and seemingly plausible solution could potentially attempt to induce unpredictability of the following: (i) the identifier included in the paging message; (2) the paging occasion of a UE in a cell. To introduce randomness, however, it is crucial to ensure that both the UE and the eNodeB (and also the MME) share a common source of randomness from which to generate subsequent pseudorandom numbers to be used as both the identifier and paging occasion. We discuss the high-level design of this countermeasure to qualitatively compare it with our proposed countermeasure.

Unpredictable identifiers with unpredictable paging occasions. In this scheme, the core network and the device use TMSI as the seed for bootstrapping a sequence of pseudo random numbers, $\mathcal{R}$. Instead of including TMSI in the i^{th} paging message, the eNodeB would include a fresh pseudo TMSI (PTMSI) that would be the i^{th} element in a chain of random numbers from the start, i.e., $\mathcal{R}_i$. At a first approximation, it seems this approach has the advantage that both parties do not have to store a significant amount of information. Due to the network unreliability, however, it is plausible that paging messages are lost and as a consequence the two parties may become desynchronized. Addressing such a case would require the device to maintain a window of possible random values to match against the value received with the paging message. Supporting this corner case would impose substantial runtime and energy overhead which obviate the actual design motivation of paging procedure to conserve more energy and thus may be infeasible in practice.

In the similar vein, one can use the TMSI as a seed for generating a sequence of n pseudo-random numbers $r_1, \ldots, r_n$ on both the device and eNodeB sides during connection initiation. The eNodeB will include a PTMSI $\langle r_i, i \rangle$ instead of the TMSI in the paging message. Once the device receives the PTMSI $\langle r, j \rangle$, it extracts the index j and checks to see whether r matches the j^{th} random number that it had generated during bootstrapping. This approach chooses to invest on the storage side to decrease the runtime overhead of checking whether the PTMSI belongs to the device.

To make the paging occasion unpredictable, in the j^{th} round of paging, a random value rInd_j is generated from a seed (which is a shared secret between the device and the eNodeB established during the connection initiation) and is used as an offset to make the device's paging frame number unpredictable. The device would wake up on every system frame number SFN if the following holds: $\text{SFN} \bmod \text{T} \equiv \text{T} \times j + \text{PFIndex} + \text{rInd}_j$ where $j \geq 0$.

The cellular paging protocol is, however, designed so to enable a UE to receive paging messages without going through the connection bootstrapping [27, 31]. Without a successful bootstrapping, it is not clear how the UE and the eNodeB (resp., the MME) could establish the necessary shared, random seeds. Even when this deployment constraint is ignored, deploying this defense would require major overhaul in both the UE and network operator sides.

6.1.2 Signature-based Defense

Another dimension of defense that can be adopted by the network operators would be to use machine learning algorithms and deep packet inspection techniques to develop a signature of the `ToRPEDO` attack (e.g., a lot of silent calls or SMS on the victim's phone number within a particular time interval) and preventing `ToRPEDO` by applying countermeasures (e.g., rate-limiting) whenever such a signature is detected [91–96]. An adversary, however, may evade the detection of such signatures by increasing delays between subsequent phone calls. Along with the resource overhead on the net-

work operator side, another critical challenge of deploying such a defense is to balance the detection rate without compromising the quality of service for benign users.

6.2 Our Proposed Noise-based Countermeasure

We now describe our noise-based countermeasure which raises the bar for attackers to infer a user's paging occasion.

The high-level idea. The basic idea of our proposed countermeasure is to increase the current paging rate (λ^{c}_{paging}) of all paging occasions to a certain level (λ^{e}) so that the adversary would need a high number of silent calls to sufficiently differentiate the paging rate of victim's paging occasion from others. To increase the paging rate, we propose that an eNodeB injects new paging messages at the paging occasions for which the paging rate is relatively lower than expected rate (λ^{e}). The eNodeB will also add new paging records to both the actual paging messages (note that, at most 16 paging records can be sent in a single paging message) and the noisy paging messages to increase the current base rate of paging records.

Noisy paging messages. An intuitive and seemingly practical choice for creating noisy paging messages would be to use fake/non-existing TMSIs so that the current devices in the network do not respond to the noisy paging messages containing the fake TMSIs. However, the adversary may distinguish the fake paging records by identifying the messages/TMSIs for which there is no response from the devices. Although identifying fake paging messages is exceedingly difficult, we do not rule out this possibility and thereby propose an eNodeB to add existing TMSIs for which the actual paging messages were recently (e.g., previous 10 minutes) requested by the network. Such noisy paging messages with legitimate TMSIs may cause a device to respond to the additional paging messages for which there is no actual pending incoming services.

CS (circuit-switch) domain records. As shown in `ToRPEDO` attack validation, the base rate of paging containing CS records is substantially low. Consequently,

the adversary only needs 2-3 silent phone calls for a successful ToRPEDO attack. To protect against this, especially in case of an incoming CSFB service, we prescribe the network to send a paging message in the PS domain first, and following it up with a cs_service_notification message to the UE through a dedicated logical channel.

6.3 Evaluation of Noise-based Countermeasure

In this section, we evaluate our countermeasure based on its effectiveness and overhead.

Network bandwidth overhead. For evaluating the operator's bandwidth requirement, we varied λ^e in the range of [0.13, 1.0] and measured the number of fake paging messages (resp., PS records) injected by the network operator. The results are shown in Figure 6.1(a). As expected, increasing λ^e results in an increase in the number of injected fake paging messages (resp., records). For $\lambda^e = 1.0$, the maximum number of injected paging messages (resp., PS records) is ~ 600 (resp., ~ 1200).

Countermeasure effectiveness. For measuring the effectiveness of our countermeasure, we varied λ^e in the range of [0.13, 1.0] and calculated the number of calls the adversary would need for a successful ToRPEDO attack. The results are shown in Figure 6.1(b). Increasing the injected noise (i.e., increase of λ^e) slows the attacker down by requiring more calls for a successful ToRPEDO attack. When λ^e reaches 1.0, we observed that ToRPEDO did not succeed with 500 calls.

UE overhead. For measuring the UE-side overhead when our countermeasure is deployed, we first calculated the number of spurious paging messages a UE would have to respond due to fake paging message injection. Figure 6.1(c) shows the results about the number of paging messages (both actual and noisy) containing an existing TMSI in a 30 paging-cycles (=38.4 seconds) time interval when the eNodeB uses actual TMSIs to generate noisy paging messages. It also shows that a device would receive ~ 1 additional spurious paging message.

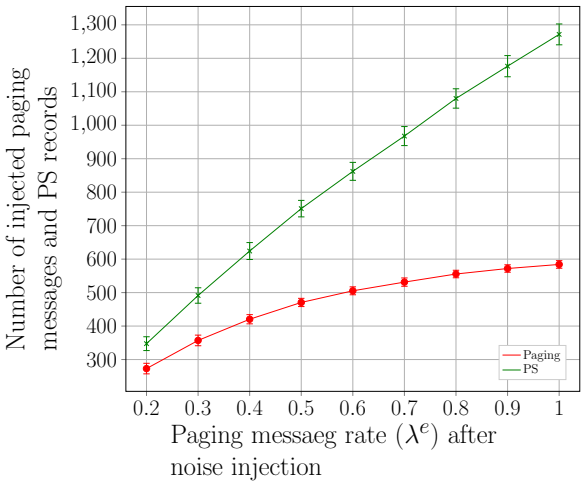

(a) # paging messages and PS records injected to increase the paging rate. The base rate were $\lambda^{\text{paging}_b} = 0.13$ and $\lambda_b^{\text{ps}} = 0.15$

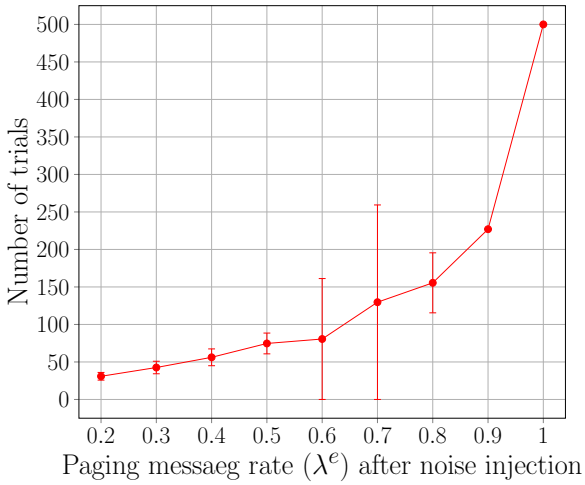

(b) vg. # of trials required to perform ToRPEDO attack against the increased paging rate using noise injection.

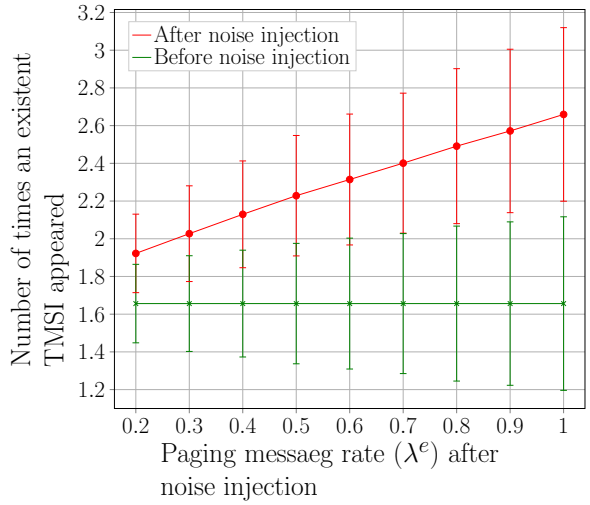

(c) Total number of (considering both noisy and actual) paging messages containing an existent TMSI in 38.4 seconds.

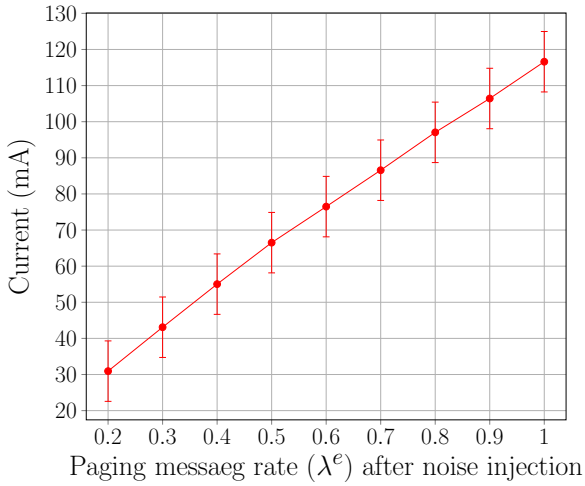

(d) Extra power consumed by a device for different levels of noises.

Figure 6.1.: Effectiveness and overhead of our proposed noise-based defense mechanism.

We then used an existing power model [97] for our test phone to calculate the energy a UE would require to respond to additional spurious paging message(s).

Table 6.1.: Qualitative comparison among three plausible defenses against the ToRPEDO attack (✓=YES, and ✗=NO).

Approach	Change in Protocol?	Change in UE implementation?	Change in network implementation?	Change in other procedures?	Backward compatible?	Overhead
Protocol-level defense	✓	✓	✓	✓	✗	HIGH
Signature-based defense	✗	✗	✓	✗	✗	HIGH
Noise-based defense	✗	✗	✗	✗	✓	LOW

Figure 6.1(d) shows results of the additional energy requirement in terms of electric current flow (in milliampere or mA) with varying λ^e. As expected, increasing λ^e results in an increase of the UE's energy requirement; the maximum value being ~ 117 mA.

Qualitative comparison. Table 6.1 compares our proposed noise-based defense with the two other plausible countermeasures discussed in Section 6.1. Our comparison is based on following aspects: does a solution require changing in the — (i) protocol, (ii) device-side implementations, (iii) network-side implementations, (iv) design of other protocols, such as attach, detach, or tracking area update procedures), (v) is the solution backward compatible, and (vi) overhead incurred by the defense. Table 6.1 summarizes that our noise-based countermeasure outperforms the protocol-level defense and the signature-based defenses with respect to every aspect.

6.4 Summary

In this chapter, we first identify and characterize plausible countermeasures against the side-channel attacks. We then design and evaluate a novel countermeasure for ToRPEDO that raises the bar for the attacker without incurring substantial overhead or violating common-sense deployment constraints.

7. RELATED WORK

In this section, we discuss existing efforts that focus on the security, privacy, and availability of cellular networks. In this context, although prior work has extensively investigated the security and privacy issues of 2G and 3G protocols [10–12, 74, 75], there is less work that addresses the same concerns for the 4G LTE [17] and 5G networks.

The closest to LTEInspector's approach is by Tu et al. [6] which focus on identifying non-trivial interactions—using an explicit-state model checker [39]—between the different control-plane protocol layers of LTE. Unlike LTEInspector, their approach, however, can neither explicitly reason about adversarial actions nor can support cryptographic constructs.

Man-in-the-Middle Attacks: Meyer et al. [16] exploit the null integrity of the security_mode_command message in 3G networks to perform a man-in-the-middle attack. In contrast, our authentication relay attack in 4G LTE allows the adversary to connect to the EPC without nullifying the security capabilities. In this attack the adversary, however, cannot decrypt or inject valid encrypted messages unless the operator uses a weak or no security context. Rupprecht et al. [59] used an implementation bug in a particular LTE dongle (Huawei E3276 USB Dongle) to demonstrate a man-in-the-middle attack for 4G LTE.The 3GPP standard [27] strictly prohibits on using null integrity algorithm by the 4G LTE capable UEs.

IMSI Catching Attacks: The IMSI catching attacks [9, 98, 99] still prevail for 4G LTE networks as they did for 2G and 3G networks. In contrast to traditional IMSI catchers where the adversary forces the UE to expose the IMSI/IMEI, the PIERCER demonstrated in this thesis forces the network to expose the user's IMSI/IMEI and thus uniquely maps a phone number to its IMSI which was supposed to be only possible by law enforcement agencies with operators' cooperation. Although the

security-conscious cellular stakeholders may have had a hunch about the plausibility of the 4G `IMSI-Cracking` attack, to the best of our knowledge, we are the first to develop and demonstrate a complete attack in both 4G and 5G.

Linkability Attacks: Arapinis et al. [14] exploit the paging messages with GUTI for linking the IMSI to the GUTI in 3G protocols. In contrast, by using paging message with IMSI in 4G LTE we demonstrate how an adversary along with other attacks (discussed in Section 3.2.2) can link the IMSIs in 3GPP [27] and the old PMSI with the new PMSI in the enhanced Authentication and Key Agreement (AKA) mechanism [20].

Traceability Attacks: Arapinis et al. [15] showed a traceability attack by exploiting an implementation bug in the 3G network which violates the 3GPP standard recommendation of adopting new temporary identity for the UE with a tracking area change. In another work, Arapinis et al. [14] demonstrate another traceability attack in which the adversary replays the auth_request for the victim UE to all the UEs in an area and detects the presence of the victim UE from the cause of the error (MAC failure or SQN synchronization failure). In contrast, our traceability attack with the *security mode command* procedure exploits the missing nonces in security_mode_command, a different implementation bug of the commercial networks.

Location tracking through TMSI. The 3GPP standard [4] suggests to use TMSI and change it frequently to hide users' IMSI/IMEIs. However, prior work [12, 17] has shown that an adversary can still exploit the operational network's misconfiguration of frequent TMSI change, and thus track a user by uniquely mapping a phone number to its TMSI which often does not get replaced even for three days [17]. The most recent work [34] along this direction exposes operational networks' vulnerability of not properly randomizing the TMSIs while reallocating them to the subscribers. As a result, some of the bytes are fixed [53] between the old and new TMSIs through which the adversary can still infer the new TMSI and track the subscriber. In contrast, our `ToRPEDO` exploits protocol standard's vulnerability of choosing fixed paging frames for a subscriber which makes all the network operators vulnerable to this attack.

Denial-of-Service (DoS) Attacks: Shaik et al. [17] demonstrate 3 DoS attacks against UEs in which downgrading to 3G/2G and denial of all network services are performed with the same tracking_area_update_reject message with just two different causes. In contrast, our DoS attacks use four new techniques as discussed in Section 3.2. As opposed to the DoS attacks against the UE, Jover et al. [19] discuss a DoS attack against the EPC using a compromised UE/eNodeB that sends huge number of attach_request messages to the EPC and thus takes the EPC down. Jermyn et al. [100] show a similar DoS attack and simulate a set of compromised UEs that exhaust the victim UEs' traffic capacity. Golde et al. [53] exploit a race condition in the paging message responses in 2G networks that enables a malicious UE to send the paging_response message before the victim UE, and thus preventing the victim UE from receiving incoming phone calls/SMS.

Data Stealing Attacks: Kim et al. [101] and Li et al. [102] address the vulnerabilities of VoLTE call setup and show caller spoofing, over-billing, and denial-of-service attacks. In contrast, our focus is on attach, detach and paging procedures of 4G LTE and 5G protocols. Sahin et al. [91] study the possible techniques to detect and measure an interconnect telecom fraud that diverts a normal phone call without explicit authorization to voice over IP chat application. Sahin et al. [92] also systematically survey different types of telephony frauds and propose a comprehensive taxonomy of these frauds.

Fake base station detection. To detect fake base stations acting as IMSI-catchers, Dabrowski et al. [18] propose to use stationary hardware units to scan frequency bands, collect cellular data and find anomalous communication patterns. This, however, has the limitation of requiring expensive hardware units and scalability. In addition, Borgaonkar et al. demonstrate that such signature-based fake base detection schemes are susceptible to new attack variants [103]. Dabrowski et al. [104] also look into detecting such fake devices using the operator side data and combine both client and operator side detections which, however, are vulnerable since the data is generated and analyzed after the cellular devices connect to the IMSI-catchers. Li

et al. [76] use crowdsourced data to detect fake base stations that broadcast fake SMS messages to scam the victims. Though they have promising results in this very specific scenario, there exists two important limitations: First, there is little to no ground truth available for this type of attack. Second, they can only detect fake base stations with known communication patterns that broadcast fake SMS messages [76]. Ney et al. [105] propose to solve this problem using sensors mounted in vehicles. This solution comes with the benefit that no subscribers need to connect to such devices to create traces which otherwise could later serve as a basis to detect them and instead use the data collected by these sensors. This, however, suffers from the limitation that such sensors would be expensive to deploy and would cause the scalability issues.

Preventing exposure of IMSI. Khan et al. [106] propose a solution to conceal the IMSI using Identity Based Encryption and provide authentication. This, however, comes with the challenge of imposing computation overhead at the Home Subscriber Network since it would require a public-private key pair for each subscriber. Pseudonym-based IMSI concealment techniques [20,107,108] might prevent the exposure of IMSI, however, the attacker could still perform downgrade attacks, and thus expose the IMSI through 4G/3G.

Mutual Authentication. The root cause of IMSI-catchers is the failure to authenticate the fake base station prior to connection. A common approach to this problem is a PKI-based solution that fully relies on certificates. A common theme in these solutions, is the core network acting as a CA and in the process, signs certificates for every MME/AMF in the network [109–111]. These solutions, however, impose a significant computational overhead at the base station and induce high communication overhead due to the lack of optimizations in authenticating a broadcast message. Though this solution proves to be computationally feasible, the IMSI can be still exposed due to the failure of SIB message's authentication.

8. CONCLUSION AND FUTURE RESEARCH DIRECTIONS

In this dissertation, we develop principled security and privacy analysis frameworks for cellular networks and design countermeasures against fake base stations and side channel attacks.

We propose LTEInspector which employs an adversarial model-based testing philosophy for exposing attacks against three critical procedures of 4G LTE. LTEInspector harnesses the strengths of both a symbolic model checkers and a protocol verifier and is demonstrated to be effective in finding 10 novel and 9 prior attacks. We have also validated most of our attacks (i.e., 8 out of 10) in a testbed.

Our work on side-channel attacks sheds light on an inherent design weakness of the 4G/5G cellular paging protocol which can be exploited by an attacker to not only obtain the victim's paging occasion but also to identify the victim's presence in a particular cell area just from the victim's soft-identity (e.g., phone number, Twitter handle) with a novel attack called `ToRPEDO`. We also demonstrate that `ToRPEDO` can enable an attacker to exploit a deployment oversight of several network operators to retrieve a victim's IMSI from his phone number using the `PIERCER` attack. To further provide evidence of `ToRPEDO`'s potency, we show that it empowers an attacker to launch a brute-force `IMSI-Cracking` attack through the use of two novels oracles we designed for 4G and 5G, respectively. Each of these attacks can also be leveraged to enhance prior attacks. All of our attacks have been validated in realistic setting for 4G using cheap software-defined radio and open-source protocol stack.

We also investigate countermeasures for preventing adversaries, from luring unsuspecting cellular devices to connect to malicious base stations, by empowering the cellular device to authenticate legitimate base stations. We accomplish this by enabling next generation cellular devices to authenticate the legitimacy of a base station, prior

to connection. We overcome the constraints imposed by both the ecosystem and stakeholders, and design an optimized PKI scheme. We leverage precomputation-based digital signature generation algorithms and employ different domain-specific optimizations to address the trilemma imposed by digital signatures.

Finally, as part of our investigation on the cellular paging protocol, we also design and evaluate a novel countermeasure for ToRPEDO that raises the bar for the attacker without incurring substantial overhead or violating common-sense deployment constraints.

Future work. In future, we would like to explore the following four directions: (i) extend our tool to support the analysis of other procedures and protocol layers (e.g., RRC and PDCP) messages; (ii) automating some of the manual tasks in LTEInspector; (iii) enrich the model features and analysis of LTEInspector to handle message data; (iv) explore other forms of side channel information, exposed by cellular network protocols, that can be exploited to launch novel security and privacy attacks; (v) evaluate the performance of different signature generation/verification schemes in authenticating broadcast messages in cellular networks; and finally (vi) design a clean-slate and backward compatible countermeasure against the side-channel attacks on the paging procedure.

REFERENCES

REFERENCES

[1] *Hackers Are Tapping Into Mobile Networks' Backbone, New Research Shows*, https://www.forbes.com/sites/parmyolson/2015/10/14/hackers-mobile-network-backbone-ss7.

[2] *Hackers Take Down the Most Wired Country in Europe*, https://www.wired.com/2007/08/ff-estonia/.

[3] *Major DDoS Attacks Involving IoT Devices*, https://www.enisa.europa.eu/publications/info-notes/major-ddos-attacks-involving-iot-devices.

[4] *3GPP Standard*, www.3gpp.org.

[5] *LTE; Evolved Universal Terrestrial Radio Access (E-UTRA) and Evolved Packet Core (EPC); Common test environments for User Equipment (UE) conformance testing (3GPP TS 36.508 version 12.3.1 Release 12)*, https://www.etsi.org/deliver/etsi_ts/136500_136599/136508/12.03.01_60/ts_136508v120301p.pdf.

[6] G.-H. Tu, Y. Li, C. Peng, C.-Y. Li, H. Wang, and S. Lu, "Control-plane protocol interactions in cellular networks," in *Proceedings of the 2014 ACM Conference on SIGCOMM*. ACM, 2014, pp. 223–234.

[7] *3GPP Standard. Release 12.*, http://www.3gpp.org/specifications/releases/68-release-12.

[8] *Cellular Service*, https://www.fcc.gov/wireless/bureau-divisions/mobility-division/cellular-service.

[9] D. Abodunrin, Y. Miche, and S. Holtmanns, "Some dangers from 2g networks legacy support and a possible mitigation," in *Communications and Network Security (CNS)*, Sept 2015, pp. 585–593.

[10] P. P. C. Lee, T. Bu, and T. Woo, "On the detection of signaling dos attacks on 3g wireless networks," in *26th International Conference on Computer Communications (INFOCOM)*, May 2007, pp. 1289–1297.

[11] N. Golde, K. Redon, and R. Borgaonkar, "Weaponizing Femtocells: The Effect of Rogue Devices on Mobile Telecommunications," in *Proceedings of the 19th Annual Network & Distributed System Security Symposium*, Feb. 2012.

[12] D. F. Kune, J. Koelndorfer, and Y. Kim, "Location leaks on the gsm air interface," in *NDSS*, 2012.

[13] I. Androulidakis, "Intercepting mobile phone calls and short messages using a gsm tester," in *18th Conference on Computer Networks, Ustron, Poland*, A. Kwiecień, P. Gaj, and P. Stera, Eds., 2011, pp. 281–288.

[14] M. Arapinis, L. Mancini, E. Ritter, M. Ryan, N. Golde, K. Redon, and R. Borgaonkar, "New privacy issues in mobile telephony: Fix and verification," in *Proceedings of the 2012 ACM Conference on Computer and Communications Security*, ser. CCS '12. ACM, 2012, pp. 205–216.

[15] M. Arapinis, L. I. Mancini, E. Ritter, and M. Ryan, "Privacy through pseudonymity in mobile telephony systems," in *NDSS*, 2014.

[16] U. Meyer and S. Wetzel, "A man-in-the-middle attack on umts," in *Proceedings of the 3rd ACM Workshop on Wireless Security*, ser. WiSe '04. ACM, 2004, pp. 90–97.

[17] A. Shaik, J. Seifert, R. Borgaonkar, N. Asokan, and V. Niemi, "Practical attacks against privacy and availability in 4g/lte mobile communication systems," in *23nd Annual Network and Distributed System Security Symposium, NDSS, San Diego, CA, USA, February 21-24*, 2016.

[18] A. Dabrowski, N. Pianta, T. Klepp, M. Mulazzani, and E. Weippl, "Imsi-catch me if you can: Imsi-catcher-catchers," in *Proceedings of the 30th Annual Computer Security Applications Conference*, ser. ACSAC '14. ACM, 2014, pp. 246–255.

[19] R. P. Jover, "Security attacks against the availability of lte mobility networks: Overview and research directions," in *Wireless Personal Multimedia Communications (WPMC), 2013 16th International Symposium on*, June 2013, pp. 1–9.

[20] F. van den Broek, R. Verdult, and J. de Ruiter, "Defeating imsi catchers," in *Proceedings of the 22Nd ACM SIGSAC Conference on Computer and Communications Security*, ser. CCS '15. ACM, 2015, pp. 340–351.

[21] *Attacks on 4G LTE Networks Could Send Fake Emergency Alerts*, https://technews.acm.org/archives.cfm?fo=2018-03-mar/mar-16-2018.html.

[22] *New Research Exposes Vulnerabilities in Cellular Networks*, https://www.cs.purdue.edu/news/articles/2018/vulnerabilities-in-4G-LTE-networks.html.

[23] *The Security of Cellular Connections*, https://www.nytimes.com/2018/08/10/technology/personaltech/security-wifi-lte-data.html.

[24] *New LTE attacks can snoop on messages, track locations and spoof emergency alerts*, https://www.zdnet.com/article/new-lte-attacks-eavesdrop-on-messages-track-locations-spoof-alerts/.

[25] *4G LTE pried open to reveal a slew of new protocol-level attacks*, https://www.theregister.co.uk/2018/03/05/4g_lte_protocol_vulnerabilities/.

[26] *4G LTE networks vulnerability allows adversaries to send fake emergency alerts*, http://www.homelandsecuritynewswire.com/dr20180405-4g-lte-networks-vulnerability-allows-adversaries-to-send-fake-emergency-alerts.

[27] *3GPP. Non-Access-Stratum (NAS) protocol for Evolved Packet System (EPS); Stage 3 Specification 3GPP TS 24.301 version 12.8.0 Release 12.*, [Online]. Available: http://www.3gpp.org/dynareport/24301.htm.

[28] *3GPP. Evolved Universal Terrestrial Radio Access (E-UTRA) and Evolved Universal Terrestrial Radio Access Network (EUTRAN); overall description; stage 2, Specification 3GPP TS 36.300 version 12.4.0 Release 12.*, [Online]. Available: http://www.3gpp.org/dynareport/36300.htm.

[29] *3GPP Release 15*, http://www.3gpp.org/release-15.

[30] *5G; Security architecture and procedures for 5G System (3GPP TS 33.501 version 15.1.0 Release 15)*, https://www.etsi.org/deliver/etsi_ts/133500_133599/133501/15.01.00_60/ts_133501v150100p.pdf.

[31] *5G; Non-Access-Stratum (NAS) protocol for 5G System (5GS); Stage 3 (3GPP TS 24.501 version 15.0.0 Release 15).*, https://www.etsi.org/deliver/etsi_ts/124500_124599/124501/15.00.00_60/ts_124501v150000p.pdf.

[32] *5G; NR; Radio Resource Control (RRC); Protocol specification (3GPP TS 38.331 version 15.2.1 Release 15).*, https://www.etsi.org/deliver/etsi_ts/138300_138399/138331/15.02.01_60/ts_138331v150201p.pdf.

[33] *3rd Generation Partnership Project; Technical Specification Group Radio Access Network; V15.0.0 NR; (2018-06) User Equipment (UE) procedures in Idle mode and RRC Inactive state (Release 15)*, http://www.3gpp.org/DynaReport/38304.htm.

[34] B. Kim, S. Bae, and Y. Kim, "Guti reallocation demystified: Cellular location tracking with changing temporary identifier," in *25th Annual Network and Distributed System Security Symposium, NDSS, San Diego, CA, USA, February 18-21*, 2018.

[35] D. Dolev and A. C. Yao, "On the security of public key protocols," Stanford, CA, USA, Tech. Rep., 1981, http://www.ncstrl.org:8900/ncstrl/servlet/search?formname=detail&id=oai

[36] K. R. Apt and D. C. Kozen, "Limits for automatic verification of finite-state concurrent systems," *Inf. Process. Lett.*, vol. 22, no. 6, pp. 307–309, May 1986.

[37] Z. Manna and A. Pnueli, "A hierarchy of temporal properties (invited paper, 1989)," in *Proceedings of the ninth annual ACM symposium on Principles of distributed computing*. ACM, 1990, pp. 377–410.

[38] A. Cimatti, E. M. Clarke, F. Giunchiglia, and M. Roveri, "Nusmv: A new symbolic model verifier," in *Proceedings of the 11th International Conference on Computer Aided Verification*, ser. CAV '99. London, UK, UK: Springer-Verlag, 1999, pp. 495–499.

[39] G. Holzmann, *Spin Model Checker, the: Primer and Reference Manual*, 1st ed. Addison-Wesley Professional, 2003.

[40] B. Blanchet, "Modeling and verifying security protocols with the applied pi calculus and proverif," *Foundations and Trends in Privacy and Security*, vol. 1, no. 1-2, pp. 1–135, 2016.

[41] S. Meier, B. Schmidt, C. Cremers, and D. Basin, "The tamarin prover for the symbolic analysis of security protocols," in *Proceedings of the 25th International Conference on Computer Aided Verification (CAV)*. Springer-Verlag, 2013, pp. 696–701.

[42] A. Armando and et al., "The avispa tool for the automated validation of internet security protocols and applications," in *Proceedings of the 17th International Conference on Computer Aided Verification*, ser. CAV'05. Springer-Verlag, 2005, pp. 281–285.

[43] J. Bengtson, K. Bhargavan, C. Fournet, A. D. Gordon, and S. Maffeis, "Refinement types for secure implementations," *ACM Trans. Program. Lang. Syst.*, vol. 33, no. 2, pp. 8:1–8:45, Feb. 2011.

[44] G. Lowe, "Breaking and fixing the needham-schroeder public-key protocol using fdr," in *Proceedings of the Second International Workshop on Tools and Algorithms for Construction and Analysis of Systems*, ser. TACAs '96. Springer-Verlag, 1996, pp. 147–166.

[45] C. J. Cremers, "Unbounded verification, falsification, and characterization of security protocols by pattern refinement," in *Proceedings of the 15th ACM Conference on Computer and Communications Security*, ser. CCS '08. ACM, 2008, pp. 119–128.

[46] A. C. Yao, "Theory and application of trapdoor functions," in *Proceedings of the 23rd Annual Symposium on Foundations of Computer Science*, ser. SFCS '82. IEEE Computer Society, 1982, pp. 80–91.

[47] J.-K. Tsay and S. F. Mjølsnes, "A vulnerability in the umts and lte authentication and key agreement protocols," in *Proceedings of the 6th MMM-ACNS*. Springer-Verlag, 2012, pp. 65–76.

[48] B. Blanchet, "Automatic verification of correspondences for security protocols," *Journal of Computer Security*, vol. 17, no. 4, pp. 363–434, Jul. 2009.

[49] M. Abadi and B. Blanchet, "Analyzing Security Protocols with Secrecy Types and Logic Programs," in *29th Annual ACM SIGPLAN - SIGACT Symposium on Principles of Programming Languages (POPL 2002)*. Portland, Oregon: ACM Press, Jan. 2002, pp. 33–44.

[50] E. A. Emerson and K. S. Namjoshi, "Reasoning about rings," in *Proceedings of the 22Nd ACM SIGPLAN-SIGACT Symposium on Principles of Programming Languages (POPL)*. ACM, 1995, pp. 85–94.

[51] R. Racic, D. Ma, and H. Chen, "Exploiting mms vulnerabilities to stealthily exhaust mobile phone's battery," in *Securecomm and Workshops*, Aug 2006, pp. 1–10.

[52] J. Serror, H. Zang, and J. C. Bolot, "Impact of paging channel overloads or attacks on a cellular network," in *Proceedings of the 5th ACM Workshop on Wireless Security*, 2006, pp. 75–84.

[53] N. Golde, K. Redon, and J.-P. Seifert, "Let me answer that for you: Exploiting broadcast information in cellular networks," in *Proceedings of the 22Nd USENIX Conference on Security*, 2013, pp. 33–48.

[54] *USRP B210*, https://www.ettus.com/product/details/UB210-KIT.

[55] *OpenLTE*, http://openlte.sourceforge.net/.

[56] *srsLTE*, https://github.com/srsLTE.

[57] *Qxdm Professional Qualcomm Extensible Diagnostic-Monitor*, www.qualcomm.com/media/documents/files/qxdm-professional-qualcomm-extensible-diagnostic-monitor.pdf.

[58] *srsUE*, https://github.com/srsLTE/srsUE.

[59] D. Rupprecht, K. Jansen, and C. Pöpper, "Putting lte security functions to the test: A framework to evaluate implementation correctness," in *Proceedings of the 10th USENIX Conference on Offensive Technologies*, ser. WOOT'16, 2016, pp. 40–51.

[60] N. Bui and J. Widmer, "Owl: A reliable online watcher for lte control channel measurements," in *Proceedings of the 5th Workshop on All Things Cellular: Operations, Applications and Challenges*, ser. ATC '16. ACM, 2016, pp. 25–30.

[61] *OpenEPC*, www.openepc.com.

[62] P. Y. Kong, "Power consumption and packet delay relationship for heterogeneous wireless networks," *IEEE Communications Letters*, vol. 17, no. 7, pp. 1376–1379, July 2013.

[63] Y. Li, C. Peng, Z. Yuan, J. Li, H. Deng, and T. Wang, "Mobileinsight: Extracting and analyzing cellular network information on smartphones," in *Proceedings of the 22nd Annual International Conference on Mobile Computing and Networking*, ser. MobiCom '16, 2016, pp. 202–215.

[64] K. B. Rasmussen and S. Čapkun, "Realization of rf distance bounding," in *Proceedings of the 19th USENIX Conference on Security*, ser. USENIX Security'10, 2010, pp. 25–25.

[65] S. R. Hussain, O. Chowdhury, S. Mehnaz, and E. Bertino, "Lteinspector: A systematic approach for adversarial testing of 4g lte," in *25th Annual Network and Distributed System Security Symposium, NDSS, San Diego, CA, USA, February 18-21*, 2018.

[66] *HLRLOOKUPS*, https://www.hlr-lookups.com/.

[67] F. Zarinni, A. Chakraborty, V. Sekar, S. R. Das, and P. Gill, "A first look at performance in mobile virtual network operators," in *Proceedings of the 2014 Conference on Internet Measurement Conference*, ser. IMC '14. ACM, 2014, pp. 165–172.

[68] H. Welte, *The reason why you see paging by IMSI in real-world GSM networks*, http://laforge.gnumonks.org/blog/20100628-the_reason_for_paging_by_imsi, 2010.

[69] *5G; System Architecture for the 5G System (3GPP TS 23.501 version 15.2.0 Release 15).*, https://www.etsi.org/deliver/etsi_ts/123500_123599/123501/15.02.00_60/ts_123501v150200p.pdf.

[70] D. Rupprecht, K. Kohls, T. Holz, and C. Pöpper, "Breaking LTE on layer two," in *IEEE Symposium on Security & Privacy (SP)*. IEEE, May 2019.

[71] *USRP B210*, https://www.crowdsupply.com/lime-micro/limesdr.

[72] A. Shaik, R. Borgaonkar, S. Park, and J.-P. Seifert, "On the impact of rogue base stations in 4g/lte self organizing networks," in *Proceedings of the 11th ACM Conference on Security & Privacy in Wireless and Mobile Networks*, ser. WiSec '18. New York, NY, USA: ACM, 2018, pp. 75–86. [Online]. Available: http://doi.acm.org/10.1145/3212480.3212497

[73] J. Ooi and N. Neninger, "Imsi catchers and mobile security," 2015.

[74] P. Traynor, M. Lin, M. Ongtang, V. Rao, T. Jaeger, P. McDaniel, and T. La Porta, "On cellular botnets: Measuring the impact of malicious devices on a cellular network core," in *Proceedings of the 16th ACM Conference on Computer and Communications Security (CCS)*, 2009, pp. 223–234.

[75] P. Traynor, P. McDaniel, and T. La Porta, "On attack causality in internet-connected cellular networks," in *Proceedings of 16th USENIX Security Symposium*, 2007, pp. 21:1–21:16.

[76] Z. Li, W. Wang, C. Wilson, J. Chen, Q. Chen, T. Jung, L. Zhang, K. Liu, X. Li, and Y. Liu, "Fbs-radar: Uncovering fake base stations at scale in the wild," 2017.

[77] Z. Zhuang, X. Ji, T. Zhang, J. Zhang, W. Xu, Z. Li, and Y. Liu, "Fbsleuth: Fake base station forensics via radio frequency fingerprinting," in *Proceedings of the 2018 on Asia Conference on Computer and Communications Security*, ser. ASIACCS '18, 2018, pp. 261–272. [Online]. Available: http://doi.acm.org/10.1145/3196494.3196521

[78] K. Nohl, *Mobile Self Defense*, 31.

[79] A. Perrig, R. Canetti, J. Tygar, and D. Song, "The tesla broadcast authentication protocol," in *Cryptobytes 5*, 2005.

[80] D. Cooper, S. Santesson, S. Farrell, S. Boeyen, R. Housley, and W. Polk, "Internet X.509 Public Key Infrastructure Certificate and Certificate Revocation List (CRL) Profile," Internet Requests for Comments, Tech. Rep. 5280, May 2008. [Online]. Available: http://www.ietf.org/rfc/rfc5280.txt

[81] D. Johnson, A. Menezes, and S. Vanstone, "The elliptic curve digital signature algorithm (ecdsa)," *International journal of information security*, vol. 1, no. 1, pp. 36–63, 2001.

[82] D. Boneh, C. Gentry, B. Lynn, and H. Shacham, "Aggregate and verifiably encrypted signatures from bilinear maps," in *International Conference on the Theory and Applications of Cryptographic Techniques*. Springer, 2003, pp. 416–432.

[83] A. A. Yavuz, A. Mudgerikar, A. Singla, I. Papapanagiotou, and E. Bertino, "Real-time digital signatures for time-critical networks," *IEEE Transactions on Information Forensics and Security*, vol. 12, no. 11, pp. 2627–2639, 2017.

[84] *Cell-Site Simulators/IMSI Catchers.*, https://www.eff.org/pages/cell-site-simulatorsimsi-catchers.

[85] J. Katz, A. J. Menezes, P. C. Van Oorschot, and S. A. Vanstone, *Handbook of applied cryptography*. CRC press, 1996.

[86] *Embedded SIM Remote Provisioning Architecture (Version 1.1)*.

[87] R. L. Rivest, A. Shamir, and L. Adleman, "A method for obtaining digital signatures and public-key cryptosystems," *Communications of the ACM*, vol. 21, no. 2, pp. 120–126, 1978.

[88] A. B. Association *et al.*, "Public key cryptography for the financial services industry: The elliptic curve digital signature algorithm," *American National Standard X*, vol. 9, 1999.

[89] D. Boneh, C. Gentry, B. Lynn, and H. Shacham, "Aggregate and verifiably encrypted signatures from bilinear maps," in *Advances in Cryptology — EUROCRYPT 2003*, E. Biham, Ed. Berlin, Heidelberg: Springer Berlin Heidelberg, 2003, pp. 416–432.

[90] A. A. Yavuz, A. Mudgerikar, A. Singla, I. Papapanagiotou, and E. Bertino, "Real-time digital signatures for time-critical networks," *IEEE Transactions on Information Forensics and Security*, vol. 12, no. 11, pp. 2627–2639, Nov 2017.

[91] M. Sahin and A. Francillon, "Over-the-top bypass: Study of a recent telephony fraud," in *Proceedings of the 2016 ACM SIGSAC Conference on Computer and Communications Security*, ser. CCS '16. ACM, 2016, pp. 1106–1117.

[92] M. Sahin, A. Francillon, P. Gupta, and M. Ahamad, "Sok: Fraud in telephony networks," in *2nd IEEE European Symposium on Security and Privacy, April 26-28, 2017, Paris, France*, Paris, France, 2017. [Online]. Available: http://www.eurecom.fr/publication/5055

[93] H. Li, X. Xu, C. Liu, T. Ren, K. Wu, Z. W. Cao, Xuezhi, Z. Y. Yu, and D. Song, "A machine learning approach to prevent malicious calls over telephony networks," in *Proceedings of the 2018 IEEE Symposium of Security and Privacy*. IEEE, 2018.

[94] B. Reaves, L. Blue, H. Abdullah, L. Vargas, P. Traynor, and T. Shrimpton, "Authenticall: Efficient identity and content authentication for phone calls," in *26th USENIX Security Symposium (USENIX Security 17)*. Vancouver, BC: USENIX Association, 2017, pp. 575–592. [Online]. Available: https://www.usenix.org/conference/usenixsecurity17/technical-sessions/presentation/reaves

[95] B. Reaves, L. Blue, D. Tian, P. Traynor, and K. R. Butler, "Detecting sms spam in the age of legitimate bulk messaging," in *Proceedings of the 9th ACM Conference on Security & Privacy in Wireless and Mobile Networks*, ser. WiSec '16. New York, NY, USA: ACM, 2016, pp. 165–170. [Online]. Available: http://doi.acm.org/10.1145/2939918.2939937

[96] S. Sinha, M. Bailey, and F. Jahanian, "Improving spam blacklisting through dynamic thresholding and speculative aggregation," in *Proceedings of the Network and Distributed System Security Symposium, NDSS 2010, San Diego, California, USA, 28th February - 3rd March 2010*.

[97] X. Chen, J. Meng, Y. C. Hu, M. Gupta, R. Hasholzner, V. N. Ekambaram, A. Singh, and S. Srikanteswara, "A fine-grained event-based modem power model for enabling in-depth modem energy drain analysis," *Proc. ACM Meas. Anal. Comput. Syst.*

[98] R. Borgaonkar and S. Udar, "Understanding imsi privacy," in *BlackHat*, 2014.

[99] K. Nohl, "Mobile self-defense." [Online]. Available: https://events.ccc.de/congress/2014/Fahrplan/system/attachments/2493/original/Mobile_Self_Defense-Karsten_Nohl-31C3-v1.pdf

[100] J. Jermyn, G. Salles-Loustau, and S. Zonouz, "An analysis of dos attack strategies against the lte ran," vol. 3, 2014, pp. 159–180.

[101] H. Kim, D. Kim, M. Kwon, H. Han, Y. Jang, D. Han, T. Kim, and Y. Kim, "Breaking and fixing volte: Exploiting hidden data channels and mis-implementations," in *Proceedings of the 22Nd ACM SIGSAC Conference on Computer and Communications Security*, ser. CCS '15. New York, NY, USA: ACM, 2015, pp. 328–339.

[102] C.-Y. Li, G.-H. Tu, C. Peng, Z. Yuan, Y. Li, S. Lu, and X. Wang, "Insecurity of voice solution volte in lte mobile networks," in *Proceedings of the 22Nd ACM SIGSAC Conference on Computer and Communications Security*, ser. CCS '15. New York, NY, USA: ACM, 2015, pp. 316–327.

[103] S. Park, A. Shaik, R. Borgaonkar, A. Martin, and J.-P. Seifert, "White-stingray: Evaluating IMSI catchers detection applications," in *11th USENIX Workshop on Offensive Technologies (WOOT 17)*. Vancouver, BC: USENIX Association, 2017. [Online]. Available: https://www.usenix.org/conference/woot17/workshop-program/presentation/park

[104] A. Dabrowski, G. Petzl, and E. R. Weippi, "The messenger shoots back: Network operator based imsi catcher detection," in *International Symposium on Research in Attacks, Intrusions, and Defenses*. Springer, Cham, 2016, pp. 279–302.

[105] P. Ney, I. Smith, G. Cadamuro, and T. Kohno, "Seaglass: enabling city-wide imsi-catcher detection," in *Proceedings on Privacy Enhancing Technologies*, 2017, pp. 39–56.

[106] M. Khan and V. Niemi, "Concealing imsi in 5g network using identity based encryption," in *axXiv preprint arXiv:1708.01868*, 2017.

[107] *Protecting IMSI and User Privacy in 5G Networks*, www.ericsson.com/res/docs/2016/protecting-imsi-and-user-privacy-in-5g-networks.pdf.

[108] M. S. A. Khan and C. J. Mitchell, "Trashing imsi catchers in mobile networks," in *Proceedings of the 10th ACM Conference on Security and Privacy in Wireless and Mobile Networks*, 2017, pp. 207–218.

[109] X. Yi, E. Okamoto, and K. Y. Lam, "An optimized protocol for mobile network authentication and security," in *ACM SIGMOBILE Mobile Computing and Communications Reviews*, vol. 2, 1998, pp. 37–39.

[110] Y. Zheng, "An authentication and security protocol for mobile computing," in *Mobile Communications*. Springer US, 1996, pp. 249–267.

[111] C.-C. Lee, I.-E. Liao, and M.-S. Hwang, "An extended certificate-based authentication and security protocol for mobile networks." in *Information Technology and Control*, vol. 38, 2009.